The E3 ligase TRIM25 negatively interferes with the translation of caspase-2 – therapeutic implications for sensitizing colon carcinoma cells to intrinsic apoptosis

Dissertation

zur Erlangung des Doktorgrades

der Naturwissenschaften

Vorgelegt beim Fachbereich 14 Biochemie, Chemie und Pharmazie

der Johann Wolfgang Goethe-Universität

in Frankfurt am Main

von

Usman Nasrullah

aus Sargodha, Pakistan

Disputation date: 29th of October, 2020

Frankfurt am Main

Vom Fachbereich 14 Biochemie, Chemie und Pharmazie der Johann Wolfgang Goethe-Universität als Dissertation angenommen.

Dekan: Prof. Dr. C. Glaubitz

Gutachter: Prof. Dr. Achim Schmidtko

Prof. Dr. Wolfgang Eberhardt

Prof. Dr. Jochen Klein

Prof. Dr.Eugen Proschak

Datum der Disputation: 29th of October, 2020

To the soul of my father,

To my beloved mother

LIST OF CONTENTS

LIST OF FIGURES

LIST OF TABLES

LIST OF ABBREVIATIONS

Abi2	Abl-interactor 2
Apaf-1	Apoptosis protease activating factor-1
Aqua bidest	Aqua biestillata
BAK	Bcl-2 homologous antagonist /killer 1
BAX	Bcl-2 associated X protein
BCL9L	B-cell CLL/lymphoma 9 protein
Bid	BH3 interacting-domain death agonist
BSA	Bovine serum albumin
CARD	Caspase Recruitment Domain
CBL	Casitas B-lineage lymphoma
CC	Coiled-Coil
DAPI	4' 6-diamidino-2-phenylindole
DD	Death domain
DED	Death effector domain
DISC	Death-inducing signaling complex
DMEM	Dulbecco's Modified Eagle Medium
DUBs	Deubiquitinases
e.g	Example
ECL	Enhanced chemiluminescence
EDTA	Ethylenediaminetetraacetic acid
EFP	Estrogen-responsive finger protein
EGFR	Epidermal growth factor receptor

ERG	ETS related gene
FACS	Fluorescence activated cell sorting
FADD	Fas-associated death domain
FCS	Fetal calf serum
h	Hours
HCC	Hepatocellular carcinoma
HEp-2	Human epithelial type 2
HuR	Human antigen R
IAPs	Inhibitors of apoptotic proteins
ICE	Interleukin-1 beta converting enzyme
IFN	Interferon
ISG 15	Interferon-stimulated gene 15
ITAFs	IRES trans-acting factors
KDa	Kilo-Dalton
MAPK	Mitogen-activated protein kinase
MAVS	Mitochondrial antiviral signaling proteins
MEFs	Mouse embryonic fibroblasts
Min	Minutes
MiRNAs	MicroRNAs
MTA1	Metastasis-associated 1 protein
Nuclear factor- κB	NF- κB
PAGE	Polyacrylamide gel electrophoresis
PARP	Poly (ADP-Ribose)-Polymerase 1

PBS	Phosphate buffered saline
PCR	Polymerase chain reaction
PI3	Phosphoinositide-3
PIDD	p53 Inducible protein along with a death domain
PKB	Protein kinase B
PRRs	Pattern recognition receptors
qPCR	Quantitative polymerase chain reaction
RAR	Retinoic acid receptor
RBP	RNA-binding protein
RIG-I	Retinoic acid-inducible gene I
RING	The really interesting new gene
rmp	Rotations per minute
SDS	Sodium dodecyl sulfate
SMAC	Second mitochondria-derived activator of caspase
SUMO	Small ubiquitin-related modifier
TEMED	Tertramethyl ethylene diamine
TNF	Tumor necrosis factor
TRADD	TNF receptor-associated death domain
TRIM	Tripartite motif
UBe2I	Ubiquitin-conjugating enzyme e2I
UTR	Untranslated region
v/v	Volume/volume
VEGF	Vascular endothelial growth factor

w/v	Weight/volume
ZAP	Zinc-finger antiviral protein
µM	Micromolar

1. SUMMARY

An overexpression of the E3 ubiquitin ligase TRIM25 is implicated in several human cancers and frequently correlates with a poor prognosis and occurrence of therapy resistance in patients. Previous studies of our group have identified the mRNA encoding the pro-apoptotic caspase-2 as a direct target of the ubiquitous RNA binding protein human antigen R (HuR). The constitutive HuR binding observed in colon carcinoma cells negatively interferes with the translation of caspase-2 mainly through binding to the 5' untranslated region (UTR) of caspase-2 and thereby confers an increased survival of tumor cells. The main objective of this thesis was to unravel novel regulatory proteins critically involved in the control of caspase-2 translation and their impact on therapeutic drug resistance of human colon carcinoma cells. By employing RNA affinity chromatography in combination with mass-spectrometry, among several putative caspase-2 mRNA binding proteins, we have identified the tripartite motif-containing protein 25 (TRIM25) as novel caspase-2 translation regulatory protein in colon carcinoma cells. The constitutive TRIM25 binding to caspase-2 mRNA in two different human colorectal carcinoma cell lines was validated by ribonucleoprotein (RNP)-immunoprecipitation (RIP)-RT-PCR assay and by means of biotin-labeled RNA-pull-down assay. Since caspase-2 is a caspase which is particularly involved in the DNA-damage-induced apoptosis, I tested the functional relevance of negative caspase-2 regulation by TRIM25 for chemotherapeutic drug-induced cell death of different adenocarcinoma cells by RNA interference (RNAi)- mediated loss-of-function and gain-of-function approaches. In the first part of the thesis, I could demonstrate that transient silencing of TRIM25 caused a significant increase in caspase-2 protein levels without affecting the

amount of corresponding mRNAs. Mechanistically, the TRIM25 silencing-triggered increase in caspase-2 was totally impaired by cycloheximide, indicating that the stimulatory effects on caspase-2 levels depend on protein synthesis. This finding was corroborated by RNP/polysomal fractionation, which revealed that the transient knockdown of TRIM25 caused a significant redistribution of caspase-2 transcripts from the fraction of RNP particles to that from translationally active polyribosomes.

The second part of my thesis aimed at the elucidation of the functional consequences of the negative caspase-2 regulation by TRIM25 for enhanced tumor cell survival. Thereby, I found that the siRNA-mediated knockdown of TRIM25 caused a significant increase in the chemotherapeutic drug-induced cleavage of caspase-3 and to elevations in cytoplasmic cytochrome c levels implicating that TRIM25 depletion did mainly affect the intrinsic apoptotic pathway. Concordantly, the ectopic expression of TRIM25 caused a reduction in caspase-2 protein levels, concomitant with an attenuated sensitivity of tumor cells to doxorubicin.

To test the functional impact of caspase-2 in the TRIM25 depletion-dependent sensitization to drug-induced apoptosis, I employed a siRNA-mediated knockdown of caspase-2. Interestingly, the strong induction of caspase-3 and -7 cleavage after doxorubicin treatment was fully impaired after the additional knockdown of caspase-2, indicating the sensitizing effects by TRIM25 knockdown depend on caspase-2.

Data from this thesis identified the TRIM25 as a novel RNA-binding protein of caspase-2 mRNA, which negatively interferes with the translation of caspase-2 and which functionally contributes to chemotherapeutic drug resistance of colon carcinoma cells. Interfering with the

negative TRIM25-caspase-2 axis may represent a promising therapeutic avenue for sensitizing colorectal cancers to conventional anti-tumor therapies.

2. ZUSAMMENFASSUNG

Eine erhöhte Expression der E3 Ubiquitin Ligase TRIM25 wird kausal mit einigen humanen Tumoren in Zusammenhang gebracht und korreliert häufig mit einer schlechten Prognose der Pateinten sowie dem Auftreten von Therapieresistenz. Jüngste Arbeiten der Arbeitsgruppe haben die für die pro-apoptotische Caspase-2L kodierende mRNA als bislang unbekanntes Target des ubiquitären mRNA-Bindeproteins „Human Antigen R“ (HuR) identifiziert. Hierbei führt die in Kolonkarzinomzellen beobachtete konstitutive Bindung von HuR v.a. an die 5´untranslatierte Region (UTR) der Caspase-2 mRNA zu einer Hemmung der Caspase-2 Translation Das Hauptziel dieser Arbeit galt der Identifizierung neuer regulatorischer Proteine, welche bei der Kontrolle der Caspase-2 Translation eine kritische Rolle spielen und deren mögliche funktionelle Bedeutung bei der Therapieresistenz von Kolonkarzinomzellen. Mit Hilfe von RNA-Affinitätschromatographie und Massenspektrometrie konnten wir neben einigen putativen Caspase-2 RNA-Bindeproteinen das „tripartite motif-containing protein 25“ (TRIM25) als ein weiteres regulatorisches Protein der Caspase-2 Translation in Kolonkarzinomzellen identifizieren. Eine konstitutive Bindung von TRIM25 an Caspase-2 mRNA konnte in zwei verschiedenen humanen Kolonkarzinomzelllinien mittels „Ribonukleoprotein (RNP)-Immunpräzipitation (RIP)-und Reverse Transkription (RT)“ PCR Assay und mittels Biotin-markierter RNA „Pulldown“ Analyse bestätigt werden. Da Caspase-2 eine besondere Relevanz bei der über DNA-Schäden induzierten Apoptose zugeschrieben wird, wurden funktionelle Auswirkungen der negativen Caspase-2 Regulation durch TRIM25 für den Chemotherapeutika aktivierten Zelltod von verschiedenen Adenokarzinomzellen mit Hilfe von RNA-Interferenz

(RNAi) vermittelten „Loss-of Function“ und „Gain-of Function“ Experimenten untersucht. Im ersten Abschnitt der Arbeit konnte ich zeigen, dass die transiente Depletion von TRIM25 zu einem signifikanten Anstieg der Caspase-2 Proteinspiegel führt während entsprechenden mRNA Spiegel unverändert bleiben. Mechanistisch wird der durch TRIM25 Depletion verursachte Anstieg von Caspase-2 vollständig durch Cyclohexemid gehemmt was nahelegt, dass der stimulierende Effekt auf die Caspase-2 maßgeblich von der Proteinneusynthese abhängt. Diese Befunde konnten mittels RNP/Polysomenfraktionierung bestätigt werden die gezeigt haben, dass der transiente Knockdown von TRIM25 eine signifikante Umverteilung von Caspase-2 mRNA von Fraktionen der RNP-Partikel hin zu den Fraktionen der translationsaktiven Polyribosomen verursacht.

Der zweite Teil meiner Arbeit galt der Aufklärung der funktionellen Konsequenzen der negativen Caspase-2 Regulation durch TRIM25 für die Therapieresistenz von Tumorzellen. Hierbei zeigte sich, dass der siRNA-vermittelte Knockdown zu einem signifikanten Anstieg der durch Chemotherapeutika-induzierten Caspase-3 Spaltung und zu einer Erhöhung der zytoplasmatischen Cytochrom C Spiegel führt. Dies lässt vermuten, dass ein sensitivierender Effekt durch genetische TRIM25 Depletion v.a. auf eine Verstärkung des intrinsischen Apoptosewegs zurückgeführt werden kann. Umgekehrt führt die ektopische Expression von TRIM25 zu einer Reduktion der Caspase-2 Proteinspiegel und funktionell zu einer verminderten Empfindlichkeit der Tumorzellen gegenüber Doxorubicin. Um die funktionelle Bedeutung der Caspase-2 für die durch TRIM25 Depletion verursachte Apoptose Sensitivierung zu bestätigen wurde zusätzlich die Caspase-2 mit Hilfe von siRNA Transfektion herunterreguliert. Interresanterweise konnte die starke Induktion der Spaltung von Caspase-3 und -7 nach

Doxorubicin Behandlung der Zellen durch den gleichzeitigen Knockdown von Caspase-2 vollständig aufgehoben werden was deutlich macht, dass Caspase-2 für die sensibilisierenden Effekte der TRIM25 Attenuation verantwortlich ist.

Zusammenfassend zeigen die Ergebnisse dieser Arbeit, dass TRIM25 ein bislang unbekanntes RNA Bindeprotein der Caspase-2 mRNA ist welches die Translation von Caspase-2 hemmt und damit maßgeblich zur Chemotherapie Resistenz von Kolonkarzinomzellen beiträgt. Der Eingriff in die negative TRIM25-Caspase-2 Regulation ist daher eine vielversprechende Therapieoption zur Sensitivitätssteigerung kolorektaler Karzinome gegenüber konventionellen Antitumortherapien.

3. INTRODUCTION

3.1. TRIM a multifunctional member of ubiquitin E3 ligases

The **tri**partite **m**otif (TRIM) belongs to a large and diverse family of proteins characterized by a canonical TRIM domain emerging in the N-terminal of the protein (Gushchina *et al.* 2018). The TRIM family represents the largest class of E3 ubiquitin ligases, which are critically involved in the transfer of the ubiquitin modifications to specific target proteins (McNab *et al.* 2011). Ubiquitination represents a dynamic, multifaceted post-translational modification in eukaryotic cells that is mainly implied in the control of proteins through proteasomal-mediated degradation (Stringer and Piper 2011; Swatek and Komander 2016). Ubiquitination modification can be distinguished between mono- and polyubiquitination, depending on the number of ubiquitin molecules that are linked to the substrate protein (Petroski and Deshaies 2003; Petroski and Deshaies 2005). The **u**biquitin-**p**roteasome **s**ystem (UPS) involves a canonical chain of events triggered by different enzymes, including the E1 ubiquitin-activating enzymes, the E2 conjugating enzymes, and the E3 ubiquitin ligases and finally **d**e**ub**iquitinases (DUBs) (Sadowski *et al.* 2012; Callis 2014; Morreale and Walden 2016). By removal of ubiquitin from target proteins, DUBs can cause the reversal of effects caused by E3 ligases and thus can play an essential role in the maturation and recycling of ubiquitin (Pfoh *et al.* 2015; Singh and Singh 2016; Harrigan *et al.* 2018). The versatility of UPS ensures a high structural diversity by using different combinations of E2 and E3 ligases. In humans, there are only two known E1 ubiquitin-activating enzymes, while more than 40 E2 conjugating enzymes and about 600 E3 ligases have been predicted by analysis of the human genome (Deol *et al.* 2019). Notably, the ubiquitin

system is not only relevant for proteasomal degradation of proteins but additionally involved in the regulation of protein-protein interactions and the activation of enzymes, e.g., the autoubiquitination of E3 ligases (Watanabe and Hatakeyama 2017). The activation of these distinct cellular features is controlled by lysine-specific ubiquitination. In addition to the proteolytic functions of lysine (K48 or K11) linked ubiquitin chain, non-proteasomal degradation through lysine (K63)-linked ubiquitin chain is essential in DNA repair, activation of protein kinase and chromatin regulation (Hatakeyama 2017). Ubiquitin molecules can furthermore induce stabilization or relocalization of the target protein to a particular cellular compartment (Conaway *et al.* 2002).

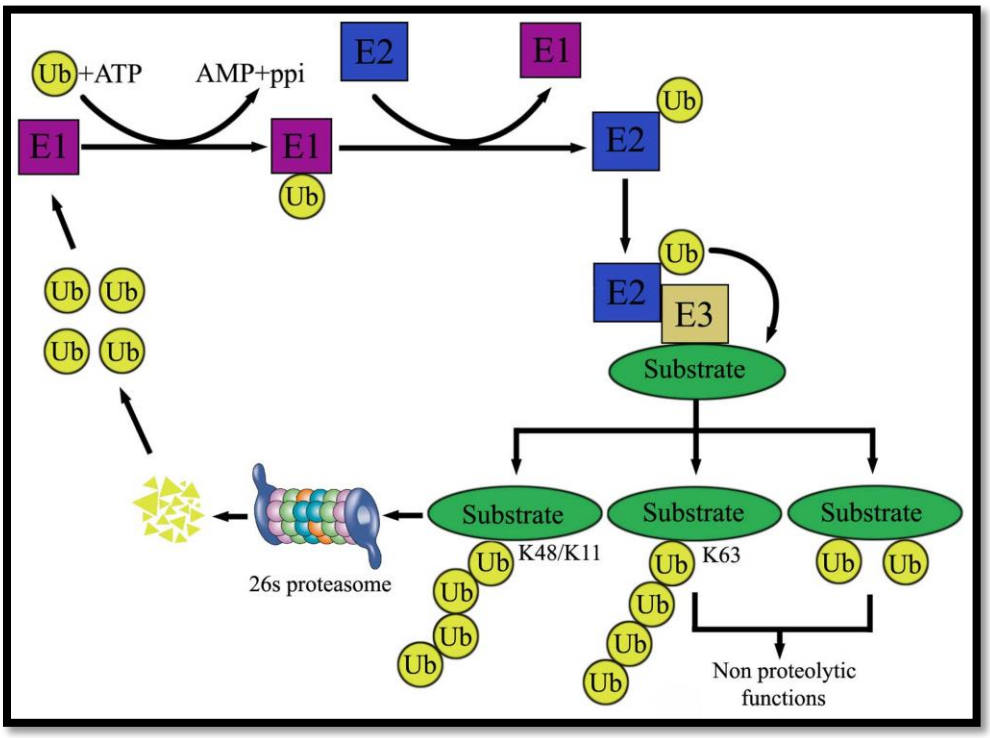

Figure 1. The role of the ubiquitin-proteasome pathway in protein degradation. Attachment of ubiquitin to E1 ubiquitin-activating enzyme charges a ubiquitin and results in an intermediate complex of an E1-ubiquitin thioester in the presence of ATP. The ubiquitin is then transferred to E2 ubiquitin-conjugating enzyme. E3 ubiquitin ligase recognizes a protein substrate and recruits an E2-ubiquitin complex, and thereby catalyzes the transfer of ubiquitin from E2 to a substrate. A single run of the reaction results in the monoubiquitination of a target protein, while

multiple runs of the reaction leading to polyubiquitination of the substrate. Polyubiquitinated proteins can either be activated (through K63) or recognized and degraded by the proteasome (through K48 linkage) (Gong *et al.* 2015).

3.2. Structural features of TRIM proteins

Structurally, members of the TRIM family have been originally defined by the presence of three distinct N-terminal domains: the **r**eally **i**nteresting **n**ew **g**ene (RING) domain (R), one or two B-boxes (B), and a **c**oiled-**c**oil region (CC), invariably ordered from the N- to the C-terminus. Based on these common structures, TRIM family members are also referred to as RBCC proteins (Reymond *et al.* 2001; Torok and Etkin 2001). To date, more than 77 TRIM evolutionarily closely related proteins have been identified in humans and mice, which have been further subdivided into 11 classes (C1 to C11). In contrast, some TRIM members lacking a typical RING domain were not included in this classification (Crawford et al., 2018). As mentioned, TRIMs represent a highly conserved family that may underline their indispensable biological functions (McNab *et al.* 2011). Besides, TRIM proteins are ubiquitously expressed and can be found in almost every eukaryotic cell type (Ozato *et al.* 2008).

The different structural domains of the TRIM/RBCC proteins not only define the family but are also inextricably associated with diverse functional abilities (Figure 2).

The RING domain is a specialized type of zinc-finger motif that is positioned at the first N-terminal 10-20 amino acids of the TRIM protein and exists in most TRIM proteins (Reymond *et al.* 2001; Torok and Etkin 2001). The insights into the functional relevance of the RING domain was initially described for the RING-domain-containing protein **C**asitas **B**-lineage **l**ymphoma

(CBL) as it could mediate the transfer of ubiquitin to target proteins (Joazeiro *et al.* 1999; Lorick *et al.* 1999; Waterman *et al.* 1999). Meanwhile, an E3 ubiquitin ligase activity has been experimentally confirmed for the RING domains of several TRIM family members, including TRIM5α, TRIM8, TRIM11, TRIM21, TRIM22, and TRIM25 (Ozato *et al.* 2008).

Growing evidence indicates that apart from ubiquitination, E3 ligase activity is also relevant for the transfer of other peptide modifications, including those of the **S**mall **U**biquitin-related **Mo**difier (SUMO), Nedd8, and **i**nterferon-**s**timulated **g**ene 15 (ISG 15) (Meroni and Diez-Roux 2005). For example, TRIM25 can modify itself and other proteins by making a conjugation with ISG15, the latter one leading to ISGylation, which represents a further significant posttranslational modification that interestingly acts independently of the RING-domain (Zou and Zhang 2006; Zou *et al.* 2007). In contrast, the RING domains of TRIM19 and TRIM63 are necessary for the association with SUMO-conjugating enzymes, such as the **ub**iquitin-conjugating **e**nzyme e2I (UBe2I) which implies a critical role of the RING domain in sumoylation (Ozato *et al.* 2008). B-box domains are zinc-binding motifs that can occur in the different forms B-box1 and B-box2, respectively (Meroni and Diez-Roux 2005). Structurally, human B-box 1 and B-box 2 domains of TRIM proteins built specific ternary structures that are similar to those from RING domains, thus implicating that these domains may origin from the same ancestry (Ozato *et al.* 2008). Since B-boxes are exclusively found in TRIM proteins, they serve as a characteristic structural feature of the TRIM family. Functionally, the B-box domains are involved in innate resistance to **h**uman **i**mmunodeficiency **v**irus (HIV) and are furthermore associated with the development of a genetic disorder such as the X-linked Opitz syndrome, which is mediated by mutations of the B-box domains of TRIM18 (Ozato *et al.* 2008). The coiled-coil domain appears

as a helical structure and frequently exists in many proteins, others than TRIMs. This helical structure plays an essential role in protein-protein interactions, especially in homo-interactions and hetero-interactions, thereby enabling TRIM proteins to build up huge multiprotein complexes essential for specific functions (McNab *et al.* 2011), e.g., the formation of the substrate-binding pocket which is critical for the E3 ligase activity of various TRIM members (Meroni and Diez-Roux 2005).

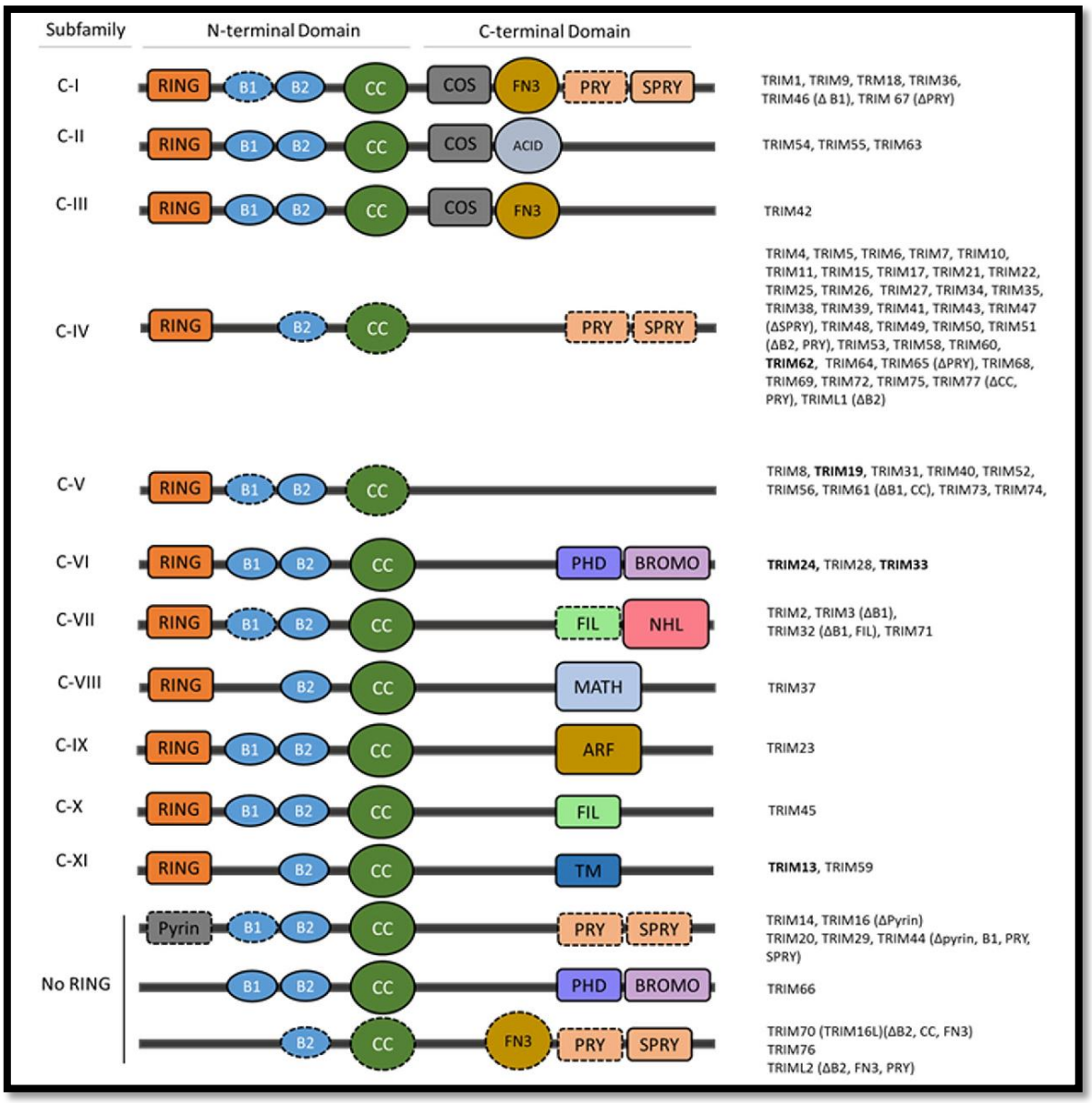

Figure 2. Structural classification of TRIM proteins: Most TRIM members contain an N-terminal RING domain, along with either one or two B-box domains (B1, B2) and a coiled-coil domain (CC) and are broadly classified into 11 subfamilies (C-I – C-XI) based on a variability of C-terminal domain. At the same time, there is an unclassified group without a RING domain (Crawford *et al.* 2018).

3.3. Biological functions of different TRIM proteins

As expected from their critical role in acting as E3 ligases of ubiquitination and related post-translational modifications (ISG15ylation, Neddylation), TRIM proteins are implied in a large variety of biological functions including protein quality control, signal transduction, cell cycle regulation, apoptosis, immune recognition and development (Watanabe and Hatakeyama 2017). In addition, some previous studies could demonstrate that several TRIM proteins can act as regulators of "autophagy" (Watanabe and Hatakeyama 2017) and can target autophagic substrates to proteolytic degradation by direct recognition (Mandell *et al.* 2014). Interestingly, many TRIMs themselves can act as autophagy cargo receptors with an essential role in autophagosome formation as described for autophagy of viral capsid proteins mediated by TRIM5a (Mandell *et al.* 2014). Besides, some TRIM proteins have been identified as critical regulators of "innate immunity" through mediating cellular signaling pathways induced either by pro-inflammatory cytokines such as **i**nter**f**ero**n** (IFN) and **t**umor **n**ecrosis **f**actor-α (TNFα) or by **p**attern **r**ecognition **r**eceptors (PRRs) such as Toll-like receptor and **r**etinoic **a**cid-**i**nducible **g**ene I (RIG-I) (Versteeg *et al.* 2014). Besides, few TRIM proteins are increasingly emerging as crucial regulators in cell proliferation and migration. One prominent example is TRIM32, which facilitates cell growth and migration of **h**uman **ep**ithelial type 2 (HEp-2) cells via binding and subsequent ubiquitination of the **Abl**-interactor 2 (Abi2) a tumor-suppressing protein (Kano *et*

al. 2008). Another example is TRIM11, which exerts a proliferative activity mainly through activation of the canonical **e**pidermal **g**rowth **f**actor **r**eceptor (EGFR)/ **m**itogen-**a**ctivated **p**rotein **k**inase (MAPK) related signaling pathway. However, the direct target of TRIM11 has not been identified so far (Di *et al.* 2013). In accordance, overexpression of TRIM14 leads to the activation of proliferative **p**rotein **k**inase B (PKB)/AKT signaling cascades in osteosarcoma cells, although the molecular mechanism of this action is not known (Xu *et al.* 2017). However, since TRIM proteins cannot directly phosphorylate proteins, both effects most probably result from indirect actions. In addition to the induction of the mitogenic Akt pathway, TRIM25 promotes proliferation and invasion of colorectal carcinoma cells through activation of the **t**ransforming **g**rowth **f**actor (TGF) β Smad signaling cascade *in vitro* and *in vivo* (Sun *et al.* 2017). A further example is TRIM52, which induces proliferation and migration of glioblastoma cell lines through a p53 dependent mechanism (Benke *et al.* 2018).

3.4. The critical role of TRIM proteins in carcinogenesis

Concerning the above mentioned diverse biological functions which are controlled by TRIM proteins, many TRIM proteins play a crucial role in different aspects of tumorigenesis. Besides, accumulating evidence revealed that malfunctions in ubiquitin-dependent degradation of some critical oncoproteins or tumor suppressors are critically involved in tumorigenesis. Accordingly, some TRIM proteins with E3 ligase activity have been identified as crucial mediators of diverse oncogenic cell functions, although these properties seem partial independent of ubiquitin-dependent degradation pathways. Consequently, various human cancers have been correlated

with either attenuated or increased expression of specific TRIMs, depending on whether they exert either tumorigenic or rather tumor-suppressive activities. A summary of TRIM-related tumors is described in Table 1.

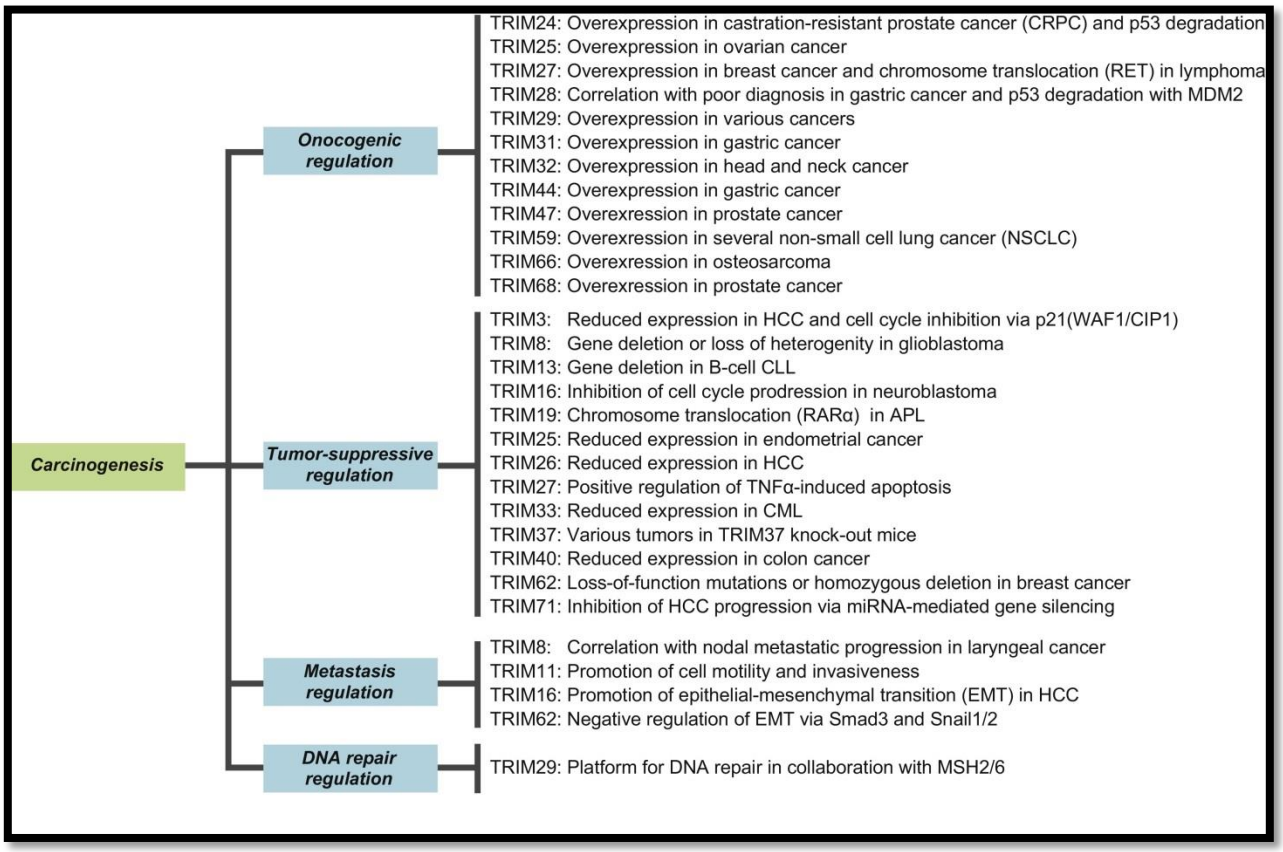

Table 1. List of prominent TRIM proteins that are implied in carcinogenesis. The specific tumorigenic function, which is characterized by a particular member of TRIM, is highlighted in blue boxes (Hatakeyama 2017).

3.5. Role of TRIM25 in host defense and cancer

Structurally, TRIM25 contains a typical RING domain, two B-boxes (B1 and B2) domains, a CC dimerization domain, and a C-terminal SPRY domain and is therefore categorized to the C-IV subfamily of TRIM proteins (see Figure 2). Similar to other TRIM members, TRIM25 was found to play a vital role in numerous cellular processes, including development, innate immunity, and

cancer (Heikel *et al.* 2016). TRIM25 was originally described as an "**e**strogen-responsive **f**inger protein" (EFP) in a screening approach that aimed for the identification of regions of human genomic DNA linked to the **e**strogen **r**eceptor (ER). The TRIM25 encoding cDNA contains a consensus estrogen-responsive element at the 3´ **u**n**t**ranslated **r**egion (UTR), which acts as a typical enhancer element. Consequently, TRIM25 expression upregulates inducible in ER-positive mammary cells (Inoue *et al.* 1993). Interestingly, in addition, to act as a target of ER-dependent signaling, TRIM25 along with some members of the TRIM family, e.g., TRIM24 and TRIM68 can directly interact with other nuclear receptors such as **r**etinoic **a**cid **r**eceptor (RAR) which is functionally relevant for the growth of hormone-dependent tumors mainly those from breast and prostate. For this reason, these TRIM proteins seem highly relevant for oncogenic pathways (Watanabe and Hatakeyama 2017).

The most studied function of TRIM25 is the regulation of RIG-I signaling, which is mainly relevant for innate antiviral immunity (Gack *et al.* 2007). RIG-I, which constitutes a pattern recognition receptor, can specifically recognize viral RNA and subsequently exposes its **c**aspase **r**ecruitment **d**omain (CARD) for the recruitment of TRIM25 via its SPRAY domain. Subsequently, TRIM25 conjugates K63 mediated polyubiquitin chains to RIG-I through its RING domain, which facilitates RIG-1 binding and subsequent activation of **m**itochondrial **a**nti**v**iral **s**ignaling proteins (MAVS) (Gack *et al.* 2007; Gack *et al.* 2008; Rajsbaum *et al.* 2012). Thereby, TRIM25-based K48-mediated ubiquitination and proteasomal degradation of the large MAVS isoform are required for downstream signaling, finally leading to the synthesis of type I IFN-1 (Castanier *et al.* 2012). For this reason, TRIM25 is overall discussed as a crucial activator of the IFN pathway, mainly at the early stages of viral infections (Gack *et al.* 2007). Besides, TRIM25 via its SPRY domain can

physically interact with the **z**ing-**f**inger antiviral **p**rotein (ZAP), which via direct binding to viral transcripts either inhibits the translation or promotes degradation of bound RNAs (Li *et al.* 2017; Zheng *et al.* 2017).

In addition to these well-documented antiviral features, accumulating evidence has revealed that TRIM25 has a substantial impact on a variety of different human cancers, including breast (Suzuki *et al.* 2005; Walsh *et al.* 2017), ovarian (Sakuma *et al.* 2005), prostate (Wang *et al.* 2016) and lung (Qin *et al.* 2016). Interestingly, both tumor-promoting as well as tumor-suppressing functions of TRIM25 have been assigned to TRIM25 depending on which tumor cell-type was investigated (Dai *et al.* 2009; Fu *et al.* 2010; Ueyama *et al.* 2010). The ability of TRIM25 to regulate the stability and activity of the tumor suppressor protein p53 represents a prominent functional link with tumorigenesis. Transient knockdown of TRIM25, e.g., leads to an accumulation of p53 levels concomitant with reduced proliferation and migration of lung cancer cells, thus indicating that TRIM25 is a negative regulator of p53 in lung cancer (Qin *et al.* 2016). In contrast, TRIM25 can increase p53 levels by preventing its ubiquitination and subsequent proteasomal degradation in human colon carcinoma cells. Interestingly, at the same time, TRIM25 inhibits the transactivation of p53 by reducing p300-dependent acetylation of p53, thus demonstrating a dual function of TRIM25 on p53 in colon carcinoma (Zhang *et al.* 2015).

Despite modulating p53 driven cell signaling, TRIM25 can promote cell growth through the proteasomal degradation of the cell cycle regulating chaperon 14-3-3σ, as demonstrated in ovarian and breast cancer (Dai *et al.* 2009; Ueyama *et al.* 2010; Zhao *et al.* 2011). The

overexpression of TRIM25 causes an increase in the proliferation and migration of lung cancer cells (Qin *et al.* 2016). In contrast, ectopic expression of TRIM25 in **h**epato**c**ellular **c**arcinoma (HCC) cells can attenuate the migration and invasion, mainly through a decrease in the expression of **m**e**t**astasis-**a**ssociated 1 protein (MTA1) (Zang *et al.* 2017). A tumor-suppressive role of TRIM25 has also been demonstrated in prostate cancer cells and is functionally due to TRIM25 dependent ubiquitination of **E**TS-**r**elated **g**ene (ERG), a transcription factor which is frequently overexpressed in prostate cancer cells (Wang *et al.* 2016). Besides the above-described examples, which rely on direct TRIM25 interactions with proteins, the presence of potential DNA-binding and dimerization-transactivation domains, including zinc finger domains, indicates that TRIM25 is also able to directly act as a transcription factor (Walsh *et al.* 2017). In accordance, a previous study using an integrated systems biology approach identified TRIM25 as a critical regulator of metastasis-related transcriptional programs. Concomitantly, TRIM25 has been established as a crucial factor of metastatic diseases, and expression of TRIM25 correlates with the poor survival of patients (Walsh *et al.* 2017).

3.6. Caspases

Caspases belong to a family of cysteine proteases that identify certain tetrapeptide motifs and cleave after a specific aspartic acid residue (Sakamaki and Satou 2009). Caspases are mainly involved in the initiation and execution of cell death and the control of inflammation through processing and activation of proinflammatory mediators, e.g., IL-1β and IL-18, which are both activated through caspase-1 dependent cleavage via the inflammasome (Bao and Shi 2007;

Kumar 2007; Martinon and Tschopp 2007; Pop and Salvesen 2009). For this reason, caspases are functionally subdivided into the apoptotic caspases (caspase-2, -3, -6, -7, -8, -9, -10) and the pro-inflammatory caspases (caspase-1, -4, -5, -11, -12) (Li and Yuan 2008) as described in Figure 3. Genetically, the caspase family constitutes 18 mammalian caspases genes (Eckhart *et al.* 2008). Principally, the caspases are inactive zymogens that require activation by cleavage either by autoactivation as in the case of the initiator caspases or by activation of upstream caspases as in the case of the executioner caspases (Pop and Salvesen 2009). All members of the caspase family contain a peptidase C14 domain consisting of about 230 amino acids with α-helical segments and a central β-sheet that are essential for homodimerization (Fuentes-Prior and Salvesen 2004). Procaspase activation involves proteolytic processing and, subsequently, producing two subunits from each caspase domain and also causing the removal of the N-terminal prodomain (Eckhart *et al.* 2008).

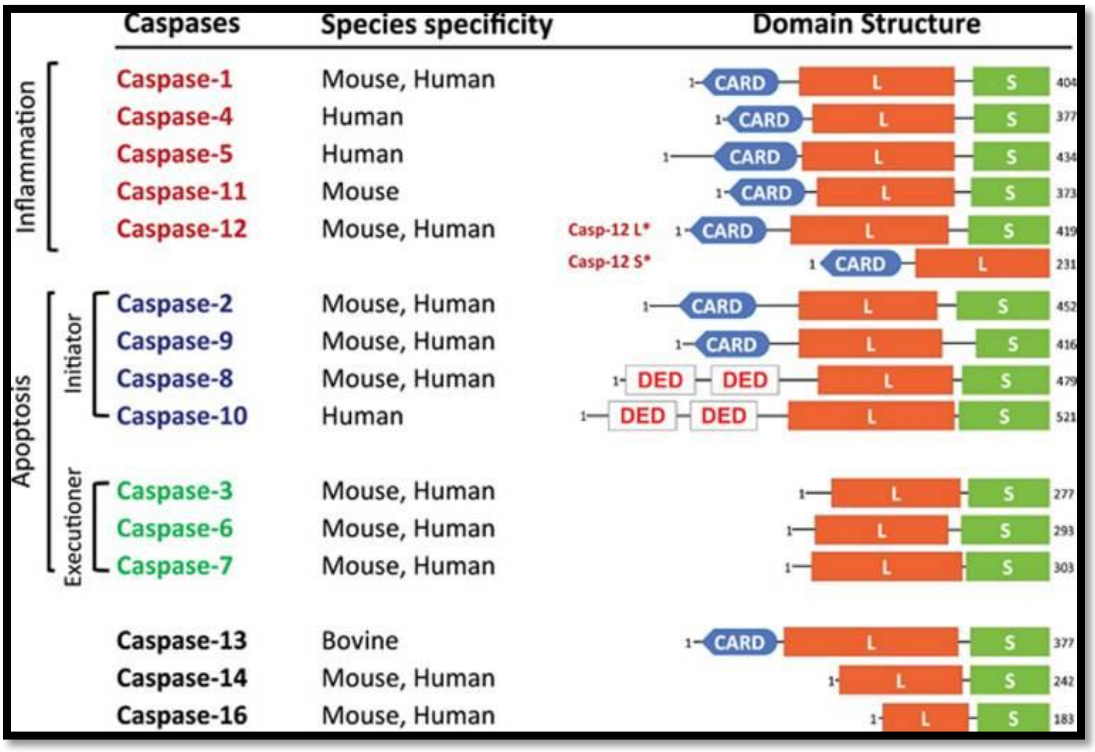

Figure 3. Structural and functional classification of mammalian caspases. Caspase-1, -4, -5, -11 and -12 are inflammatory caspases. Apoptotic caspase-2, -8, -9, and -10 belong to the initiator caspases, while caspase-3, -6, and -7 are summarized as key executioner caspases (Shalini *et al.* 2015).

3.7. Classification and activation of caspases

Since caspases share multiple cellular processes other than apoptosis and inflammation, they are additionally categorized based on the structural characteristics into initiator caspases (caspase-1, -2, -4, -5, -8, -9, -10, -11, -12) and effector or executioner caspases (caspase-3, -6, -7) (Boatright and Salvesen 2003; Li and Yuan 2008). Initiator caspases have pro domains that are characterized by either the **d**eath **e**ffector **d**omain (DED) or by the CARD. Both domains are critical anchors for autoactivation and interaction with adaptor proteins (Degterev *et al.* 2003; Li and Yuan 2008). Initiator caspases are activated through the "induced proximity" upon an interaction between adaptor proteins and pro domains resulting in the dimerization of caspases (Parrish *et al.* 2013). On the contrary, the executioner caspases have only short pro domains that require cleavage either by initiator caspases or by the action of the serine protease granzyme. In addition to a short prodomain, the executioner caspases share a common structure of a short (p10) and a large (p20) catalytic subunit (Lavrik *et al.* 2005). These caspases act downstream of initiator caspases and act directly on specific cellular substrates, including nuclear proteins, plasma membrane proteins, and mitochondrial proteins. The cleavage of these substrated critically contributes to cell death (Li and Yuan 2008; Parrish *et al.* 2013). Similarly, the initiator caspases, in addition to executioner caspases, can cleave various other cellular substrates, including the **B**H3 **i**nteracting-domain **d**eath agonist (Bid), **r**etino**b**lastoma (Rb), and **i**nhibitors of **a**poptotic **p**roteins (IAPs) (Jin and El-Deiry 2005).

3.8. Apoptosis

Apoptosis, in contrast to necrosis, is a programmed and evolutionarily highly conserved cell death pathway essential for homeostasis of adult organisms but also highly relevant during embryogenesis (Elmore 2007). Apoptosis describes a morphologically distinct form of cell death. Microscopically, it is characterized by cell shrinkage and by the extensive blebbing of plasma membranes as well as chromatin condensation in the nucleus (Kerr *et al.* 1972). Phagocytosis by macrophages is induced by the presentation of phosphatidylserine to the outer plasma membrane (Norbury and Hickson 2001). Importantly, in clear contrast to necrosis, apoptosis does not lead to the release of intracellular constituents to the extracellular space and, therefore, does not induce inflammation or other immune responses. Mechanistically, the activation of apoptosis is achieved by two main pathways the intrinsic and the extrinsic pathway, respectively.

3.9. The extrinsic pathway of cell death

The extrinsic or death receptor-related apoptosis pathway is initiated primarily by the interaction of membrane-bound death receptors belonging to the superfamily of TNF with their respective TNF family ligands (Guicciardi and Gores 2009; Zaman *et al.* 2014). Death receptors are characterized by a specialized protein-protein interaction domain called the **d**eath **d**omain (DD), which is crucial for the induction of apoptotic signaling (Fulda and Debatin 2003). Some prominent examples of most critical death receptor ligands include TNFR1/TNFα, FasR/FasL, TRAILR1 (DR4)/TRAIL, and TRAILR2 (DR5)/TRAIL (Locksley *et al.* 2001). The binding of the Fas

ligand to its respective receptor induces the recruitment of an adaptor protein named **F**as-**a**ssociated **d**eath **d**omain (FADD). The adaptor protein binds with the procaspase -8, −10, and results in the formation of a complex called **d**eath-**i**nducing **s**ignaling **c**omplex (DISC) (Zaman *et al.* 2014; Goldar *et al.* 2015; Liu *et al.* 2017). The activation of initiator caspases by DISC is followed by the activation of the executioner caspase-3 and caspase-7, which leads to the cleavage of specific protein targets including **P**oly (**A**DP-**R**ibose)-**P**olymerase 1 (PARP) relevant for DNA cleavage apoptosis (Degterev *et al.* 2003; Pfeffer and Singh 2018). In some cases, cells require an amplification step from caspase-8 in addition to the extrinsic pathway to undergo the process of apoptosis. In such an instance, caspase-8 targets the **B**H3 **i**nteracting-domain **d**eath agonist (BID) for the generation of a cleavage fragment t-Bid that directly activates the **m**itochondrial **o**uter **m**embrane **p**ermeability (MOMP), which initiates the intrinsic pathway of apoptosis as will be described in more detail in 3.10 (Plati *et al.* 2008; Kiraz *et al.* 2016)

3.10. The intrinsic pathway of cell death

The intrinsic apoptosis is dependent on mitochondria and mitochondrial proteins (Pistritto *et al.* 2016). This pathway is activated mainly via the mitochondria-mediated release of signaling proteins in response to diverse stress conditions (Green and Kroemer 2004). Some of the prominent stimuli for this pathway include deprivation of growth factors, high cytosolic concentrations of Ca^{++}, hypoxia, oxidative stress, and DNA damaging agents (Kroemer *et al.* 2007; Hassan *et al.* 2014). Many of these apoptotic stimuli cause an upregulation of BH3 proteins, which subsequently activate pro-apoptotic factors including **B**cl-2 **a**ssociated **X** protein

(BAX) and the **B**cl-2 homologous **a**ntagonist/**k**iller 1 (BAK) which both can neutralize the antiapoptotic proteins, i.e., Bcl-2, Bcl-xL, and Mcl-1 thereby leading to the disruption of the MOMP (Lomonosova and Chinnadurai 2008; Pistritto *et al.* 2016). The increased member permeability results in the release of several intermembrane proteins such as cytochrome c, **s**econd **m**itochondria-derived **a**ctivator of **c**aspase (SMAC) (Danial and Korsmeyer 2004; Pfeffer and Singh 2018). Cytochrome c binds with Apaf-1 (**a**poptosis **p**rotease **a**ctivating **f**actor-1) and thereby, promotes the formation of the "apoptosome" complex which is required for the activation of caspase-9 ultimately resulting in the activation of the executioner caspase-3 and caspase-7 (Slee *et al.* 1999; Kuribayashi *et al.* 2006; Hassan *et al.* 2014; Green and Llambi 2015).

3.11. Caspase-2

Caspase-2 was first identified as a "death protease" related to **ce**ll **d**eath protein 3 (CED-3) and **I**nterleukin-1 β **c**onverting **e**nzyme (ICE) by two separate research groups irrespectively (Xue *et al.* 1996; Schweizer *et al.* 2003). Initially, caspase-2 was named as **n**euronally **e**xpressed **d**evelopmentally **d**own-regulated (NEDD-2) as it was detected in a subtractive hybridization screening of mouse genes in neural precursor cells in mice while termed as ICH-1 (ICE and CED-3 homolog) in humans (Kumar *et al.* 1994; Wang *et al.* 1994). Caspase-2 represents the evolutionarily most conserved members of the caspase family (Dorstyn and Kumar 2009; Bouchier-Hayes and Green 2012; Kitevska *et al.* 2014). Caspase-2 is a target of differential splicing giving rise to three different isoforms of human procaspase-2 (Droin *et al.* 2000). Interestingly, the longer isoform (caspase-2L) is pro-apoptotic, whereas the shorter isoform

(caspase-2S) bearing an additional exon has mainly antiapoptotic features (Droin *et al.* 2000; Han *et al.* 2013). In contrast, the functional role of a third transcript variant with a missing exon is still enigmatic. Caspase-2L constitutes a long CARD pro-domain, which is vital for establishing interaction with an adaptor protein **r**eceptor-interacting protein-**a**ssociated **I**CH-1 homologous with a **D**eath **D**omain (RAIDD) (Droin *et al.* 2000; Krumschnabel *et al.* 2009). A characteristic attribute of caspase-2 is its additional nuclear localization due to a classical **n**uclear **l**ocalization **s**ignal (NLS) at the C terminus of the prodomain, which is recognized by importin α/β (Kumar 2009; Puccini *et al.* 2013). Structurally, due to the existence of a CARD domain, caspase-2 resembles a typical initiator caspase. However, based on its substrate specificity, caspase-2 additionally shares the feature of effector caspases as they typically cleave their substrates after aspartate at the so-called "P1 position" (Bouchier-Hayes 2010). However, the exact role of caspase-2 in apoptotic pathways is still not fully understood. The expression of caspase-2 is under the control of some **mi**cro**R**NAs (miRs). The miR-dependent repression of caspase-2 has been demonstrated for several miRs, namely miRs-17, -34a, -96, and -125b (Upton *et al.* 2008), miR-149 (Shen *et al.* 2016), and miR-708 (Song *et al.* 2013). Besides, transcription of the caspase-2 gene in colon carcinoma cells is under the control of the **B**-cell **C**LL/**l**ymphoma 9 **l**ike protein (BCL9L), and dysregulation of this factor can result in the pathological tolerance towards aneuploidy colon carcinoma cells (Lopez-Garcia *et al.* 2017). Finally, as mentioned before, caspase-2 is a target of alternative splicing giving rise to two proteins with antagonistic apoptosis regulatory functions (Wang *et al.* 1994). In support of the reported tumor-suppressive capacity of caspase-2L, reduced expression of caspase-2L is observed in several human cancers, including gliomas, lymphomas, testicular, and renal cancers (ATLAS 2020, March 6)

The activation of caspase-2 can be achieved by different mechanisms (Butt *et al.* 1998; Read *et al.* 2002; Badawi *et al.* 2018). A prominent mechanism of caspase-2 activation is the formation of PIDDosome, a multiprotein complex consisting of **p**53 **I**nducible protein along with a **d**eath **d**omain (PIDD) and the adapter protein RAIDD (Tinel and Tschopp 2004). However, several *in vivo* studies in mice demonstrated the activation of caspase-2 through a PIDD independent pathway, thus implicating the existence of alternative modes of activation of caspase-2 (Kim *et al.* 2009; Manzl *et al.* 2009). An alternative mode of caspase-2 activation is initiated by proteolytic cleavage caused by effector caspases such as caspase-3, as demonstrated in Jurkat cells (Li *et al.* 1997). An additional mechanism of caspase-2 activation is conferred through the action of caspase-8, together with a DISC in the course of CD95 triggered apoptosis (Lavrik *et al.* 2006; Olsson *et al.* 2009). A further mode of PIDD independent caspase-2 activation is an induction by bacterial pore-forming toxins, which can induce efflux of K^+, resulting in the dimerization and subsequent autoproteolysis of caspase-2 (Imre *et al.* 2012). Finally, caspase-2 activation can be achieved through proximity-driven oligomerization of the protein leading to an autocatalytic activation of the enzyme by a mechanism nominated as "induced proximity" (Casiano *et al.* 1998). This model has been validated experimentally by ectopic expression of caspase-2, leading to the activation of caspase-2 without additional stimuli (Badawi *et al.* 2017). However, the existence of this mechanism *in vivo* is still questionably.

Previously, our group could demonstrate a negative regulation of caspase-2 translation by the RNA-binding protein human antigen R (HuR) which mainly interferes with the **i**nternal **r**ibosomal **e**ntry **s**ite (IRES)-mediated translation in colorectal carcinoma cells (Winkler *et al.* 2014; Badawi *et al.* 2018).

3.12. Functional roles of caspase-2

The role of caspase-2 in regulating important cellular processes and its possible involvement in disease has been challenging to determine since first studies with caspase-2 knockout mice did not show any notable developmental defects (Bergeron *et al.* 1998). Nevertheless, caspase-2 has been involved in apoptosis induced by various stimuli such as DNA damage, **r**eactive **o**xygen **s**pecies (ROS), and disruption of the cytoskeleton (Puccini *et al.* 2013). In accordance, several *in vivo* studies have confirmed an indispensable role of caspase-2 in DNA-damage induced apoptosis (Sohn *et al.* 2011). Accordingly, it is postulated that caspase-2 serves as a kind of "damage sensor," which enables cells to initiate the process of apoptosis as a last resort in response to catastrophic signals (Baliga *et al.* 2004). Importantly, caspase-2 constitutes an effector of both stress-induced and p53-mediated apoptosis (Guo *et al.* 2002; Upton *et al.* 2008). Another vital function of caspase-2 is to serve as a potential tumor suppressor. Importantly, **m**ouse **e**mbryonic **f**ibroblasts (MEFs) from caspase-2 knockout mice with defects in the regulation of cell cycle checkpoints showed an increased genomic instability that can promote tumorigenicity (Ho *et al.* 2009). In several tumors, the affected tissues revealed a strongly reduced expression of caspase-2, -6 and -7, concomitant with increased resistance to apoptosis, e.g., gastric cancer (Yoo *et al.* 2004). More recent studies with caspase-2 knockout mice show increased vulnerability to tumor formation triggered by overexpression of specific oncogenes, thereby corroborating a tumor-suppressive role of caspase-2 also *in vivo* (Ho *et al.* 2009). Concerning the postulated tumor-suppressive capacity of caspase-2, ultimately, dysfunction of the features, as mentioned above, is often associated with increased tumorigenesis (Puccini *et al.* 2013). Besides, several publications could demonstrate caspase-2

as a novel regulator of autophagy, a critical intracellular pathway relevant to the disposal of cellular debris and misfolded proteins (Tiwari *et al.* 2014). The authors of the study demonstrated that increased autophagy and restricted apoptosis. Mechanistically, the effects are due to an increase in AMP-activated protein kinase activity accompanied by an inhibition of the rapamycin mTOR pathway resulting in increased autophagy (Tiwari *et al.* 2014).

Finally, caspase-2-mediated apoptosis is crucial for deleting mitotically stressed and aneuploid cells as these defective cells have a high capacity to induce tumorigenic transformation (Dawar *et al.* 2017; Lopez-Garcia *et al.* 2017). Mechanistically, the caspase-2 mediated cleavage of the p53 inhibiting E3 ligase Mdm2 is a part of a p53 pathway that is relevant for caspase-2 which acts as a guardian of genomic stability

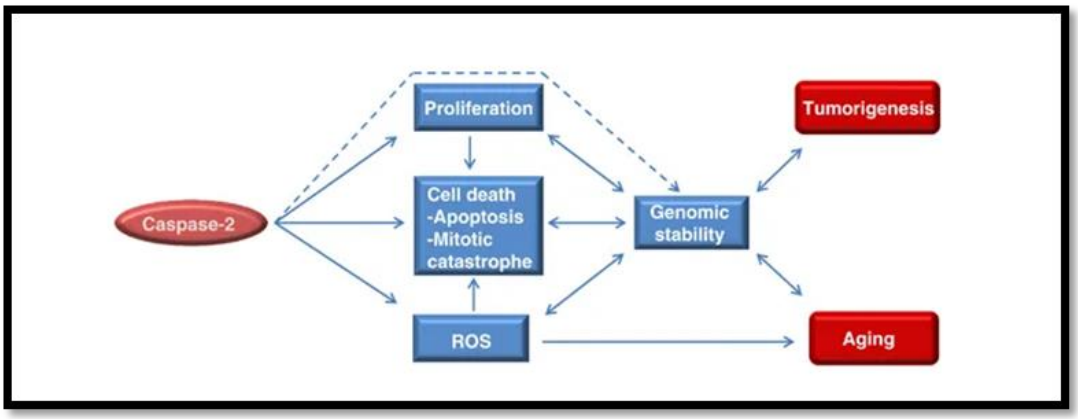

Figure 4. Functional relevance and interrelationships of caspase-2 in cellular processes (Olsson *et al.* 2015).

3.13. Colorectal cancer

Colo**r**ectal **c**ancer (CRC) is the third most commonly prevailing cancer and the second leading cause of cancer deaths worldwide (Keum and Giovannucci 2019). Although the progression of CRC is slow, yet the mortality rates are high, mainly because of the metastasis of the primary

tumor (Marley and Nan 2016; Ferlay *et al.* 2018). Pathologically, in most cases, tumors appear spontaneously with a wide range of risk factors that contribute substantially to a sporadic spread of CRC (Marley and Nan 2016; Oines *et al.* 2017). Several risk factors such as age, unhealthy dietary habits, a variety of diseases including obesity, diabetes, and chronic inflammatory diseases such as ulcerative colitis or Crohn´s disease, contribute towards the high probability of CRC (Gillen *et al.* 1994; Marley and Nan 2016; Oines *et al.* 2017).

Moreover, mutations either acquired through inheritance such as **f**amilial **a**denomatous **p**olyposis (FAP) or caused by defects DNA repair are discussed as crucial risk factors that frequently predispose individuals towards the progression of CRC (De Rosa *et al.* 2015). On the molecular level, CRC has also been linked with chromosomal and microsatellite instabilities that may affect tumor suppression and expression of the oncogene. Data acquired through pathway analysis reveal the genetic mutations that, in addition to external risk factors, influence signaling pathways critical for maintaining the homeostasis of self-renewing tissue and keeping the integrity of the intestine (Eberhardt *et al.* 2019). Some eminent examples include MAPK, **t**umor **p**rotein 53 (TP53), Wnt/β-catenin, **p**hospho**i**nositide-3 (PI3) kinase, and TGF β signaling pathways (Senda *et al.* 2005; De Rosa *et al.* 2015; Liu *et al.* 2015; Aghabozorgi *et al.* 2019). The changes in these signaling pathways play a crucial role in the transformation of colonic epithelial and metastasis of CRC (Eberhardt *et al.* 2019). During the last decade, it has been revealed that in addition to genetic events modification in post-transcriptome, including mechanisms controlling various phases of RNA maturation, i.e., trafficking, degradation, and translation can crucially contribute to CRC progression (Audic and Hartley 2004; Legrand *et al.* 2019).

Dysregulation of apoptosis is another essential hallmark of human cancers, including CRC, and at the same time critically contributes to therapy resistance. The current treatment of advanced CRC encompasses the use of diverse chemotherapeutics including 5- fluorouracil (5-FU) and cisplatin in combination with monoclonal antibodies such as Bevacizumab and Cetuximab which target the **v**ascular **e**ndothelial **g**rowth **f**actor (VEGF) and the receptor for the **e**pidermal **g**rowth **f**actor (EGF), respectively. Despite the improved therapy, the five-year survival rate for CRC is still below 13% (Siegel *et al.* 2014). One of the major problems which limit the therapeutic benefit of current therapeutics is the occurrence of drug resistance, which is partially due to a reduced sensitivity towards therapy-induced cell death. It is, therefore, a plausible therapeutic option to render colon carcinoma cells susceptible to current treatment regimens by interfering with major mechanisms of apoptosis resistance. A major demand for this approach is the identification of detailed signaling mechanisms and modules conferring cell survival mechanisms in colon carcinoma cells.

4. MATERIALS AND METHODS

4.1. Materials

4.1.1. Chemicals

Table 2. Chemicals

Chemical	Company
Acetic acid	Merck Biosciences, Schwalbach
Acrylamide/Bisacrylamide-Solution (37, 5: 1)	Roth, Karlsruhe
Agarose	Eurogentec, Cologne
Ammonium persulfate	Sigma Aldrich, Steinheim
Ampicillin	Sigma Aldrich, Steinheim
Bovine Serum Albumin	Sigma Aldrich, Steinheim
Bromophenol	Sigma Aldrich, Steinheim
Calcium chloride	Roth, Karlsruhe
Chloroform	Merck, Darmstadt
Coomassie Brilliant-Blue	AppliChem, Darmstadt
Cycloheximide	Sigma Aldrich, Taufkirchen
DAPI	Sigma Aldrich, Steinheim
DEPC	Sigma Aldrich, Steinheim
Desoxy nucleotide triphosphates	MBI Fermentas, St. Leon-Roth
D-Galactopyranoside (X-Gal)	AppliChem, Darmstadt
Disodium hydrogen phosphate	Merck, Darmstadt
DMEM	Gibco, Darmstadt
DMSO	AppliChem, Darmstadt
DTT	AppliChem, Darmstadt
EDTA	Sigma Aldrich, Steinheim
EGTA	Sigma Aldrich, Steinheim
Ethanol	Merck, Darmstadt
FCS	Biochrom, Berlin

Glycerol	Sigma Aldrich, Steinheim
Glycin	Roth, Karlsruhe
Hydrochloric acid	Sigma Aldrich, Steinheim
Isopropanol	Sigma Aldrich, Steinheim
Magnesium chloride	Merck, Darmstadt
Manganese chloride	Merck, Darmstadt
Micro-BCA protein assay	Thermo Scientifc, Dreieich
NP-40	Sigma Aldrich, Steinheim
Opti-MEM	Gibco, Darmstadt
Paraformaldehyde	Sigma Aldrich, Steinheim
Penicillin-Streptomycin	Gibco, Darmstadt
Ponceau S	Amersham Pharmacia, Munich
Potassium chloride	Merck, Darmstadt
Potassium dihydrogen phosphate	Merck, Darmstadt
Propidium iodide	Sigma Aldrich, Steinheim
Protease inhibitor-Cocktail Complete (R)	Roche Biochemicals, Munich
Protein ladder	Fermentas, St. Leon-Rot
Protein-G-Sepharose (TM) 4 fast Flow	GE Healthcare, Munich
Puromycin	Life Technologies, Darmstadt
Rubidium chloride	Sigma Aldrich, Steinheim
SDS	Roth, Karlsruhe
Skim milk powder	Sigma Aldrich, Steinheim
Sodium chloride	Sigma Aldrich, Steinheim
Sodium dihydrogen phosphate-Monohydrate	Merck, Darmstadt
Sodium fluoride	Sigma Aldrich, Steinheim
Sodium hydroxide	Roth, Karlsruhe
Sodium phosphate-Dihydrate	Roth, Karlsruhe
ß-Glycerophosphate	Sigma Aldrich, Steinheim
SYTOX Blue dead cell stain	Life Technologies, Darmstadt
TEMED	Sigma Aldrich, Steinheim
Tri reagent	Sigma Aldrich, Steinheim

Trichlor acetic acid	Sigma Aldrich, Steinheim
Tris-HCl	Sigma Aldrich, Steinheim
Triton X-100	Sigma Aldrich, Steinheim
Trizma (R) base (Tris-Base)	Sigma Aldrich, Steinheim
Trizol	Sigma Aldrich, Taufkirchen
Trypsin-EDTA	Gibco, Darmstadt
Trypton/Pepton from Casein	Roth, Karlsruhe
Tween-20	Sigma Aldrich, Steinheim

4.1.2. Instruments

Table 3. Instruments

Device	Company
Applied Biosystem 7500 Real-time PCR system	Perkin Elmer, Rodgau
BD FACS Canto II	BD Biosciences, Heidelberg
Cell chamber	Roth, Karlsruhe
CO_2 Incubator BBD 6220	Heraeus, Hanau
Detection system (BAS 1500 Fuji Film)	Raytest, Straubenhardt
Electrophoresis chamber	Bio-Rad, Munich
Film developer Agfa CP 1000	Agfa Healthcare, Bonn
Gene Amp PCR system 9700	Applied Biosystems, Weiterstadt
Heat block, Thermomixer compact	Eppendorf, Hamburg
Herasafe Sterile bank	Thermo Scientifc, Langenselbold
LSM 510 Confocal Scanning Microscope	Carl Zeiss MicroImaging GmbH, Göttingen
Megafuge 1.0 R	Heraeus, Hanau
Microfuge Fresco 21	Heraeus, Hanau
Microplate Reader Sunrise	Tecan, Switzerland
Microscope Axiovert 25	Zeiss, Jena
Mini-Protean 3 cell	Bio-Rad, Munich

Nanodrop ND-1000 Spectrophotometer	Peqlab Biotechnology GmbH, Erlangen
Rotating Mixer	Rettberg, Göttingen
Semidry-Blot-Apparatus	Bio-Rad, Munich
Spectrophotometer, Uvikon 810P	Kontorn Instruments, Rossdorf
Ultracentrifuge Optima TLX (Rotar TLA 120.2)	Beckman Coulter, Krefeld
UV-Gel camera, GelDoc 1000	Bio-Rad, Munich

4.1.3. General Materials

Table 4. General Materials

Material	Company
Amersham Hyperfilm (TM) MP X-ray films	GE Healthcare, Munich
Cell Culture Conical Tubes (15ml)	Greiner Bio-One, Frickenhausen
Cell Culture Conical Tubes (50ml)	Greiner Bio-One, Frickenhausen
Cell Culture Dishes	Greiner Bio-One, Frickenhausen
Cell Culture Flasks (175 cm^2)	Greiner Bio-One, Frickenhausen
Cell Culture Flasks (75 cm^2)	Greiner Bio-One, Frickenhausen
Cell Culture Plates (-6, -12, -24, -96 well)	Greiner Bio-One, Frickenhausen
Cryogenic Storage Vials	Greiner Bio-One, Frickenhausen
Eppendorf Safe-Lock Tubes (2 ml)	Eppendorf, Hamburg
Eppendorf Safe-Lock Tubes (1.5 ml)	Eppendorf, Hamburg
Hamilton-Pipette	Hamilton, Laboratory, Manitowoc, USA
Microtiter Plates	Greiner Bio-One, Frickenhausen
Nick Columns; Sephadex G50 DNA grade	Amersham Pharmacia, Freiburg
Nitrocellulose membrane	GE Healthcare, Munich
Polyvinyl difluoride (PVDF) Membrane	Millipore, Darmstadt
Stripette (R) cell culture pipette	Corning Incorporated, Corning NY, USA
Whatman Blotting paper (3 mm)	Macherey-Nagel, Düren

4.1.4. Kits and Reagents

Table 5. Kits and Reagents

Kit and Reagent	Company
5'EndTag (TM) labeling RNA Kit	Vector Laboratories, UK
Lipofectamine 2000 (TM) Transfection reagent	Invitrogen, Karlsruhe
Micro-BCA Protein assay kit	Thermo Scientifc, Dreieich
Nucleo Spin RNA Kit	Machery-Nagel, Düren
Oligofectamine (TM) Transfection reagent	Invitrogen, Karlsruhe
RiboMAX (TM) Large Scale RNA Production systems	Promega GmbH, Mannheim
Rotitest (R) Annexin V	Carl Roth, Karlsruhe
Western Lightning Plus-ECL, Enhanced Chemiluminescence Substrate	Perkin Elmer, Rodgau

4.1.5. Enzymes

Table 6. Enzymes

Enzyme	Company
DNA-Polymerase (5 U/µl)	Thermo Scientifc , Fermentas, Dreieich
Go-Taq hot-start polymerase (40 U/µl)	Promega, Mannheim
M-MuLV Reverse Transcriptase	Thermo Scientifc , Fermentas, Dreieich
RiboLock RNase Inhibitor	Thermo Scientifc , Fermentas, Dreieich

4.1.6. Antibodies

4.1.6.1. Primary antibodies

Table 7. Antibodies

Antibody	Catalog number	Company	Dilutions
β-actin	#A2228	Merck, Darmstadt	1:15.000
Caspase-2	#611022	BD Bioscience, Fulda	1:1.000
Caspase-3	#9662	Cell Signaling, Frankfurt	1:1.000
Caspase-7	#9494	Cell Signaling, Frankfurt	1:1.000
Caspase-8	#9746	Cell Signaling, Frankfurt	1:1.000
Cytochrome c	#4272	Cell Signaling, Frankfurt	1:1.000
HuR	#sc-5261	Santa Cruz, Heidelberg	1:1.000
PARP	#9542	Cell Signaling, Frankfurt	1:1.000
Phospho-S6 ribosomal protein (Ser240/244)	#2215	Cell Signaling, Frankfurt	1:500
TRIM25	#sc-166926	Santa Cruz, Heidelberg	1:1.000
TRIM25	#115737	Abcam, Berlin	1:1.000

4.1.6.2. Secondary antibodies

Antibody	Catalog number	Company	Dilutions
Goat anti-mouse IgG-HRP	#sc-2054	Santa Cruz, Heidelberg	1:10.000
Goat anti-rabbit IgG-HRP	#sc-20559	Santa Cruz, Heidelberg	1:10.000
Alexa Fluor 488 anti-rabbit	#A32731	Thermo Scientifc, Dreieich	1:50
Alexa Fluor 594 anti-mouse	#A11005	Thermo Scientifc, Dreieich	1:50

4.1.7. Oligonucleotides

Table 8. Oligonucleotides

Oligonucleotide	Oligonucleotide sequence (5´- 3´)
TRIM25 (Forward)	5´ -CCG CAA ATG TTC CCA GCA CA-3´.
TRIM25 (Reverse)	5´ -TGC AGT CAT CCG CAC ATC CT-3´.
Caspase-2 (Forward)	5´ -ACA GGG GAC GCA GGA TAT TGG GA-3´.
Caspase-2 (Reverse)	5´ -GGT GGC CTT GCT TGG TCT CCC T-3´.
GAPDH (Forward)	5´ -CAC CAT CTT CCA GGA GCG AG-3´.
GAPDH (Reverse)	5´ -GCA GGA GGC ATT GCT GAT-3´.

4.1.8. Taqman probes for Real-time PCR

Table 9. Taqman probes for Real-time PCR

Probe	Catalog number	Company
TRIM25	#Hs01116121_m1	Applied Biosystems, Weiterstadt
Caspase-2	#Hs00892481_m1	Applied Biosystems, Weiterstadt
GAPDH	#4310884E	Applied Biosystems, Weiterstadt

4.1.9. Small interfering RNAs (siRNAs)

Table 10. Small interfering RNAs (siRNAs)

siRNA	Catalog number	Company
siTRIM25	#15204	Thermo Scientific, Dreieich
siTRIM25 (FlexiTube mixture)	#3213123	Qiagen, Hilden
siTRIM25 (1)	SI0000072170	"
siTRIM25(2)	SI0000072163	"
siTRIM25(3)	SI0000072156	"
siTRIM25(4)	SI0000072156	"

siControl	#D001206-13	Dharmcon, Lafayette, USA
siCaspase-2	#SI00299551	Qiagen, Hilden

4.2. Methods

4.2.1. Cell culture

All cell lines were cultured in sterile conditions under a laminar flow hood. Routinely, cells were cultured in 175 cm² culture flasks at 37°C in a humidified atmosphere containing 5% of CO_2. For splitting cells into fresh culture flasks, cells were washed once using PBS and subsequently trypsinized with 5 ml of Trypsin/EDTA (0.05% v/v) for 5 min at 37°C. The detachment of cells was controlled and visualized by microscopy. After the complete detachment of cells, 5 ml of culture media was added to the culture flask, and thereafter cells were collected by centrifugation at 800 rpm for 5 min by use of a desk centrifuge. Afterward, the cell pellet was resuspended into 10 ml of fresh culture media. The diluted cells were further transferred into sterile culture flasks and routinely further diluted in a ratio of 1:5 (v/v).

Table 11. Cell lines

Cell lines	Culture media	Additional components
DLD-1 (Human colon cancer cells, p53 mutated) Derived from "The German Collection of Microorganisms and Cell Cultures" (Braunschweig, Germany)	DMEM	10% (v/v) FCS 1% (v/v) Pen-Strep
RKO (Human colon cancer cells, p53 wild type) Derived from LGC-Promochem (Wiesbaden, Germany)	DMEM	10% (v/v) FCS 1% (v/v) Pen-Strep
HEK-293 (Human embryonic kidney cells) Derived from LGC-Promochem (Wiesbaden, Germany)	DMEM	10% (v/v) FCS 1% (v/v) Pen-Strep

DLD-1 CRISPR-Cas9-control	DMEM	10% (v/v) FCS 1% (v/v) Pen-Strep 0.25% (v/v) Puromycin
DLD-1 CRISPR-Cas9-caspase-2 K.O	DMEM	10% (v/v) FCS 1% (v/v) Pen-Strep 0.25% (v/v) Puromycin

4.2.2. Long term storage of cells/thawing of cells

For long term storage, subconfluently grown colon carcinoma cells (70-90% confluent) from 175 cm^2 culture flasks were trypsinized and collected by centrifugation. Subsequently, the cells were resuspended in 1.5 ml of FCS, and 0.5 ml portions transferred to a sterile cryotube and incubated on ice for 30 min before the cell suspension was supplemented with the same volume of FCS/20% DMSO (v/v). The cell suspension was incubated at -80°C for 48 h before being ready for long-term storage in liquid nitrogen. Frozen cells were thawed rapidly in a water bath at 37°C and, after that, added directly to a 75 cm^2 flask with 15 ml of prewarmed growth media containing 10% FCS (v/v) plus antibiotics. The next day, the growth media was replaced with fresh growth media.

4.2.3. Treatment of cells with chemotherapeutics

For experiments with different chemotherapeutic drugs, human colon carcinoma cells grown on tissue flasks were trypsinized and seeded on 60 mm Petri dishes dish containing 2 ml of DMEM

plus 10% FCS and 1% Penstrep for a period of at least 24 h before the drugs were directly applied for a period of 6 h to maximal 24 h before cells were harvested for specific approaches.

4.2.4. Small interfering RNA (siRNA)

The specific number of cells (5.5 x 10^5) were counted by using a Neubauer cell chamber and subsequently seeded on a 60 mm dish containing antibiotics free DMEM and 10% FCS for 24 h. The next day, cells should have reached a confluency of 30-50% prior to transfection procedures. The media was changed with 1 ml of Opti-MEM. For single knockdown experiments, either one TRIM25 specific siRNA duplex (TRIM25 siRNA #1) or, alternatively, a mixture of either four different TRIM25 siRNA duplexes (see section 4.1.9) (TRIM25 siRNA #2) or a scrambled siRNA with a final concentration of 50 nM was added to a transfection mix containing 1 ml of Opti-MEM plus 6 µl of oligofectamine per 60 mm dish. For double knockdown experiments targeting TRIM25 plus caspase-2, the concentration of siRNA duplexes was reduced to a final concentration of 25 nM for each siRNA. Subsequently, the mixture was incubated for 30-40 min at RT to allow the formation of siRNA-lipid complexes. After that, the mixture was added dropwise to the cells. 24 h after transfection, the transfection medium was removed and replaced with medium containing antibiotics free DMEM plus 10% FCS for further incubations. Routinely, the transfection efficiency was controlled by Western blot analysis 48 h after the addition of siRNAs. In contrast, different periods of transfection ranging from 24 h to 72 h were used for time-course experiments.

4.2.5. Ectopic expression of proteins

Routinely, 1x 10^6 cells were cultured on a 60 mm dish containing growth media supplemented with FCS (10% v/v) plus Penstrep (1%). The next day, cells should have reached a confluency of 70-90% prior to transfection. The growth media range with 1 ml of Opti-MEM per 60 mm dish. Routinely, 6 µg of pCMV-Flag-TRIM25 plasmid DNA or alternatively, the same amount of empty pCMV-Flag vector per dish, were added to 1 ml of Opti-MEM plus 10 µl of lipofectamine 2000. Afterward, the transfection mixture was incubated for 5 min at RT before the DNA-lipid complex was added dropwise to the cells under gentle shaking. After 4 h, the Opti-MEM medium containing the transfection mix was replaced with growth media containing 10% FCS (v/v) plus antibiotics. Routinely, the ectopic expression of TRIM25 was monitored by Western blot analysis after 24 h to 48 h.

4.2.6. Isolation of total cell lysates

Cells seeded on 60 mm dishes were washed once with 1 ml of ice-cold PBS before incubated with 1 ml of ice-cold PBS/EDTA (5mM) before scraped by the use of a cell scraper. Cell suspensions were collected by centrifugation for 5 min at 6.500 rpm (5.000 x g) before the cell pellets were resuspended with 60-100 µl ice-cold lysis buffer. Subsequently, cell lysis was achieved by five freeze-thaw cycles by alternate use of liquid nitrogen and a heat block. Finally, cell debris was separated by centrifugation for 30 min at 13.000 rpm (11.000 x g), and the proteins in supernatants stored at -20°C.

Lysis buffer for total cell homogenates

Substance	Final concentration	Amount
NaCl	137 mM	5.48 ml 5 M
Tris/HCl, pH 8.0	20 mM	4 ml 1 M
EDTA, pH 8.0	5 mM	2 ml 0.5 M
Glycerol	10%	20 g
Triton X-100	1%	2 g
Aqua bidest.		200 ml (adjusted volume)

A mixture of inhibitors containing 1x of "Complete Protease inhibitor (25x)'' and for inhibition of protein phosphatases, Na_3VO_4 (final 1 mM) and NaF (final 1 mM) was added immediately before use.

4.2.7. Preparation of nuclear and cytoplasmic cell fractions

Human colon carcinoma cells grown on 60 mm Petri dishes were harvested in ice-cold PBS/0.5 mM EDTA as described in section 4.2.6 and collected by short centrifugation for 5 min at 6.500 rpm (5.000 x g) in a microfuge before the cell pellets were resuspended in 70-100 µl of ice-cold hypotonic buffer A. Subsequently, lysates were kept on ice for 10 min after which $1/16^{th}$ of a 10% solution of Nonidet NP40 was added. The cell lysates tubes were vigorously vortexed for 10 sec before centrifuged for 3 min at 10.000 rpm (7.000 x g) in a microfuge. The supernatants which represent the crude "cytoplasmic fractions" were transferred to a fresh Eppendorf tube and stored at -20°C. The remaining pellets were resuspended in 20-30 µl ice-cold high salt buffer C and vigorously rocked for 30 min on a shaker machine in the cold room. Finally, the samples were centrifuged at 13.000 rpm (11.000 x g) for 30 min and supernatants stored as crude "nuclear extracts" at -20°C. The protein concentrations of both fractions were determined as described in 4.2.8.

Buffer A

Substance	Final concentration	Amount
HEPES, pH 7.9	10 mM	500 µl (from 1 M stock solution)
KCl	10 mM	500 µl (from 1 M stock solution)
EDTA	0.1 mM	10 µl (from 0.5 M stock solution)
EGTA	0.1 mM	10 µl (from 0.5 M stock solution)
Aqua bidest.		50 ml (adjusted volume)

A mixture of inhibitors containing 1x of "Complete Protease inhibitor (25x)'' and for inhibition of protein phosphatases, Na_3VO_4 (final 1 mM) and NaF (final 1 mM) was added freshly before use.

Buffer C

Substance	Final concentration	Amount
HEPES, pH 7.9	20 mM	1 ml (from 1 M stock solution)
Glycerin	25%	12.5 g
NaCl	0.4 M	8 ml (from 2.5 M stock solution)
EDTA	1 mM	100 µl (from 0.5 M stock solution)
EGTA	1 mM	100 µl (from 0.5 M stock solution)
Aqua bidest.	50 ml	50 ml (adjusted volume)

A mixture of inhibitors containing 1x of "Complete Protease inhibitor (25x)'' and for inhibition of protein phosphatases, Na_3VO_4 (final 1 mM) and NaF (final 1 mM) was added freshly before use.

4.2.8. Quantification of protein contents

The BCA protein assay kit was used to determine protein concentrations. BCA assay is based on the Biuret reaction, which involves the reduction of Cu^{++} ions to Cu^{+} ions under alkaline conditions. Cu^{+} is detected by a reagent that contains bicinchoninic acid. The chelation of two

molecules BCA with one Cu^{+} ion results in a change in color, giving rise to a purple-colored complex with the absorbance, linearly increasing with the protein concentration of samples (Smith *et al.* 1985). A standard curve was established by using BSA in concentrations from 2.5-200 µg/ml. Usually, 1 µl of each protein sample was diluted with 100 µl of **d**ouble-**d**istilled water (ddH_2O). Subsequently, 100 µl of standards and unknown samples in duplicate were pipetted into a 96 well plate, and 100 µl of ddH_2O was used as a blank. 100 µl of working reagent (25 parts of reagent A, 25 parts of reagent B, and 1 part of reagent C) was added to each well. The plate was covered and incubated at 60°C for 1 h. The absorbance was measured at 562 nm on a microplate reader (Elisa Reader) using MEGALLAN V 3.00 software.

4.2.9. Western blot analysis

4.2.9.1. SDS gel electrophoresis

Sodium **d**odecyl **s**ulfate-**p**oly**a**crylamide **g**el **e**lectrophoresis (SDS-PAGE) is a widely used technique that allows the separation of proteins according to their molecular weight and the differences in their electrophoretic mobility. SDS is an anionic detergent that denatures the proteins and thereby imparting a negative charge to the linearized proteins (Laemmli 1970). The separation of proteins by SDS gel electrophoresis was performed in a polyacrylamide gel. The gels were cast in two phases. During the first phase, the resolving or lower gel was prepared, applied to a gel caster system, and isopropanol was added on the top of the gel to smoothen the surface before polymerization. After polymerization of the lower gel, the isopropanol was discarded from the top, and the prepared stacking or upper gel solution was poured on the

head of the resolving gel. Immediately the well comb was immersed between the two glass plates before the upper gel was allowed to polymerize after the addition of TEMED and APS. The gels were either stored in wet paper towels at 4°C or immediately used for gel electrophoresis. 15-30 µg of respective protein lysates were mixed with 4 x SDS-Laemmli buffer and heated for 5 min at 95°C. Subsequently, the samples were loaded in the pockets of the gel by using a Hamilton syringe. Additionally, 5 µl of a page ruler prestained protein ladder was loaded as a molecular weight marker. The gel was run in 1 x SDS-PAGE running buffer at a constant voltage of 100 V for 70 min.

Stacking buffer (Upper Tris)

Substance	Final concentration	Amount
Tris/HCl, pH 6.8	0.5 M	30.4 g
Aqua bidest.	500 ml	500 ml (adjusted volume)

Resolving buffer (Lower Tris)

Substance	Final concentration	Amount
Tris/HCl, pH 8.8	1.5 M	181.65 g
Aqua bidest.		1.000 ml (adjusted volume)

Ammonium persulfate (APS) solution

Substance	Final concentration	Amount
APS	10% (w/v)	1 g

Aqua bidest.		10 ml (adjusted volume)

4 x Laemmli buffer

Substance	Final concentration	Amount
Glycerol	40% (v/v)	8 ml
SDS	10% (w/v)	2 g
Tris/HCl pH 6.8	125 mM	5 ml (0.5 M stock solution)
DTT	50 mM	154 mg
Bromphenol blue	0.01% (w/v)	2 mg
Aqua bidest.	20 ml	20 ml (adjusted volume)

10 x PAGE buffer (Electrodes buffer)

Substance	Final concentration	Amount
Tris	0.25 M	60 g
Glycine	1.92 M	288 g
SDS	1%	20 g (100 ml from 20 % Stock solution)
Aqua bidest.	2.000 ml	2.000 ml (adjusted volume)

Coomassie-solution substance

Substance	Final concentration	Amount
Coomassie-Brilliant-Blue R250	0.1% (w/v)	0.25 g
Isopropanol	25% (v/v)	62.5 ml

Acetic acid	10% (v/v)	25 ml
Aqua bidest.		162.5 ml (adjusted volume)

Destaining solution

Substance	Final concentration	Amount
Acetic acid	10% (v/v)	100 ml
Ethanol p.a	10% (v/v)	100 ml
Aqua bidest.		800 ml (adjusted volume)

Stacking gel recipe for different gels (for 2 gels)

Substance	Amount
Stacking buffer (Upper Tris)	1.25 ml
Polyacrylamide (30%) Bisacrylamide (0.8%)	0.7 ml
Aqua bidest.	3 ml
APS (10%)	30 µl
TEMED	10 µl

Resolving gel (for 2 gels)

Substance	Amount
Resolving buffer (Lower Tris)	2.5 ml
Polyacrylamide (30%) Bisacrylamide (0.8%)	4 ml
Aqua bidest.	3.4 ml
SDS (from 20% stock solution)	100 µl
APS (from 10% stock solution)	100 µl

TEMED	5 µl

4.2.9.2. Transfer of Proteins to Nitrocellulose Membrane

After gel electrophoresis, the proteins which are separated in the gel were transferred to a nitrocellulose membrane by employing a semi-dry blotting method. Thereby, the SDS-gel and the nitrocellulose membrane were sandwiched between two stacks of three blotting papers, which had been soaked in the Towbin transfer buffer. The blotting was performed at 70 mA (constant current) for 70 min, thereby allowing a transfer of negatively charged proteins onto the nitrocellulose membrane towards the positively charged electrode of the blotting system. Ponceau S Rouge dye was used to visualize transferred proteins on the membrane.

Towbin Transfer buffer

Substance	Final concentration	Amount
Tris base	25 mM	3.03 g
Glycine	192 mM	14.4 g
Isopropanol	20%	200 ml
Aqua bidest.		1.000 ml (adjusted volume)

4.2.9.3. Immunodetection

After blotting, the nitrocellulose membrane was incubated in a blocking buffer (3% non-fat dry milk dissolved in 1x TBST) for 1 h at RT to saturate unspecific antigen binding. Thereafter, the membrane was washed three times with 1 x TBST for 5 min before incubated with the primary antibody. The primary antibody was diluted at the concentration summarized in Table 7 in 1 x

TBST (final concentration: 200 ng antibodies per ml) was added to the membrane for 1 h at RT or, alternatively, overnight at 4°C on a rocking platform. Next, the membrane was washed three times with 1 x TBST for each time 5 min before adding respective species-specific secondary antibody diluted 1:10.000 in 1 x TBST (final concentration: 40 ng antibodies per ml) for 1 h on a rocking platform. Routinely, the secondary antibodies used were conjugated with **h**orse**r**adish **p**eroxidase (HRP), which allows the detection of the immune complexes by chemiluminescence after the addition of the HRP substrate. Thereby, blots were washed 3-5 times with 1 x TBST before incubated with 1 ml of ECL substrates A plus B in a ratio of 1:1 (v/v) for 3-5 min. The ECL substrate contains an enhancer solution which is oxidized in the presence of H_2O_2 by horseradish peroxidase and resulting in the emission of light. Finally, the membranes were exposed to photographic Amersham hyper film in a dark room. Films were developed in a commercial developer machine and immunopositive signals quantified by the use of ImageJ software.

10 x Tris-buffered Saline-Tween (TBST)

Substance	Final concentration	Amount
Tris/HCl, pH 7.6	20 mM (w/v)	24 g
NaCl	150 mM (w/v)	88 g
Aqua bidest.		900 ml (adjusted volume)

4.2.10. Immunoprecipitation of Flag-tagged TRIM25

Isolation of the Flag-tagged protein (TRIM25) and associated proteins or RNA was accomplished by using monoclonal anti-Flag-M2 antibodies coupled to superparamagnetic iron impregnated agarose beads (Sigma). In order to reduce nonspecific binding of proteins, the magnetic beads were preconditioned as followed: Anti-Flag M2 Magnetic beads were washed three times with 0.5 ml of ice-cold TBS buffer using a magnetic stand before the beads were incubated with 0.5 ml of transfer (t)RNA (10 µg tRNA/ml PBS) for 1 h at 4°C under constant rotation. Subsequently, the beads were washed three times, with 0.5 ml before use. In parallel, the cell lysates used for immunoprecipitation were divided into equally sized aliquots (0.5-1.0 mg protein per aliquot) with an adjusted volume of each aliquot up to 1 ml with cold lysis buffer described before in section 4.2.6. 40 µl of preconditioned beads were added to each aliquot of cell lysates and incubated for 16 h at 4°C under constant vertical rotation. The next day, the beads were shortly centrifuged at 10.000 rpm (7.000 x g) for 60 sec at 4°C by using a microfuge. The supernatants were removed, and subsequently, the beads were washed with 0.5 ml of ice-cold TBS buffer. The washing step was repeated six times by using a magnetic rack. After the final washing step, the wash buffer was completely removed before dried beads were dissolved in a volume of 15-30 µl of Laemmli-buffer boiled for 10 min at 95°C before loaded on an SDS-PAGE gel as described in section 4.2.9.1. Alternatively, for isolation of Flag-tagged protein associated mRNA by Ribonucleoprotein-Immunoprecipitation (RNP-IP) assay, 1 ml of Tri-reagent was added to the dried beads and followed as described in section 4.2.13.

4.2.11. Immunoprecipitation of endogenous TRIM25

Usually, cell lysates from colon carcinoma cells grown on either two 60 mm dishes or one 100 mm dish sufficed for one RNP-IP reaction. The amount of precipitating antibody to be used for precipitation of a certain amount of protein was chosen by following the manufacturer´s recommendations. Usually, 12 µg of a monoclonal anti-TRIM25 mouse antibody or the same amount of mouse-IgG were used for one precipitation reaction with 0.5 to 1.0 mg of protein. Before, the cell lysates designated for one IP reaction was precleaned by incubation with 30 µl of protein-G sepharose beads for 2 h at 4°C under constant rotation. Subsequently, the beads were discarded after a short centrifugation step while the precleaned lysates (supernatants) were transferred into a fresh RNase free Eppendorf tube before divided into two equal portions (300-500 µg protein each tube) and adjusted to a final volume of 1 ml with cold lysis buffer. Afterward, each tube was complemented with 50 µl of FCS along with monoclonal anti-TRIM25 antibodies or, alternatively, with the same amount of mouse IgG and subsequently incubated overnight at 4°C under constant rotation. The next day, 70 µl of protein-G sepharose beads (note that beads had been washed three times with 0.5 ml of ice-cold lysis buffer supplemented with protease and phosphatase inhibitors) was added to the IP reaction and incubated for 2 h at 4°C under constant rotation. After that, the antigen-antibody-bound beads were centrifuged at 10.000 rpm (7.000 x g) for 1 min at 4°C and subsequently washed three times for 20 min with 0.5 ml of low salt and high salt wash buffer at 4°C. After the last washing step, the beads were thoroughly dried by using a Hamilton syringe. Analysis of TRIM25 interacting proteins was analyzed by Western blot analysis, as described in section 4.2.9.1.

4.2.12. Ribonucleoprotein-Immunoprecipitation (RNP-IP)

TRIM25 bound RNA was isolated by means of RNP-IP. Therefore, TRIM25 was immunoprecipitated as described in 4.2.11. Antibody complexed RNA from one 60 mm culture dish, which had attached to sepharose beads, was isolated by the addition of 1 ml of Trizol together with 0.2 ml of chloroform and subsequently mixed by vigorous vortexing for 10 sec. Afterward, the aqueous phase containing nucleic acids was separated from the organic phase by centrifugation for 15 min at 13.000 rpm (11.000 x g) at 4°C in a microfuge. The aqueous layer (upper phase) was carefully transferred to an RNase-free Eppendorf tube. For precipitation of total RNA, 800 µl of isopropanol, along with 3.5 µl of glycoblue was added and incubated overnight at -20°C. The next day, the RNA was collected by centrifugation at 13.000 rpm (11.000 x g) for 20 min at 4°C in a microfuge. After the supernatants were carefully drained off, and the RNA pellet was washed with 0.5 ml of 70% ice-cold ethanol and subsequently dried at 37°C for 5 min. Thereafter, the RNA was resuspended in a volume of 10-15 µl of DEPC-treated water and heated at 65°C for 10 min to resolve the RNA. Finally, the RNA content was determined by using a Nanodrop spectrophotometer by measuring the absorbance at OD_{260} and OD_{280} nm, respectively.

High Salt Buffer

Substance	Final concentration	Amount
NaCl	300 mM	3.5g
Tris/HCl, pH 7.4	50 mM	10 ml 1M Tris/HCl
EDTA pH, 8.0	2 mM	0.8 ml 0.5 M EDTA
EGTA pH, 8.0	2 mM	0.8 ml 0.5 M EGTA

SDS	0.1%	0.2 g
TWEEN	0.2%	0.4 g
Aqua bidest.		200 ml (adjusted volume)

Low Salt Buffer

Substance	Final concentration	Amount
NaCl	100 mM	1.2g
Tris/HCl, pH 7.4	50 mM	10ml 1M Tris/HCl
EDTA, pH 8.0	2 mM	0.8 ml 0.5 M EDTA
EGTA, pH 8.0	2 mM	0.8 ml 0.5 M EGTA
SDS	0.1%	0.2 g
TWEEN	0.2%	0.4 g
Aqua bidest.		200 ml (adjusted volume)

4.2.13. Isolation of total RNA from cell culture

Before the RNA isolation, cells grown on a 60 mm petri dish were washed once with ice-cold PBS before 1 ml of Trizol was directly added to the cells. Subsequently, the cells were scraped from the Petri dishes by use of a rubber policeman and the lyzed cell suspension collected in an RNA free Eppendorf tube. The following steps were similar, as described in section 4.2.12.

4.2.14. Reverse transcriptase (RT) reaction

The process of DNA synthesis from an RNA template through reverse transcription results in a complementary DNA (cDNA), which is required for the amplification of a specific cDNA by PCR.

In this study, the RevertAid RT Reverse Transcription Kit (Thermo Scientific) was used for cDNA synthesis. First-strand cDNA synthesis was accomplished by preparing a master mix according to the manufacturer´s instructions.

Component	Volume
Random Hexamer Primer	1 µl
5 X reaction buffer	4 µl
dNTP mix (10 mM each dNTP)	2 µl
RNase inhibitor (stock 40U /µl)	1 µl
M-MulV Reverse Transcriptase	1 µl
Aqua bidest.	20 µl (adjusted volume)

1 µg of RNA was used for cDNA synthesis and added to the master mix as described in the table above. For random hexamer primed cDNA synthesis, the mix was incubated for 5 min at 25°C, followed by 60 min at 37°C. The reaction was terminated by heating the sample at 70°C for 5 min. The newly synthesized cDNA was used as a template for real-time PCR and stored at -20°C.

4.2.15. Polymerase Chain Reaction (PCR)

4.2.15.1. Semi-quantitative RT-PCR

The Semi-quantitative RT-PCR was performed by using GoTaq DNA Polymerase (Promega). All reagents were thawed on ice. A master mix was prepared by following the manufacturer's instructions as followed:

Component	Volume
5 X Green Reaction Buffer	3 µl
Upstream primer (50 µM)	1 µl
Downstream primer (50 µM)	1 µl
dNTP Mix (10 mM)	2 µl
GoTaq DNA Polymerase (5U/µl)	0.15 µl
$MgCl_2$ (25 mM)	3 µl
Aqua bidest.	15 µl (adjusted volume)

Finally, 2 µl of cDNA was added to the RT-PCR master mix. The reaction mixture was briefly centrifuged before incubated in a thermocycler by choosing 32-35 cycles with the following temperatures setting.

Step	Temperature	Time
Initial Denaturation	94°C	4 min
Denaturation	94°C	30 sec
Annealing	55°C	45 sec
Extension	72°C	45 sec
Final Extension	72°C	5 min

The PCR conditions described above were employed for the amplification of different cDNAs used in this study (TRIM25, caspase-2, and GAPDH, respectively). The samples were either stored at -20° C or directly used for further analysis.

4.2.15.2. Electrophoretic separation of DNA

Separation of PCR products from a size range of 0.2 to 2 kbp was separated by using 1% -1,5% agarose gels by employing vertical electrophoresis. DNA was visualized by Midori Green DNA Stain (Nippon Genetics GmbH), which was added directly to the hardened gel at a dilution of 1:20.000. DNA samples from PCR reactions were directly transferred to the gel wells, and electrophoresis was performed in 1x TBE buffer at a constant voltage of 110 V for approximately 1 h. DNA was visualized under a UV transilluminator and documented by using Gel Doc software.

4.2.15.3.Quantitative RT PCR (qRT PCR)

TaqMan gene expression Assay was utilized for the qRT PCR analysis. The sensitivity of Real-time PCR systems has been increased by the insertion of fluorogenic labeled probes utilizing the 5' nuclease activity of the Taq DNA polymerase. The qRT PCR reaction was performed in 96 well PCR plates (Applied Biosystems) sealed with a transparent heat Sealing film and ran in AB7500 fast system according to the following protocol.

Ingredient	Volume
Probe mix Lo-ROX	5 µl
TaqMan(R) probe	0.5 µl
RNase free water	3.5 µl
cDNA (derived from RevertAid RT Reverse Transcription Kit)	1 µl

Cycles	Temperature (°C)	Time
Initial denaturation	95°C	120 sec

Denaturation	95°C	5 sec
Polymerization and signal generation	62°C	30 sec

The changes in the gene expression were analyzed by relative quantification of the mean Ct value of a housekeeper gene that served as a reference. With the help of the reference gene, the relative expression of cDNA was calculated by the $2^{-\Delta\Delta CT}$ formula.

4.2.16. Biotin pull-down assay

Biotin labeling of proteins or nucleic acids is often used to specifically enrich proteins bound to labeled baits. The underlying principle is based on the fact that Biotin has a strong affinity to avidin and streptavidin, which is directly coupled to immobilized columns or beads. Biotin maleimide has become a widely used method for non-radioactive labeling of proteins and nucleic acids. Since it is a robust and sensitive technique, it is widely used for a large variety of biochemical applications such as RNA pull-down assays.

4.2.16.1. Linearization of plasmid DNA

For linearization 5 µg of the plasmid DNA was subjected to digestion by choosing the *BamH*1 restriction site, which is located within the polylinker region of the pCR2.1-5'-UTR-caspase-2 plasmid and upstream of the T7 promoter binding sequence. The reaction mixture constituted the following components.

1 µl of *BamH*1 (10 U/µl)

2 µl 10 x buffer

5 µg of plasmid DNA,

Adjust to a final volume of 20 µl with aqua bidest

The reaction was incubated for 1 h at 37°C before the linearization was confirmed by loading 1/10 of the reaction mixture onto a 1% agarose gel.

4.2.16.2. Synthesis of mRNA by *in vitro* transcription

In vitro RNA transcription of the linearized template, DNA was generated by using the RiboMAX large Scale RNA production system kit (Promega). According to the manufacturer´s instructions, the following reagents were added.

20 µl 5 x transcription buffer

30 µl ribonucleoside triphosphate (rNTPs) mix

5 µg of linearized plasmid

10 µl T7 RNA polymerase enzyme mix

The final volume was adjusted to 100 µl with DEPC water. The reaction mixture was added with 5 µl RQ1 RNase free DNase (1 U/µg) and incubated at 37°C for 3 h. Thereafter, the RNA was isolated by employing LiCl precipitation as followed:

12.5 µl of LiCl (4M)

375 µl absolute ethanol (ice cold)

100 µl *in vitro* transcribed RNA

All components were vortexed and precipitated overnight at -80°C. The next day, the RNA was isolated by centrifugation at 13.000 rpm (11.000 x g) for 20 mins, and subsequently, the RNA pellet was washed with 70% ethanol. The pallet was dried at 37°C for 5 min and resuspended in 2 µl of DEPC water. The RNA concentration was determined by using a Nanodrop spectrophotometer.

4.2.16.3. Biotinylation of RNA

The synthesized RNA was labeled with biotin by using the 5' End labeling system Kit (Vector Laboratories). The reaction components were mixed according to the manual of the kit as followed:

1 µl of universal reaction buffer

1 µl alkaline phosphatase

60 µg of RNA

The final volume was adjusted to 10 µl deionized H_2O. The reaction mixture was incubated for 30 min at 37°C. Thereafter, the components were added in the following order:

2 µl universal reaction buffer

1 µl ATPγS

2 µl T4 polynucleotide kinase

Deionized water was added to a total volume of 20 µl. The reaction mixture was incubated for 30 min at 37°C. After that, 10 µl of Biotin Maleimeide was added, and the whole mixture was kept at room temperature for a further 2 h.

4.2.16.4. Pull down reaction

The streptavidin-coupled agarose beads were washed thrice with 0.5 ml of **R**NA-**i**ncubation **b**uffer (RIB). After that, the precleaned beads were incubated with 15 µg of the biotinylated RNA at 4°C for 2 h under continuous rotation. Subsequently, 300 µg of total or cytoplasmic cell lysates were added to the beads before the volume was adjusted to 500 µl with RIB. The reaction was kept at 4°C for 1 h under continuous rotation. Thereafter, the mixture was centrifuged at 3.000 rpm (2.000 x g) for 2 min, and the supernatant was removed. The beads were washed three times with cold RIB, and the last traces of wash buffer were removed by using the Hamilton syringe. Dried beads were resuspended with 35 µl of 4 x Laemmli buffer and heated for 10 min at 95°C. The beads were centrifuged at 10.000 rpm (7.000 x g) for 2 min, and the supernatant loaded on PAGE SDS gels and analyzed by Western blot analysis using TRIM25 specific antibodies.

4.2.17. Polysomal fractionation

The first day, 5.5 x 10^5, cells were seeded on a 60 mm dish containing 2 ml of antibiotics free DMEM and 10% FCS. The next day, the cells were transfected with a mixture of siRNA

oligonucleotides and oligofectamine (Invitrogen), as described in section 4.2.4. After that, the transfected cells were kept for 48 h. Before harvesting, the cells were treated with cycloheximide (CHX, 25µg/ml) for 15 min and later washed once with 1 ml of ice-cold PBS. Subsequently, the cells were added with 1 ml of ice-cold PBS/EDTA (5mM) and scarped on ice. Cell suspensions were centrifuged at 6.500 rpm (5.000 x g) for 5 min, and the supernatants were removed before the pellets were resuspended in a Polysomal lysis buffer. After that, the protein concentrations of the samples were determined as described in 4.2.8. 1 ml of sucrose cushion buffer was added along with 1 mg of lysate to Beckman Coulter (#343778) tubes. The tube was adjusted using a weight balance before being applied to ultracentrifugation at 48.000 rpm for 2 h at 4°C. The supernatant was collected in a fresh Beckman Coulter tube and subjected to the second centrifuge at 83.000 rpm for 3 h at 4°C. The pellet containing the polysomal fraction was dissolved in 100 µl of PUB buffer, and RNA isolated by using the Trizol. The supernatant from the second centrifugation step was discarded, and the pellet containing RNP fractions was dissolved in 100 µl of PUB buffer, and RNA was isolated as described in 4.2.12. RNA from both fractions was quantified using a NanoDrop Spectrophotometer by measuring the absorbance at OD_{260} and OD_{280} nm, respectively. After cDNA synthesis, individual mRNAs contents were measured by semiquantitative RT-PCR using GoTaq hot-start polymerase and by Real-Time PCR (qRT PCR) as described in sections 4.2.14 and 4.2.15, respectively.

Polysomal lysis buffer

Substance	Final concentration	Amount
NaCl	50 mM	5 ml 1M
Tris/HCl, pH 7.4	50 mM	5 ml 1M

EDTA, pH 8.0	2 mM	0.4 ml 0.5 M
EGTA, pH 8.0	2 mM	0.4 ml 0.5 M
Glycerol	10%	10 g
Triton X-100	1%	1 g
Aqua bidest.		100 ml (adjusted volume)

A mixture of inhibitors containing 1x of "Complete Protease inhibitor (25x)'' and for inhibition of protein phosphatases, Na_3VO_4 (final 1 mM) and NaF (final 1 mM) was added freshly before use.

Sucrose Cushion Buffer

Substance	Final concentration	Amount
Tris/HCl, pH 7.4	50 mM	12.5 ml 1M
$MgCl_2$	5 mM	1.25 ml 1 M
KCl	20 mM	6.25 ml 1 M
Sucrose	2M	171.2g
KCl	20 mM	6.25 ml 1 M
Aqua bidest.		250 ml (adjusted volume)

PUB Buffer

Substance	Final concentration	Amount
NaCl	50 mM	2 ml 1M
Tris/HCl, pH 7.4	50 mM	0.5 ml 1M
EDTA, pH 8.0	2 mM	1 ml 0.5 M
SDS	20%	2.5 ml
Aqua bidest.		50 ml (adjusted volume)

4.2.18. Statistical analysis

Software	
Imaging processing	ImageJ 1.41, Wayne Rasband
	ZEN 2009 Software, Carl Zeiss, Jena
	Quantity One, BIO-RAD Laboratories Inc.
	CorelDraw Graphics Suite X4, Coral, Ottawa
Graphs	Graph Pad Prism 5, Graph Pad Software Inc.
Presentations	Microsoft Office Powerpoint 2010
Protein measurement	Tecan Magellan 7.2
Calculation tables	Microsoft Office Excel 2010
Text writing	Microsoft Office Word 2010
FACS data analysis	BD FACS Diva (TM) software

Data were represented as means ± standard deviations (SD). All analyses and graphs were performed using Graph Pad Prism. Significance was tested by student's T-test or one way ANOVA, and P values < 0.05 were considered statistically significant.

5. AIM OF THE STUDY

By using RNA affinity chromatography, our research group has previously identified the tripartite motif-containing protein 25 (TRIM25) as a bona fide caspase-2 mRNA binding protein in colon carcinoma cells. The main objective of this study was to investigate the impact of TRIM25 on caspase-2 expression and the identification of underlying mechanisms. Furthermore, the functional impact of TRIM25 on caspase-2 was elucidated by loss of function and gain of function experiments. Based on the knowledge that caspase-2 downregulation is part of a cell survival pathway in colon carcinoma cells, I further tested whether RNAi-mediated silencing or alternatively, the ectopic expression of TRIM25 has any impact on the sensitivity of human colon carcinoma cells towards chemotherapeutic drug-induced apoptosis.

Results from this study should provide novel mechanistic insights into the apoptosis regulatory activity of the E3 ligase TRIM25, which could be relevant for therapy resistance of tumor cells. Targeting of TRIM25 may, therefore, represent a novel therapeutic option to increase the efficacy of clinically used cancer therapies.

6. RESULTS

6.1. Identification of TRIM25 as a novel caspase-2 mRNA-binding protein

Previously, our group identified a novel cell survival mechanism through which the translation of the pro-apoptotic caspase-2L is constitutively inhibited by the ubiquitous mRNA-binding protein **h**uman **a**ntigen **R** (HuR) in different human colon carcinoma cell lines (Winkler *et al.* 2014; Badawi *et al.* 2017; Badawi *et al.* 2018). Thereby, HuR does mainly interfere with the IRES-dependent translation of caspase-2 through direct interaction with the 5'UTR of the mRNA (Badawi *et al.* 2018). As already described in the introduction part, the IRES-mediated translation is controlled by several canonical initiation factors that act in concert with accessory proteins summarized as "**I**RES **t**rans-**a**cting **f**actors" (ITAFs). To identify other caspase-2 translation regulatory proteins, streptavidin-tethered RNA affinity chromatography in combination with **l**iquid **c**hromatography/**m**ass **s**pectrometry (LC/MS) was utilized (in collaboration with the functional proteomic core unit of the Goethe University Frankfurt). To discriminate between RNA-binding proteins, which mainly associate with the coding region of caspase-2 mRNA or those which exclusively bind to the 5'UTR of caspase-2 for affinity chromatography, biotin-labeled *in vitro* transcribed mRNAs containing either the 5'-UTR or the **c**o**d**ing **r**egion (cdr) of caspase-2 were used as baits. The proteins derived from total cell homogenates of DLD-1 bound exclusively to the different biotin-labeled RNAs were evaluated by mass spectrometry. The analysis of peptides with Uniprot human reference proteome database revealed that along with several eukaryotic translation initiation factors and some renowned RNA-binding proteins such as HuR, **h**eterogeneous **n**uclear **r**ibo**n**ucleo**p**rotein A1

(hnRNPA1) and **p**olypyrimidine **t**ract **b**inding **p**rotein 1 (PABP1), the **tri**partite **m**otif-containing protein (TRIM) 25, synonymously **e**strogen-**r**esponsive **f**inger protein (Efp), was identified as a protein which bound exclusively to the 5'UTR of caspase-2 mRNA but not with cdr. To validate the results from mass spectrometry, I performed RNP-IP by TRIM25 immunoprecipitation. Thereby, DLD-1 cells showed significant and robust binding of TRIM25 to caspase-2 mRNA, as indicated by the amplification of cDNA from TRIM25 antibody-associated RNA **(Fig. 5A)**. To test the specificity of TRIM25 binding, IgG was used as a control. In contrast to TRIM25 IP, mouse IgG failed to produce appropriate amplicons demonstrating a faint affinity of IgG towards caspase-2 mRNA **(Fig. 5A)** (Nasrullah *et al.* 2019). Furthermore, Western blot analysis affirmed the specific binding of the antibody used for RNP-IP. The binding of endogenous TRIM25 to caspase-2 mRNA was also demonstrated in another colon carcinoma cell line RKO, thus indicating that the binding of TRIM25 is not a cell-type-specific phenomenon **(Fig. 5B)** (Nasrullah *et al.* 2019).

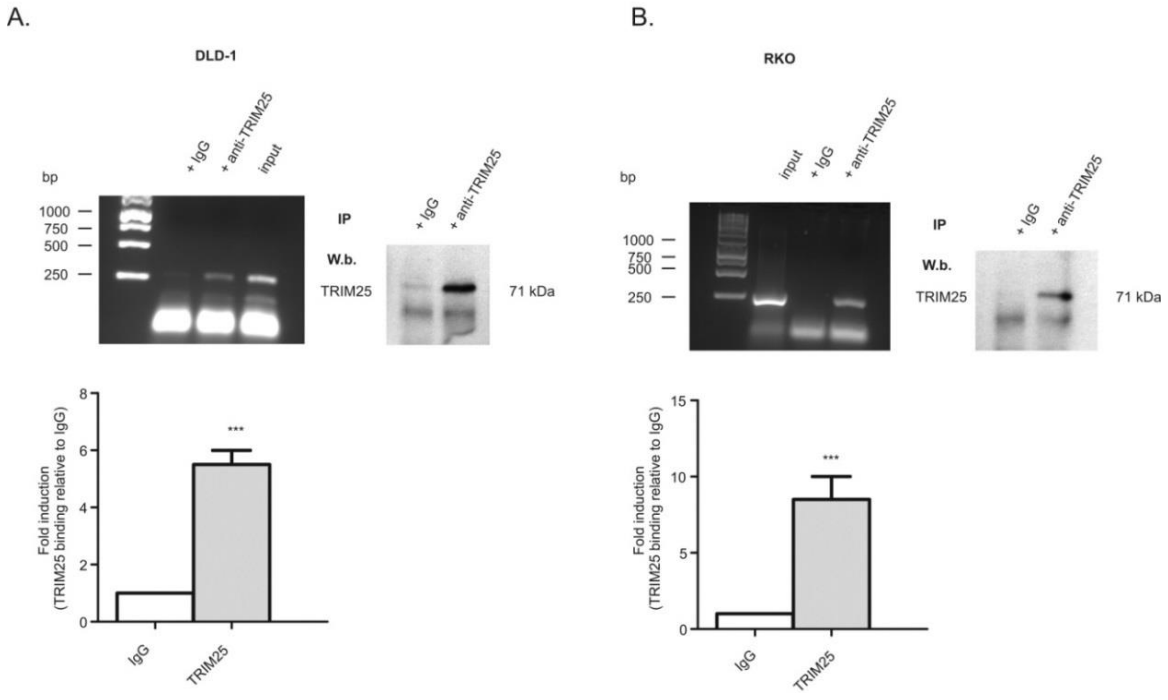

Figure 5. **TRIM25 is a bona fide mRNA-binding protein of caspase-2 in the human colorectal cell lines**, DLD-1 **(A)** and RKO **(B)**. The total cell lysates of colon carcinoma cells were used for RNP-IP assays and followed by RT-PCR. The precipitation of TRIM25-bound mRNA was carried out by the addition of monoclonal TRIM25-specific antibodies (anti-TRIM25) or, alternatively, the equivalent amount of mouse IgG (IgG) as a negative control. The precipitated RNA samples were used for semiquantitative RT-PCR using primer sets encompassing the coding region of caspase-2. The specificity of immunoprecipitation (IP) of TRIM25 in both cell lines was validated by using Western blot analysis, as shown on the right-hand panel. The Input levels of caspase-2 mRNA were also monitored by RT-PCR (input). Graphs shown in the lower parts of the panels represent means ± SD (n = 3) and illustrate the relative caspase-2 binding to TRIM25 (filled bars) in relation to IgG (empty bars). *** $p \leq 0.001$ vs. IgG.

6.2. TRIM25 negatively interferes with caspase-2 translation

6.2.1. Gain of function approach

In the next approach, I tested whether a similar way as reported for HuR-caspase-2 mRNA interactions (Winkler *et al.* 2014), the binding of TRIM25 to caspase-2 mRNA could affect the protein expression of caspase-2. For this purpose, I employed gain of function experiments. For overexpression of TRIM25, colon carcinoma cells were transiently transfected with different amounts of pFLAG-CMV-TRIM25 vector coding for Flag-tagged TRIM25. Thereby, the highest expression of TRIM25 was obtained with 6 µg of plasmid DNA **(Fig. 6A)**. Notably, due to higher transfection efficiencies, the following gain of function experiments was performed in RKO cells. Interestingly, the increase in TRIM25 protein was accompanied by a reduction in caspase-2 levels. In comparison, the transfection of the same amount of empty vector (pCMV-Flag) failed to impact the protein content of caspase-2 **(Fig. 6B)** (Nasrullah *et al.* 2019). In contrast, although the ectopic expression of TRIM25 in HEK cells leads to a robust increase in TRIM25 protein levels, the content of caspase-2 protein remained unchanged **(Fig. 6C)** (Nasrullah *et al.* 2019). These data implicate that besides HuR, TRIM25 may constitute another negative regulator of caspase-2 in colon carcinoma cells.

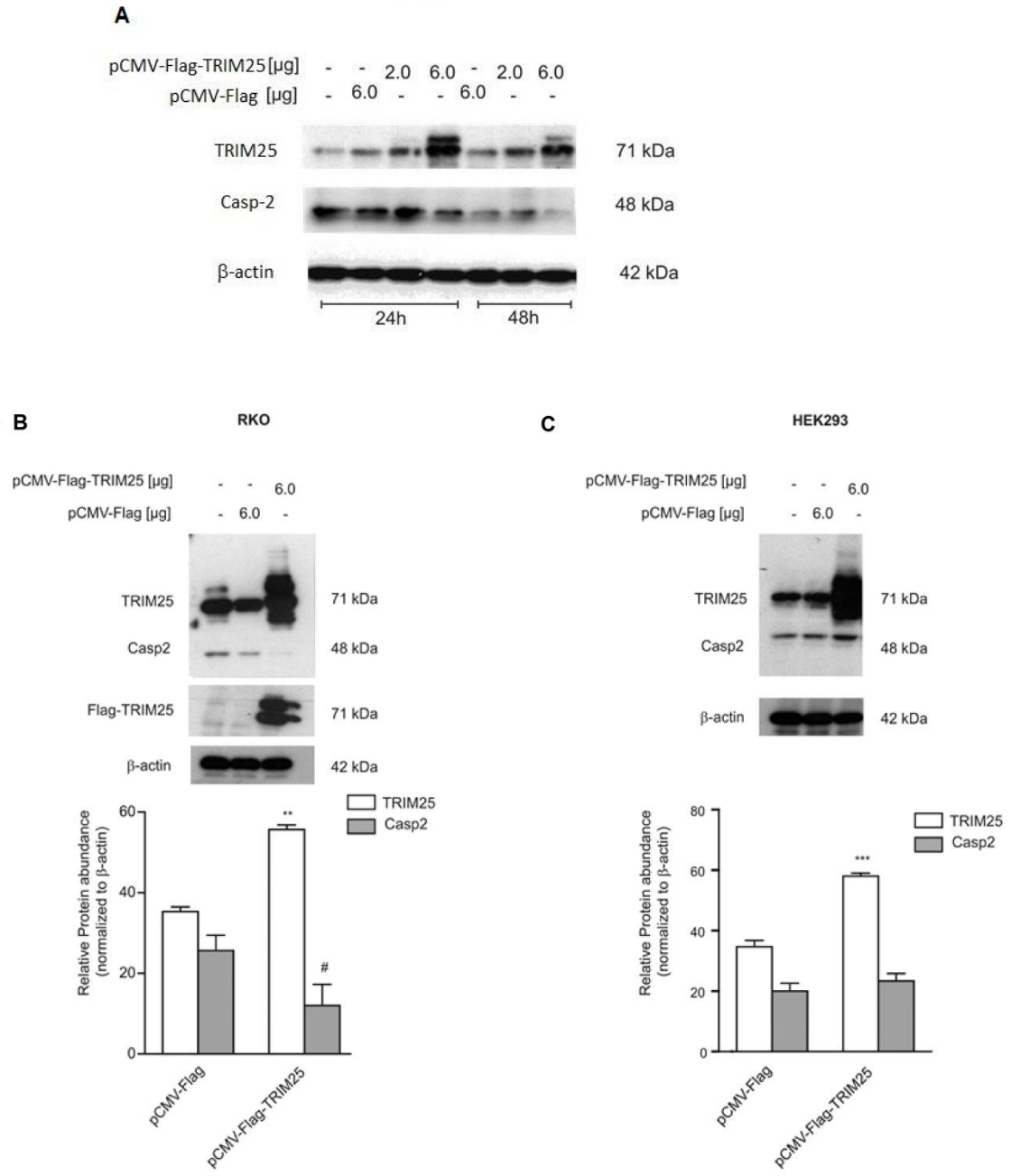

Figure 6. The ectopic expression of TRIM25 decreases caspase-2 protein levels in colon carcinoma cells. Subconfluent RKO **(A)** cells were either transfected with 6 µg of empty pCMV-Flag vector (pCMV-Flag) or with 2 µg or 6 µg of Flag-tagged human TRIM25 (pCMV-Flag-TRIM25) respectively for the period of 24 h and 48 h before cells were harvested for total cell extracts. 20 µg of total cell lysates were analyzed by Western blot for the detection of TRIM25 and caspase-2, and β-actin was used as a loading control. Data represent two independent experiments with similar results. Subconfluent RKO **(B)** or HEK293 **(C)** cells either mock-transfected (-) or transfected with the designated amount of Flag-tagged human TRIM25 (pCMV-Flag-TRIM25) or, alternatively, with the equivalent amount of empty pCMV-Flag vector (pCMV-Flag). Subsequently, 48 h post-transfection, the amounts of endogenous and ectopic TRIM25 as well as caspase-2 were monitored by Western blot analysis with β-actin was used as a loading control. The graphs at the bottom indicate means ± SD (n = 3) and depict the relative abundance of TRIM25 (empty bars) and caspase-2 (filled bars) protein levels in both transfected cell populations. ** $p \leq 0.005$, *** $p \leq 0.001$ (TRIM25), and # $p \leq 0.05$ (Casp2), respectively, vs. empty vector-transfectants.

6.2.2. TRIM25 is a potential target of auto-ubiquitination

Based on the observation that ectopic expression of TRIM25 revealed different immunopositive bands, I questioned for the origin of these differentially migrating bands. The upper band with the lowest migration properties was seen with endogenous TRIM25 and with ectopic TRIM25 protein **(Fig. 6B).** The fact that this low migrating band was not observed in the lysates derived from untreated HEK cells indicates that it may originate from a cell-type-specific posttranslational modification **(Fig. 6C)**. This issue was further addressed by performing Western blot analysis with an anti-Flag-specific antibody **(Fig. 6B)**. Thereby, I found that both upper bands were recognized by the anti-Flag antibodies indicating that they originate from TRIM25. In clear contrast, the fast migrating band was not recognized by the anti-flag-specific antibodies suggesting that it may either represent an unspecific protein or results from a TRIM25 degradation product devoid of the Flag-tag. Since the distance of both Flag-positive bands was approximately between 5-8 kDa, it was tempting to speculate that the upper band may represent ubiquitination since ubiquitin itself has a molecular weight of about 8.0 kDa. Immunoprecipitation of endogenous TRIM25 and subsequent Western blot analysis with either TRIM25 or a ubiquitin-specific antibody revealed a ubiquitin-positive band at 79 kDa, which migrated higher than the TRIM25 positive signal at 71 kDa **(Fig. 7).** These data suggest that TRIM25 is a putative target of mono-ubiquitination. However, further experiments are needed to investigate the possible functional consequences of this specific post-translational modification of TRIM25, especially whether it is relevant for TRIM25 affinity to the caspase-2 mRNA.

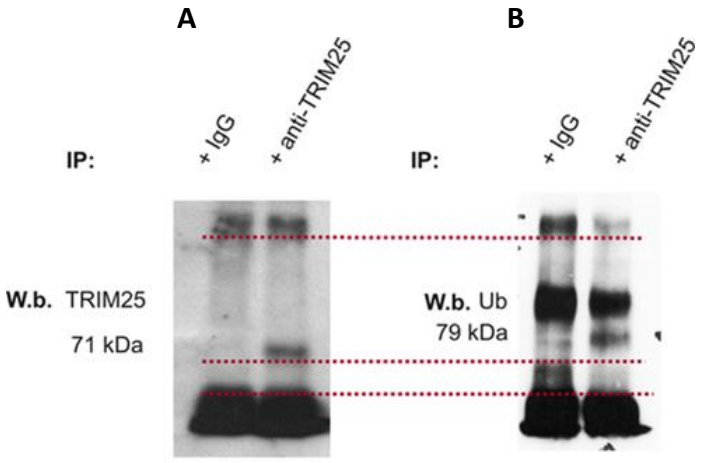

Figure 7. **TRIM25 is a target of mono-ubiquitination**. Subconfluent RKO cells were harvested, and total protein extracts were subjected to IP with antibodies specific for either TRIM25 or species-specific control IgG. **(A)** samples were subjected to SDS-PAGE and immunoblotted with anti-TRIM25 to validate the specificity immunoprecipitation (IP) or, alternatively **(B)** with anti-ubiquitin antibody to recognize ubiquitination.

6.2.3. Loss of function approach

Besides, to gain of function, a loss-of-function approach was used to confirm an inverse correlation between both proteins. Based on our previous observations that forced upregulation of caspase-2 by HuR is only a transient phenomenon probably because of some unknown compensatory mechanisms activated in tumor cells, I chose a transient silencing approach. Monitoring of knockdown efficiency revealed a robust and stable decrease in TRIM25 protein levels upon transfection of 25pg of gene-specific siRNA duplexes in both colon carcinoma cell lines tested **(Fig. 8A, B)** (Nasrullah *et al.* 2019). In contrast, no effects on protein expression of TRIM25 were noticed after the transfection of cells with scrambled siRNAs (siCtrl.) **(Fig. 8A, B)**. Conversely to the effects from overexpression experiments, caspase-2 levels showed a time-dependent increase upon silencing of TRIM25 **(Fig. 8A, B)**, with the modulatory effect was most apparent at 48 h after siRNA transfection **(Fig. 8C, D)** (Nasrullah *et al.* 2019).

Notably, the protein content of caspase-2 dropped substantially after culturing for 72 h. A similar induction of caspase-2 protein upon TRIM25 silencing was observed when I used siRNA duplexes subjected to another sequence of TRIM25, which clearly indicates that induction of caspase-2 is not due to off-target effects **(Fig. 8E, F)** (Nasrullah *et al.* 2019).

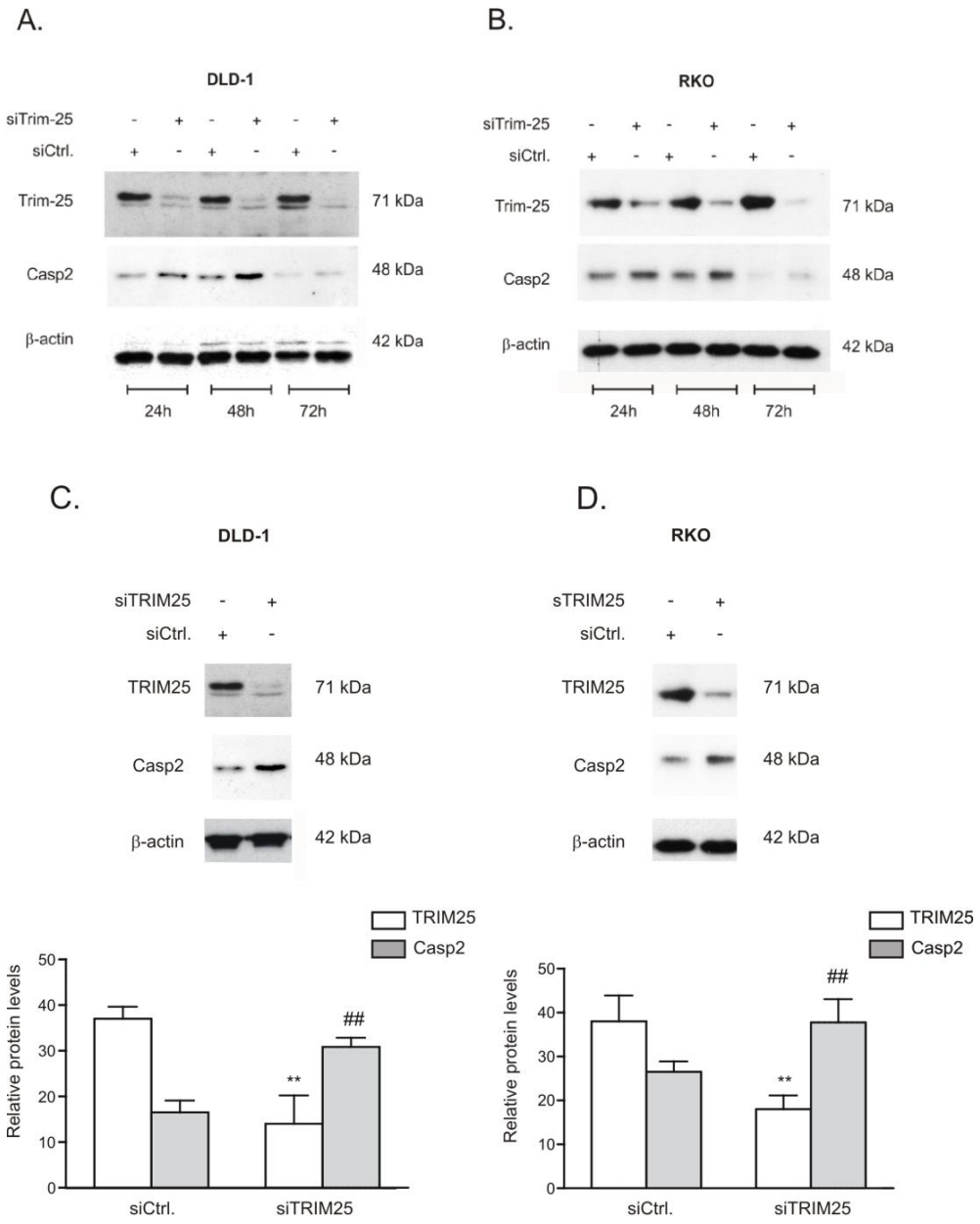

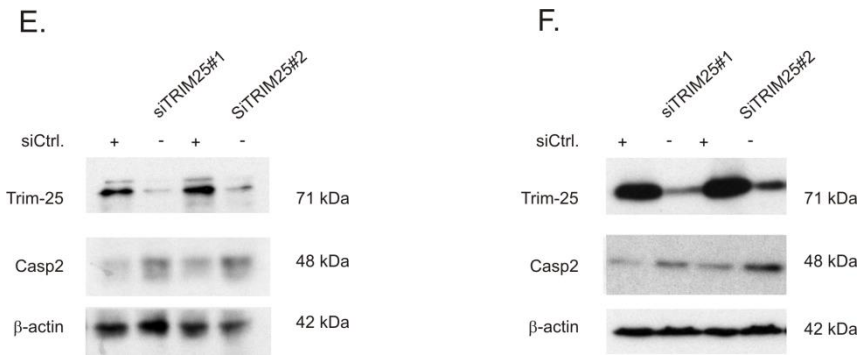

Figure 8. The silencing of TRIM25 increases caspase-2 protein levels in colon carcinoma cell lines. The subconfluent DLD-1 **(A)** or RKO **(B)** cells were transfected with control siRNA duplexes (siCtrl.) or with siRNA duplexes of TRIM25 (siTRIM25) for the indicated time periods. Subsequently, cells were harvested, and total protein lysates (20 µg) were subjected to SDS-PAGE. The abundance of TRIM25 and caspase-2 was analyzed by Western blot analysis, and β-actin was used as a loading control Data shown are representative for three independent experiments giving similar results. Subconfluent DLD-1 **(C)** or RKO **(D)** cells were transfected with control siRNA duplexes (siCtrl.) or with siRNA duplexes of TRIM25 (siTRIM25). Then, 48 h post-transfection, cells were harvested for total protein extracts. 20 µg of total cell homogenates were subjected to SDS-PAGE and probed with anti-TRIM25, anti-caspase-2, and anti-β-actin, respectively. Values in the graphs at the bottom show means ± SD (n = 3) and depict the relative protein levels of TRIM25 (empty bars) and caspase-2 protein (filled bars). ** $p \leq 0.005$, (TRIM25) and ## $p \leq 0.005$ (Casp2), respectively, vs. control siRNA-transfected (siCtrl.) cells (Nasrullah et al. 2019). The increased levels of caspase-2 caused by TRIM25 silencing in DLD-1 **(E)** and RKO **(F)** cells were analyzed after 48 h of siRNA transfection and validated with two separate sets of siRNA duplexes complementary to distinct regions of the TRIM25 mRNA (siTRIM25#1 and siTRIM25#2) as described in the section 4.1.9.

6.2.4. Effect of TRIM25 silencing on caspase-2 mRNA abundance

To further test whether silencing of TRIM25 would additionally affect the steady-state mRNA levels of caspase-2, I performed quantitative PCR. As expected, time-dependent silencing of TIRM25 also occurred on the mRNA level **(upper panels Fig. 9A, B)** (Nasrullah *et al.* 2019). In contrast to the substantial changes in TRIM25 mRNA, there was no significant change in caspase-2 mRNA levels independent of which time point and of which cell line was assessed **(lower panels of Fig. 9A, B)** (Nasrullah *et al.* 2019)**.** Collectively, these data indicate a negative regulation of caspase-2 by TRIM25 exclusively on the protein level.

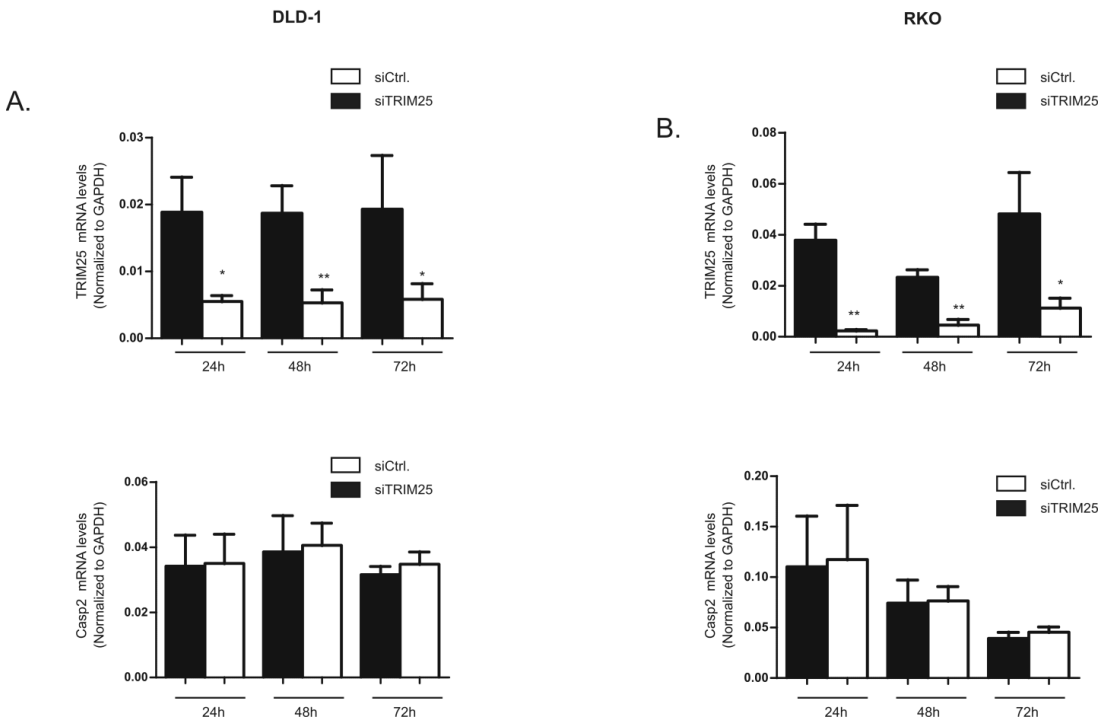

Figure 9. **Time-course of TRIM25 (upper panels) and caspase-2 (lower panels) mRNA levels after transient RNAi-mediated TRIM25 knockdown**. DLD-1 **(A)** or RKO **(B)** cells were transiently transfected with control duplexes (siCtrl.) or with siRNA duplexes of TRIM25 (siTRIM25) for the indicated periods before cells were harvested and extracted for total cellular RNAs. The changes in steady-state TRIM25 mRNA (black bars) and caspase-2 mRNA (white bars) were evaluated by quantitative PCR in relation to GAPDH steady-state mRNA levels. Data represent means ± SD (n = 3), * $p \leq 0.05$, ** $p \leq 0.01$ siCtrl. cells vs. siTRIM25-transfected cells**.**

6.3. Elevation in caspase-2 protein upon transient knockdown of TRIM25 depends on *de novo* protein synthesis

Next, I investigated whether the increase in caspase-2 upon TRIM25 silencing is either due to an enhanced translation or due to increased stability of the caspase-2 protein. For this purpose, a series of experiments were conducted with cycloheximide, an antibiotic derived from *Streptomyces griseus,* which interferes explicitly with eukaryotic translation. Thereby, 24 h post-transfection of siRNAs (siCtrl. or siTRIM25), cycloheximide was added, and cells harvested after different periods. Monitoring the time-course of caspase-2 protein contents after the

application of cycloheximide revealed a clear and significant suppressive effect by cycloheximide mainly at 24 h **(Fig. 10A)** (Nasrullah *et al.* 2019). In contrast, the levels of TRIM25 were not influenced by cycloheximide in DLD-1 cells, thus implicating high stability of the TRIM25 protein **(Fig. 10B)** (Nasrullah *et al.* 2019). Similar results were observed in the human colon carcinoma cell line RKO **(Fig. 10C)** (Nasrullah *et al.* 2019). These results clearly indicate that TRIM25 silencing-induced rise in caspase-2 protein depends on *de novo* protein synthesis but not via increased protein stability.

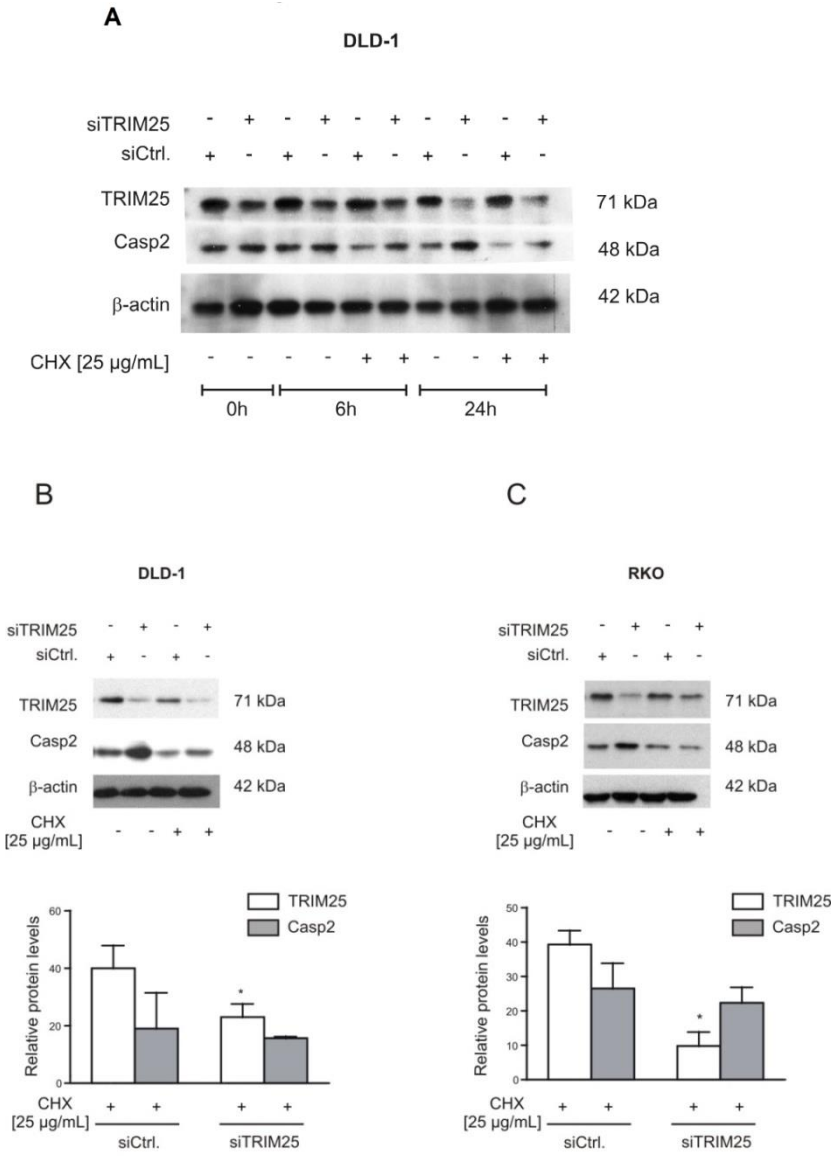

Figure 10. The increase in caspase-2 protein levels by TRIM25 knockdown depends on *de novo* synthesis. The subconfluent DLD-1 **(A)** cells were transfected with control siRNA duplexes (siCtrl.) or with siRNA duplexes of TRIM25 (siTRIM25) for 24 h before the translation was blocked by the addition of cycloheximide (CHX, 25 µg/ml) (0 h). After the indicated periods, cells were harvested, and total protein lysates (20 µg) were subjected to SDS-PAGE and probed with anti-TRIM25, anti-caspase-2, and anti-β-actin, respectively. Data represent two independent experiments with similar results. The subconfluent DLD-1 **(B)** or RKO **(C)** cells were transfected with control duplexes (siCtrl.) or with siRNA duplexes of TRIM25 (siTRIM25) for 24 h before the translation was blocked by the addition of cycloheximide (CHX, 25 µg/mL). The cells were harvested for total protein extraction after an additional 24 h. The abundance of TRIM25 and caspase-2 was analyzed by Western blot analysis, with β-actin used as a loading control. Graphs at the lower panels show means ± SD (n = 3) and represent the relative protein levels of TRIM25 (empty bars) and caspase-2 (filled bars) * $p \leq 0.05$ (TRIM25) vs. control siRNA-transfected (siCtrl.) cells.

6.4. TRIM25 silencing induces a redistribution of caspase-2 mRNA from RNPs to polysomes

The hypothesis that TRIM25 binds to the 5' UTR of caspase-2 mRNA and thereby may influence the translation of caspase-2 mRNA was validated by the use of polysomes/RNP fractionation experiments. To test whether siRNA mediated knockdown of TRIM25 would affect the occupancy of polyribosomes with caspase-2 mRNA as a read-out for caspase-2 translational active polysomes. Thereby, total lysates from siRNA transfected DLD-1 cells were layered on a sucrose gradient for separation of polysomes from translational inactive RNP particles through ultracentrifugation. Instead of separating panels of diverse polysomal fractions, a protocol for crude separation of only two fractions was chosen due to the limited yield of input material. Results from these experiments revealed a significant increase in the polysome-to-RNP ratio of caspase-2 mRNA abundance relative to GAPDH mRNA, which indicates a shift of caspase-2 mRNA distribution from RNPs to polysomes under TRIM25 depleted conditions **(Fig. 11)** (Nasrullah *et al.* 2019). Together, these results suggest that in DLD-1 cells, TRIM25 interferes negatively with the translation of caspase-2.

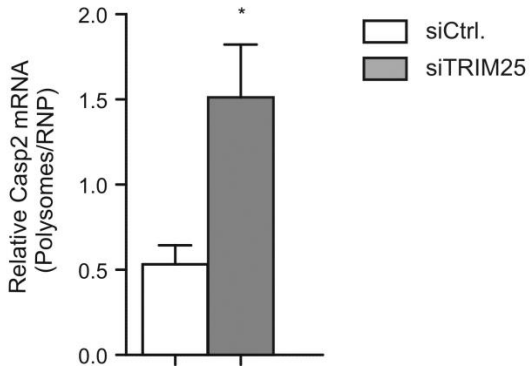

Figure 11. TRIM25 knockdown caused a significant accumulation of caspase-2 mRNA in the translationally active polysomes. Subconfluent DLD-1 cells were transfected with control siRNA duplexes (siCtrl.) or with siRNA duplexes of TRIM25 (siTRIM25) for 48 h, and the fractions of translational inactive RNPs were segregated from translational active polysomes by employing sequential ultracentrifugation. The caspase-2 mRNA content was determined by qRT-PCR using primer pairs complementary to the coding region of caspase-2. The graph shows means ± SD (n = 3) and represent the amount of caspase-2 mRNA levels normalized to GAPDH mRNA in polysomes in relation to those in RNP fractions from control siRNA (empty bars) and TRIM25 siRNA-transfected cells (filled bars) * $p \leq 0.05$ (TRIM25) vs. control siRNA-transfected (siCtrl.) cells.

6.5. TRIM25 silencing sensitizes colon carcinoma cells to drug-induced apoptosis

Based on the functional role of caspase-2 in DNA damage-induced cell death (Badawi et al., 2017, 2018), in the next set of experiments, I tested for any functional consequences of TRIM25 silencing by monitoring drug-induced apoptosis. First, intrinsic apoptosis was monitored by cleavage of caspase-3 and -7, which both caspases act as primary effector caspases, e.g., in the induction of DNA-damage induced apoptosis. Before analyzing for caspase activation after the TRIM25 silencing, I compared the apoptosis sensitivity toward different chemotherapeutic drugs in two different colon carcinoma cell lines. First, the clinically established antitumor compounds with different modes of action, including doxorubicin, an inhibitor of topoisomerase-II, and paclitaxel, a stabilizer of microtubule, were applied at different doses and in time-course experiments, respectively. Importantly, a clear drug-induced caspase-3 cleavage in the two

colon carcinoma cell lines, DLD-1 (**Fig. 12A, B**) (Badawi *et al.* 2018) and RKO (**Fig. 12C, D**) (Badawi *et al.* 2018), were only found with doxorubicin. Since paclitaxel failed to produce a substantial increase in cleavage of caspase-3 three other chemotherapeutics including the alkylating compound cisplatin (CDDP), the nucleotide analog 5'-fluorouracil (5´FU) and etoposide (Etopo.) another topoisomerase inhibitor were tested in RKO cells **(Fig. 12 E)**.

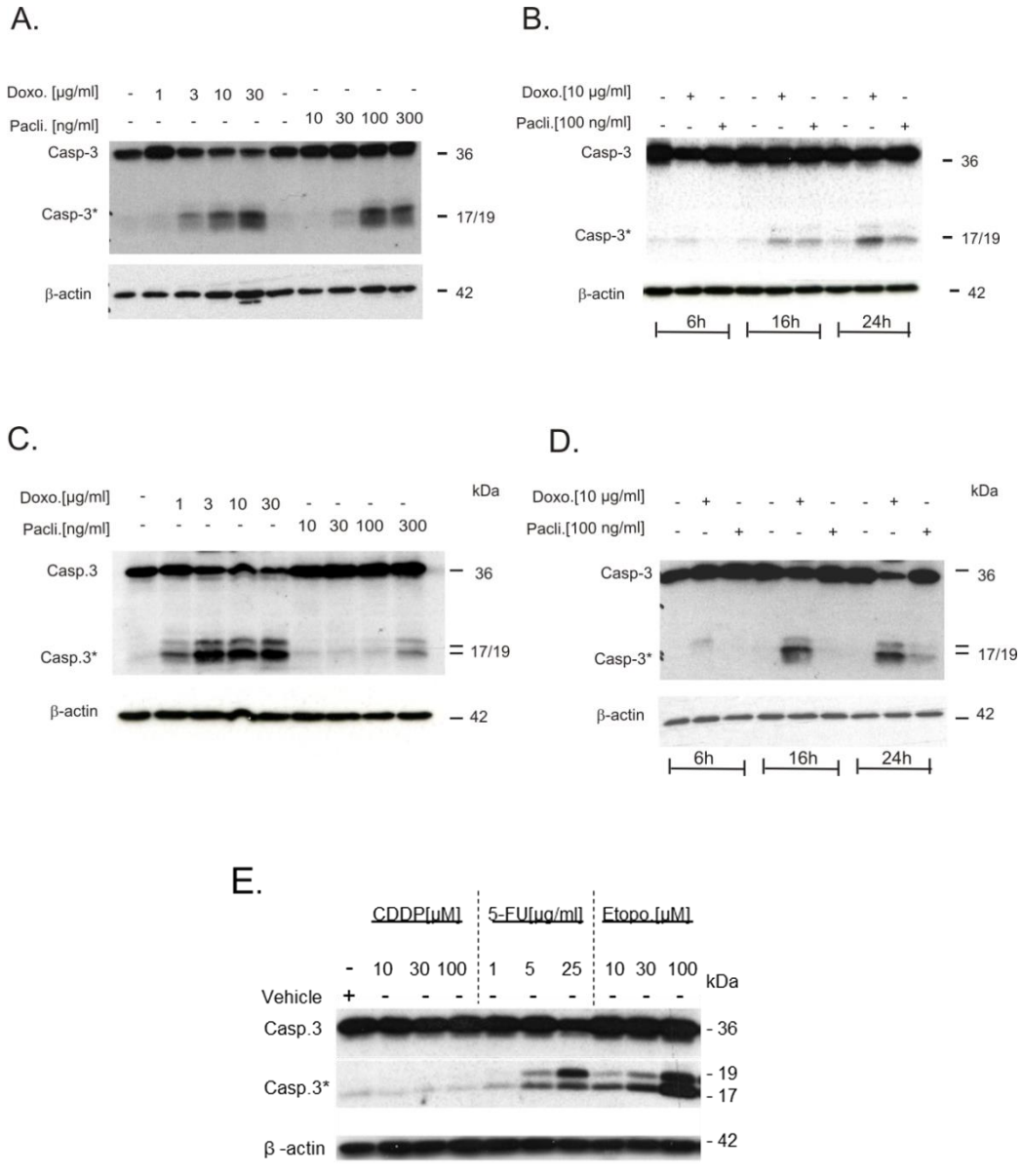

Figure 12. Concentration and time-dependent induction of caspase-3 cleavage. (A) DLD-1 cells were stimulated for the indicated doses of doxorubicin (Doxo.) or paclitaxel (Pacli.) for 24 h. The cells were harvested, and equal amounts of protein (20 µg) from total cell lysates were subjected to SDS-PAGE and successively immunoblotted with anti-caspase-3 and anti-β-actin antibodies, respectively. The cleaved caspase-3 (Casp-3*) at 19 and 17 kDa are represented by an asterisk symbol. **(B)** DLD-1 cells were stimulated with doxorubicin (Doxo.) or paclitaxel (Pacli.) for indicated time periods. Subsequently, cells beings harvested for total protein lysates were assessed by Western blot analysis as 20 µg of total cell homogenates were subjected to SDS-PAGE and successively immunoblotted with anti-caspase-3 and anti-β-actin antibodies, respectively. An asterisk symbol depicts the cleavage products of pro-caspase-3 (Casp-3) at 19 and 17 kDa by (Casp-3*). Data represent three independent experiments with similar results. **(C)** RKO cells were stimulated for the indicated doses of doxorubicin (Doxo.) or paclitaxel (Pacli.) for 24 h. The cells were harvested, and equal amounts of protein (20 µg) from total cell lysates were subjected to SDS-PAGE and successively immunoblotted with anti-caspase-3 and anti-β-actin antibodies, respectively. The cleaved caspase-3 (Casp-3*) at 19 and 17 kDa are represented by an asterisk symbol. **(D)** RKO cells were stimulated with doxorubicin (Doxo.) or paclitaxel (Pacli.) for indicated time periods. Subsequently, cells beings harvested for total protein lysates were assessed by Western blot analysis as 20 µg of total cell homogenates were subjected to SDS-PAGE and successively immunoblotted with anti-caspase-3 and anti-β-actin antibodies, respectively. An asterisk symbol depicts the cleavage products of pro-caspase-3 (Casp-3) at 19 and 17 kDa by (Casp-3*). Data represent three independent experiments with similar results. **(E)** Dose-dependent induction of caspase-3 cleavage of chemotherapeutic drugs. RKO cells were stimulated for the indicated doses of cisplatin (CDDP) or 5'-FU or etoposide (Etopo.) for 24 h. The cells were harvested, and equal amounts of protein (20 µg) from total cell lysates were subjected to SDS-PAGE and successively immunoblotted with anti-caspase-3 and anti-β-actin antibodies, respectively. The cleavage products of pro-caspase-3 (Casp-3) at 19 and 17 kDa are depicted by an asterisk symbol (Casp-3*). Data shown are representative of two independent experiments giving similar results.

Besides doxorubicin, etoposide-induced the most robust increase in caspase-3 cleavage, and these two drugs were used for further experiments. As mentioned before, the drugs were applied 48 h after transfection, the time point when caspase-2 levels peaked upon transient TRIM25 knockdown **(Fig. 8C, D)**. Cleavage of caspase-3 and -7 was monitored after an additional 24 h when drug-induced caspase-3 cleavage was most robust in both cell lines **(Fig. 13A, B)**. Western blot analysis revealed a faint basal and more robust processing of effector caspase-3 and -7 by both drugs, which were significantly increased after silencing of TRIM25 in both cell lines tested **(Fig. 13A, B)** (Nasrullah *et al.* 2019).

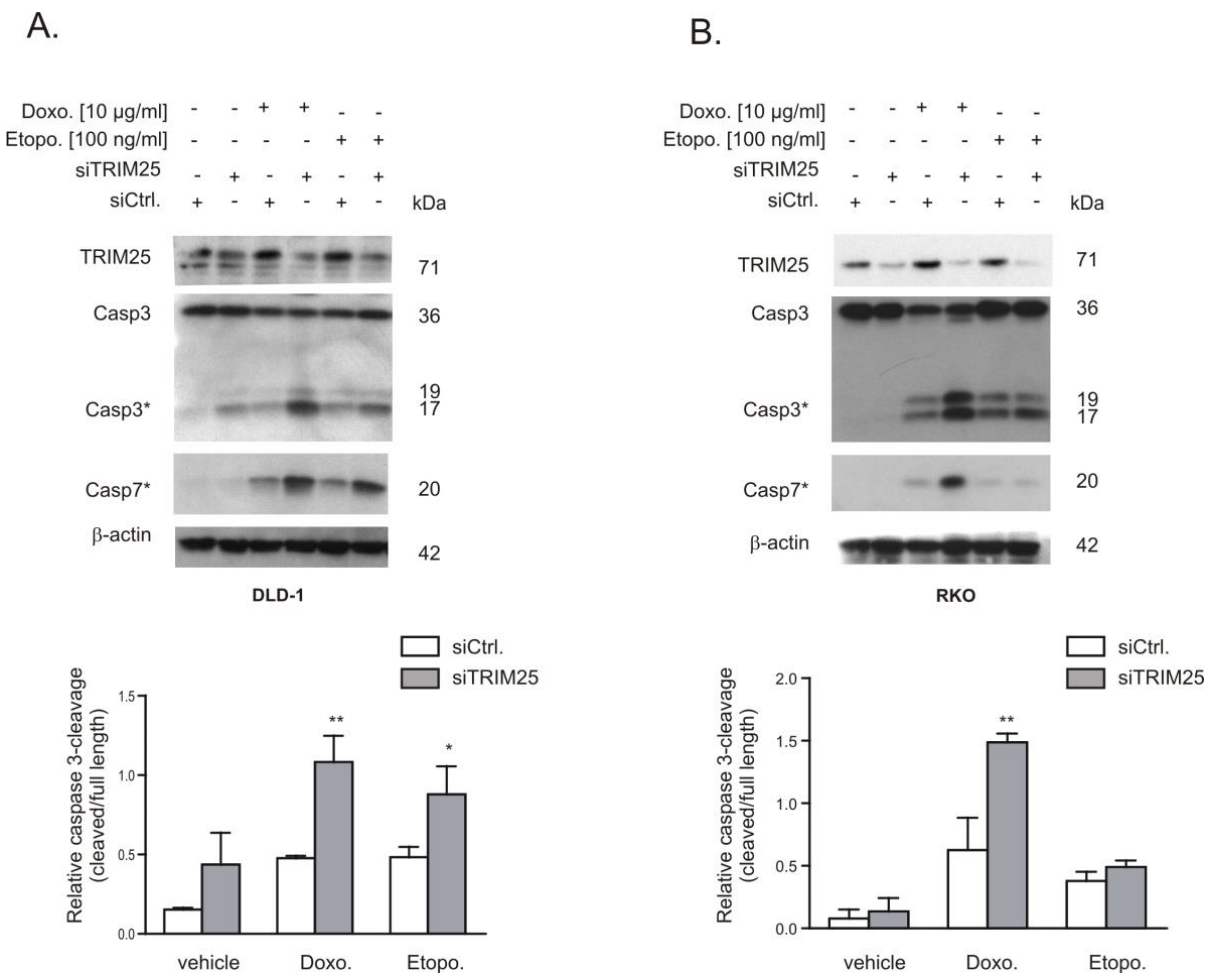

Figure 13. **Increase in chemotherapeutic drug-induced apoptosis in colon carcinoma cells upon transient silencing of TRIM25**. Subconfluent DLD-1 cells **(A)** or RKO cells **(B)** were either transfected with control siRNA duplexes (siCtrl.) or with siRNA duplexes targeting TRIM25 (siTRIM25) for 24 (A) or 48 (B) before stimulation with the indicated doses of doxorubicin (Doxo.) or etoposide (Etopo.) for an additional 24 h. Subsequently, the cells were lysed for total protein extraction, and cleavage products of caspase-3, caspase-7, and knockdown efficiency of TRIM25 were determined by Western blot analysis with β-actin was used as a loading control. Graphs at the lower panels summarize the densitometric analysis of cleaved caspase-3 (Casp3*) levels in relation to full-length caspase-3. Data show means ± SD (n = 3) * $p \leq 0.05$, ** $p \leq 0.01$ siTRIM25 (filled bars) vs. siCtrl. (empty bars) transfected cells.

Importantly, in contrast to doxorubicin, etoposide-induced caspase-3 cleavage was not significantly amplified by TRIM25 silencing in RKO cells **(Fig. 13B).** The dichotomy of sensitivity towards TRIM25 knockdown observed in both colon carcinoma cell lines indicates that the different p53 states in both cell lines may play a limiting role in the apoptosis-sensitizing

mechanisms by TRIM25 silencing as has been previously reported in human embryonic stem cells (Neochoritis *et al.* 2015).

6.6. TRIM25 dependent increase in caspase-3 cleavage is accompanied by an elevated cytochrome c release

To further confirm a modulation of intrinsic apoptosis by TRIM25, I monitored for changes in mitochondrial cytochrome c release to the cytoplasm. Therefore, colonic carcinoma cells were biochemically fractionated for nuclear and cytoplasmic lysates, and the content of cytoplasmic caspase-2 was subsequently analyzed by Western blot analysis. We observed low levels of cytochrome c in both cell lines. Interestingly, RNAi-based attenuation of TRIM25 was concomitant with a moderate increase in cytochrome c levels **(Fig. 14A, B)**. However, the TRIM25 silencing-dependent modulation in cytochrome c release remained unchanged regardless of doxorubicin treatment **(Fig. 14A, B)** (Nasrullah *et al.* 2019). By contrast, cleavage of cytoplasmic caspase-3 was exclusively observed in siTRIM25 transfected cells treated with doxorubicin independent of the cell line tested. Interestingly, by monitoring changes in caspase-8, an initiator caspase, a substantial decrease in procaspase-8 levels was only observed in doxorubicin-treated cells, indicating activation of this particular caspase by chemotherapeutic drugs. These data in accord with a previous study that demonstrated the induction of FAS-mediated cell death by doxorubicin via a drug-induced increase in Fas expression (Kim *et al.* 2009). Again, the same modulatory effects on caspase-8 were observed in RKO cells **(Fig. 14B).** Together, these data imply that the increased sensitivity of colon carcinoma cells to doxorubicin-induced apoptosis upon transient knockdown of TRIM25 results from convergent

activation of mitochondrial apoptosis via silencing of TRIM25 and drug-mediated activation of receptor-triggered apoptosis.

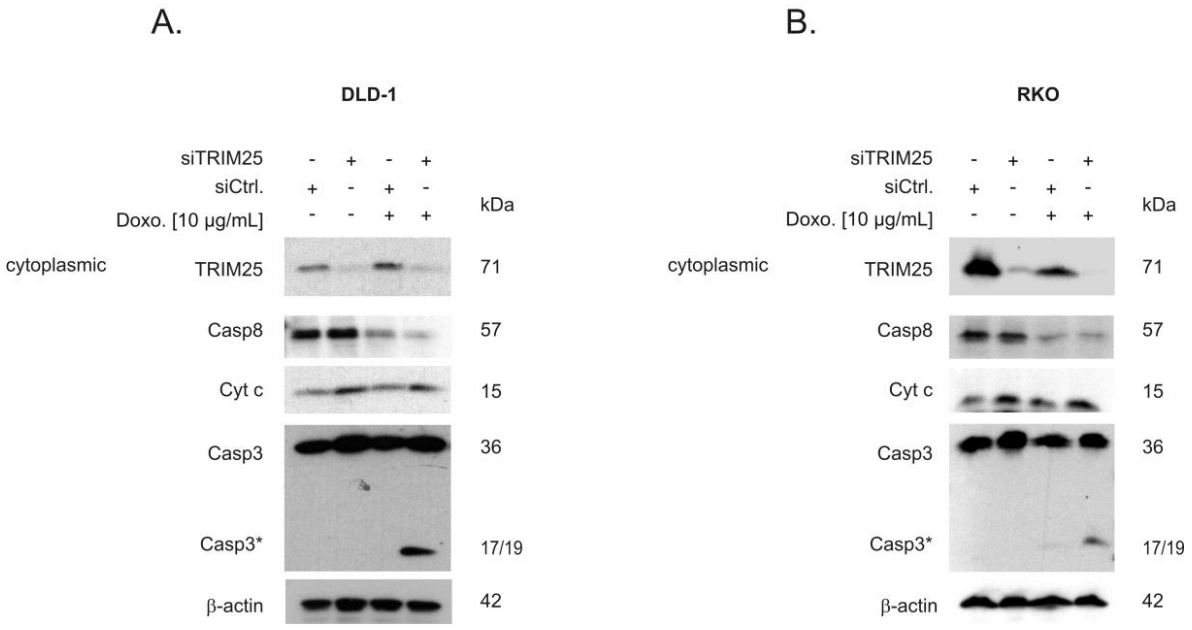

Figure 14. The transient knockdown of TRIM25 via increased mitochondrial cytochrome c release enhances doxorubicin-induced caspase-3 cleavage. Subconfluent DLD-1 cells **(A)** or RKO cells **(B)** were transfected with control siRNA duplexes (siCtrl.) or with siRNA duplexes against TRIM25 (siTRIM25) for 48 h before being stimulated with the indicated doses of doxorubicin (Doxo.). After an additional 24 h, cells were harvested for cytoplasmic cell lysates. The content of cytoplasmic cytochrome c (Cyt c), mature caspase-8, cleavage of caspase-3, and knockdown efficiency of TRIM25 was determined by Western blot analysis using β-actin as a loading control. Data are representative of two independent experiments giving similar results.

6.7. Modulatory effects of chemical caspase-2 inhibition on drug-induced caspase-3 cleavage

The next approach aimed at the investigation of a functional role of caspase-2 in the sensitization of colon carcinoma cells to drug-induced apoptosis. First, I tested for a modulatory influence of the pharmacological caspase-2 inhibitor Z-VDVAD-FMK, a synthetic peptide that consists of the caspase-2 specificity determining substrate VDVAD and a **f**luoro **m**ethyl **k**etone (FMK) linker peptide. The fact that the inhibitory peptide is chemically coupled to a

benzyloxycarbonyl group (Z) results in the irreversible inhibition of the enzyme. 50 µM of Z-VDVAD-FMK was added after 48 h of siRNA transfection and 1 h before the administration of chemotherapeutic drugs. Interestingly, the coincubation of transfected cells with doxorubicin or etoposide plus Z-VDVAD-FMK did not cause a full blockage of caspase-3 cleavage. Instead, it induced a shift in caspase-3 cleavage with a reduced generation of a p17 caspase-3 fragment concomitant with an increase in the levels of p19 cleavage product **(Fig. 15A)**. Since the processing of the pro-caspase-3 protein follows a two-step cleavage giving rise to three different cleavage products, the results indicate that caspase-2 is mainly involved in the last processing step of caspase-3 processing (Han et al. 1997).

The same observation was made in untransfected DLD-1 cells. In contrast, the addition of Z-VAD-FMK, a pan-caspase inhibitor, caused a complete loss in caspase-3 processing, which indicates that the switch in caspase-3 cleavage by Z-VDVAD is not due to the direct interference with caspase-3 activation but is instead a consequence of the impaired caspase-2 activity **(Fig. 15B)** (Badawi *et al.* 2018).

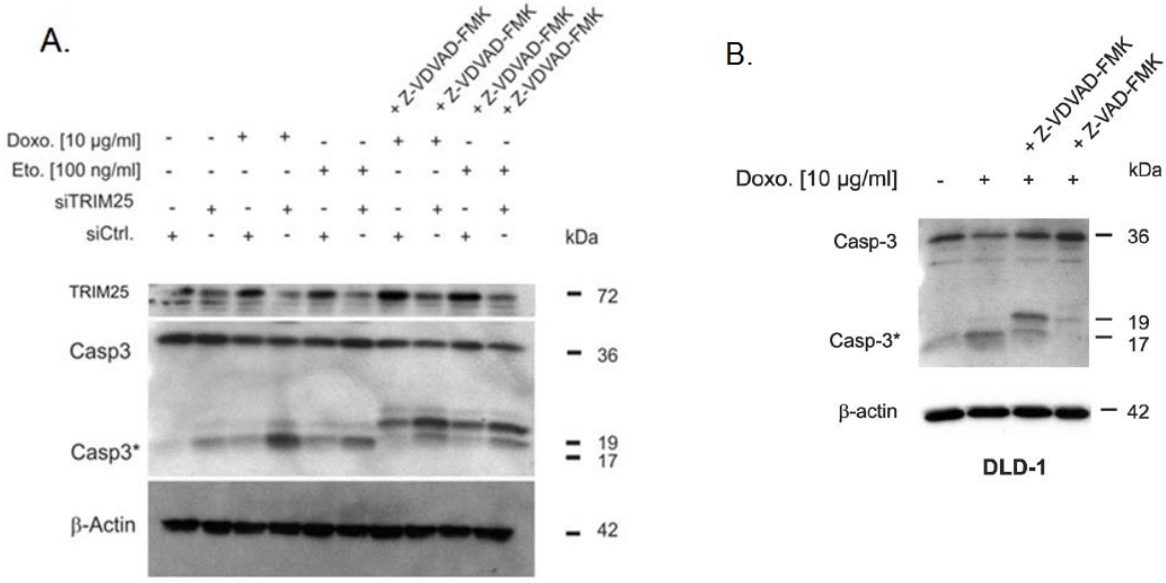

Figure 15. **Modulatory effects of caspase-2 inhibitor on drug-induced caspase-3 cleavage. (A)** Subconfluent DLD-1 cells were transfected with control siRNA duplexes (siCtrl.) or with siRNA duplexes against TRIM25 (siTRIM25) for 24 h before cells were stimulated with the indicated doses of doxorubicin (Doxo.) or etoposide (Etopo.) for an additional 24 h in the absence or presence of Z-VDVAD-FMK (50 µM) which was added 1 h prior to the chemotherapeutic drugs. After 24 h, the cells were lysed for total protein extraction, and cleavage products of caspase-3 and knockdown efficiency of TRIM25 were determined by Western blot analysis with β-actin as a loading control. Data shown are representative of two independent experiments giving similar results. **(B)** DLD-1 cells were stimulated with either vehicle (−) or with (10 µg/ml) doxorubicin (Doxo.) either in the presence of Z-VDVAD-FMK (50 µM) or Z-VAD-FMK (50 µM) which were added 1 h before doxorubicin stimulation. After 24 h, the cells were lyzed for total cell extracts, and cleavage products of caspase-3 were monitored by Western blot analysis (cleavage products are indicated by asterisk symbol.

6.8. Caspase-2 is critical for apoptosis sensitization by TRIM25 silencing

In addition to pharmacological caspase-2 inhibition, the impact of caspase-2 in TRIM25 silencing-dependent apoptosis sensitization was assessed by RNAi-mediated knockdown. Again, effects of caspase-2 knockdown on the drug-induced cleavage of the effector caspases -3 and -7 were tested by Western blot analysis. Importantly, the transfection of two different sets of caspase-2-specific siRNA duplexes resulted in a similar reduction in caspase-2 contents in DLD-1 cells **(Fig. 16A)** (Badawi *et al.* 2018). In order to keep a constant amount of siRNAs, for double knockdown experiments, only half-amounts of each gene-specific siRNAs were administered. Western blot analysis confirmed a significant knockdown efficiency of TRIM25 and caspase-2 in both colon carcinoma cell lines, although reduced amounts of siRNAs were used **(Fig. 16B, C)**. Transient TRIM25 knockdown significantly sensitized DLD-1 colon carcinoma cells to caspase-3 cleavage by doxorubicin when compared to the effects obtained after transfection of control siRNA (Fig. 16B). Moreover, these results are in accord with the TRIM25 silencing-dependent effects on cytosolic caspase-3 cleavage **(Fig. 14A, B).** Importantly, the additional knockdown of caspase-2 completely reversed the sensitizing effects by TRIM25 depletion, as indicated by the fact that the doxorubicin-induced caspase-3 cleavage was reduced to background levels **(Fig. 16B)** (Nasrullah *et al.* 2019). A similar caspase-2-dependent effect in doxorubicin-induced

caspase-3 cleavage was also observed in RKO cells **(Fig. 16C)** (Nasrullah *et al.* 2019). In contrast to caspase-3, the TRIM25 dependent increase in caspase-7 cleavage was not fully rescued by the additional knockdown of caspase-2, indicating the existence of caspase-2 independent mechanisms, which may contribute to the sensitization of caspase-7 in RKO cells upon TRIM25 knockdown. Conversely, to the inhibitory effects observed in loss of function experiments, overexpression of caspase-2 resulted in a time-dependent increase in basal caspase-2 and -3 cleavage **(Fig.16D)** (Badawi *et al.* 2018). Intriguingly, overexpression of caspase-2 induced a substantial increase in caspase-2 cleavage without affecting the levels of the full-length protein, indicating that ectopically expressed caspase-2 protein is immediately and completely processed. Besides, the overexpression of caspase-2 induced cleavage of caspase-3 (Casp3**), indicating that ectopic overexpression of caspase-2 can induce caspase-3 cleavage even in the absence of chemotherapeutic agents.

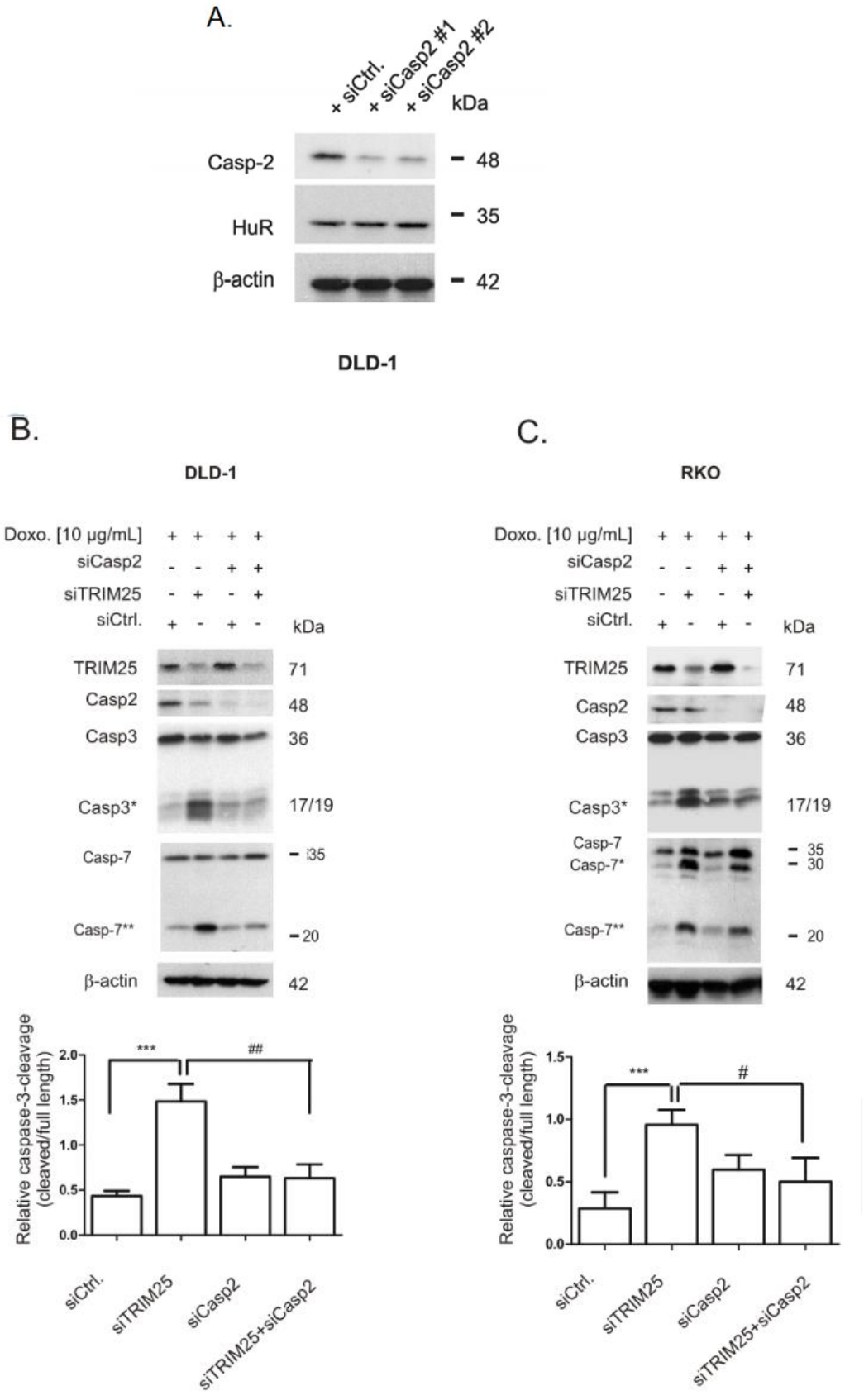
A.
+ siCtrl.
+ siCasp2 #1
+ siCasp2 #2
kDa
Casp-2
48
HuR
35
β-actin
42
DLD-1
B.
DLD-1
Doxo. [10 µg/mL]
siCasp2
siTRIM25
siCtrl.
kDa
TRIM25
71
Casp2
48
Casp3
36
Casp3*
17/19
Casp-7
35
Casp-7**
20
β-actin
42
Relative caspase-3-cleavage (cleaved/full length)
***
##
siCtrl.
siTRIM25
siCasp2
siTRIM25+siCasp2
C.
RKO
Doxo. [10 µg/mL]
siCasp2
siTRIM25
siCtrl.
kDa
TRIM25
71
Casp2
48
Casp3
36
Casp3*
17/19
Casp-7
Casp-7*
35
30
Casp-7**
20
β-actin
42
Relative caspase-3-cleavage (cleaved/full length)
***
#
siCtrl.
siTRIM25
siCasp2
siTRIM25+siCasp2

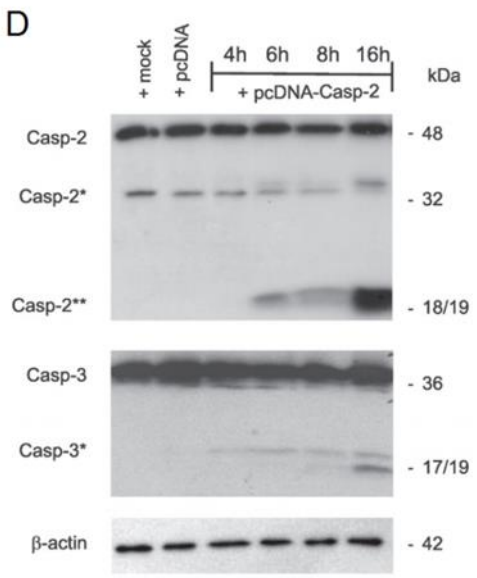

Figure 16. Caspase-2 is indispensable for doxorubicin-induced apoptosis in TRIM25 depleted colon carcinoma cells. (A) Transient knockdown of caspase-2 by two separate sets of siRNAs duplexes complementary to distinct regions of the coding region of caspase-2 mRNA (siCasp2#1 and siCasp2#2) was analyzed 48 h after transfection. HuR was used as a negative control and β-actin as a loading control. Data are representative of two independent experiments giving similar results. Subconfluent DLD-1 **(B)** or RKO **(C)** cells were transfected with control siRNA duplexes (siCtrl.) or with siRNA duplexes targeting caspase-2 (siCasp2) or TRIM25 (siTRIM25) or both in combination for 24 (B) 48 (C) h before cells were stimulated to doxorubicin for an additional 24 h. Thereafter, the cells were harvested for total protein extraction, and the cleavage of caspase-3, caspase-7, and knockdown efficiency of TRIM25 and caspase-2 was determined by Western blot analysis using β-actin for equal protein loading. Graphs in the lower panels summarize a densitometric analysis of cleaved caspase-3 (Casp3*) levels in relation to full-length caspase-3. Values show means ± SD (n = 3) *** $p \leq 0.005$ siTRIM25 vs. siCtrl. and # $p \leq 0.05$, ## $p \leq 0.01$ siTRIM25/Casp2 vs. siTRIM25**. (D)** Ectopic expression of caspase-2 caused a time-dependent increase in caspase-2 and caspase-3 cleavage- Subconfluent DLD-1 colon carcinoma cells were either mock-transfected (mock) or transfected with 1 µg of empty pcDNA vector (pcDNA) for 24 h, or with the equivalent amount of pcDNA3-Caspase-2 (pcDNA-Casp2) coding for full-length caspase-2 for the indicated time period before cells were harvested for total cell extracts. 20 µg of total cell lysates were analyzed by Western blot for the detection of unprocessed as well as cleaved caspase-2 and caspase-3 (indicated by asterisks).

6.9. Overexpression of TRIM25 results in reduced sensitivity to drug-induced apoptosis

In addition, to gain of function experiments with TRIM25, I tested for possible modulatory effects by ectopic expression of TRIM25 by employing transient overexpression. Monitoring for TRIM25 levels 72 h post-transfection revealed a clear increase in TRIM25 protein. In order to analyze a possible sensitizing effect of TRIM25 overexpression towards chemotherapeutic drug-

induced apoptosis, RKO cells were transiently overexpressed either with pFLAG-CMV-TRIM25 vector or with the same amount of the empty vector pCMV-Flag for 48 h before the cells were stimulated with either doxorubicin (Doxo) or etoposide (Etopo.) for additional 24 h. Before, I affirmed the specific binding of Flag-tagged TRIM25 binding to caspase-2 mRNA by employing RNP-IP RT-PCR using magnetic beads carrying immobilized flag-specific antibodies. PCR analysis revealed a strong and specific binding of Flag-tagged TRIM25 to caspase-2 mRNA when compared to empty vector (pCMAV-Flag) **(Fig. 17A)** (Nasrullah *et al.* 2019). As expected by results from silencing experiments, overexpression of TRIM25 resulted in a clear reduction in drug-induced cleavage of caspase-3 and caspase-7 independent of which drug was employed **(Fig. 17B)** (Nasrullah *et al.* 2019). These data reinforce the hypothesis that TRIM25 may constitute a novel suppressor of intrinsic apoptosis.

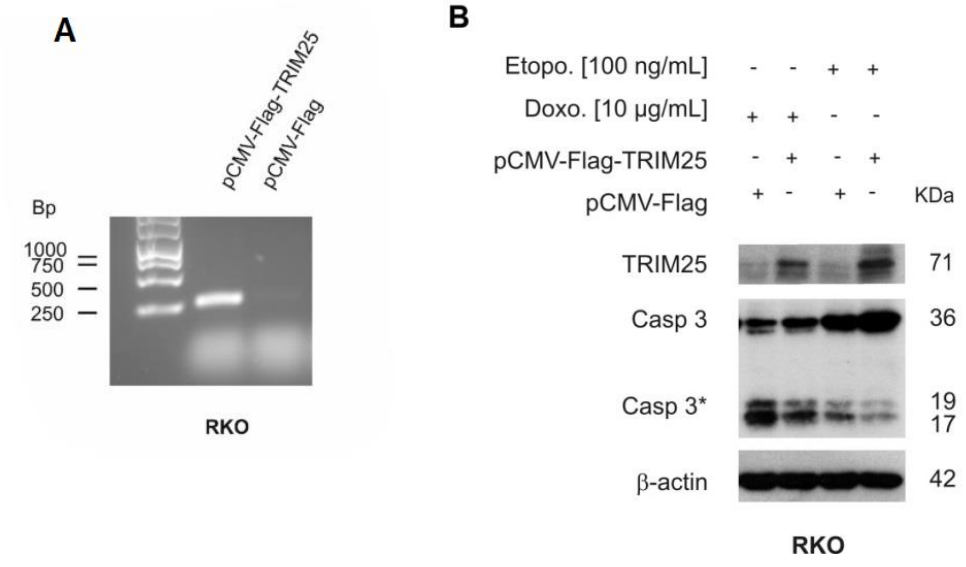

Figure 17. Ectopic expression of TRIM25 attenuates drug-induced cleavage of caspase-3 and caspase-7. (A) Explicit binding of Flag-tagged TRIM25 to caspase-2 mRNA in human colon carcinoma cells. The total cell lysates of RKO cells expressing either Flag-tagged human TRIM25 (pCMV-Flag-TRIM25) or pCMV-Flag (pCMV-Flag) were used to perform RNP-IP assays. Anti-Flag-M2 magnetic beads were utilized to isolate TRIM25-bound mRNA and subsequently followed by RT-PCR. The precipitated RNA samples were examined by semiquantitative RT-PCR using

primer sets encompassing the coding region of caspase-2. Data shown are representative of three independent experiments giving similar results. **(B)** Subconfluent RKO cells were either transfected for 48 h with 6 µg of Flag-tagged human TRIM25 (pCMV-Flag-Trim25) or an equivalent amount of empty pCMV-Flag vector (pCMV-Flag) before being stimulated with either the vehicle (-) or with the indicated chemotherapeutic drugs. After an additional 24 h, cells were harvested, and 20 µg of total cell lysates were analyzed by Western blot for detection of cleaved caspase-3 as well as the overexpression of TRIM25 and β-actin was used for equal protein loading. Data represent three independent experiments with similar results.

6.10. Increased TRIM25 binding to the 5'UTR of caspase-2 by doxorubicin

The next question which I addressed was whether the negative TRIM25-caspase-2 axis could reflect a physiological anti-apoptotic program of colon cancer cells and additionally may represent a drug-induced cell survival pathway. To answer this question, I investigated whether the treatment of cells with doxorubicin would influence the constitutive binding of TRIM25 to the 5'UTR of caspase-2 mRNA. For the detection of a UTR-specific TRIM25 binding, I used a streptavidin-tethered pull-down assay containing a biotinylated *in-vitro* transcribed mRNA encompassing the entire 5'UTR of caspase-2 (described in 4.2.16). Since in both tumor cell lines which were tested, activation of effector caspases-3 and -7 cleavage was only observed with doxorubicin, the following experiments were performed with this chemotherapeutic drug. Western blot analysis of total cell lysates from DLD-1 cells stimulated with doxorubicin revealed a substantial increase in TRIM25 affinity to 5'UTR-caspase-2 **(Fig. 18, left panel)** (Nasrullah *et al.* 2019). Besides, a similar drug-evoked increase in TRIM25-caspase-2 RNA-binding was observed in the cytoplasmic fractions from DLD-1 cells, indicating that the RNA binding of TRIM25 occurs mainly in the cytoplasm **(Fig. 18, right panel**) (Nasrullah *et al.* 2019).

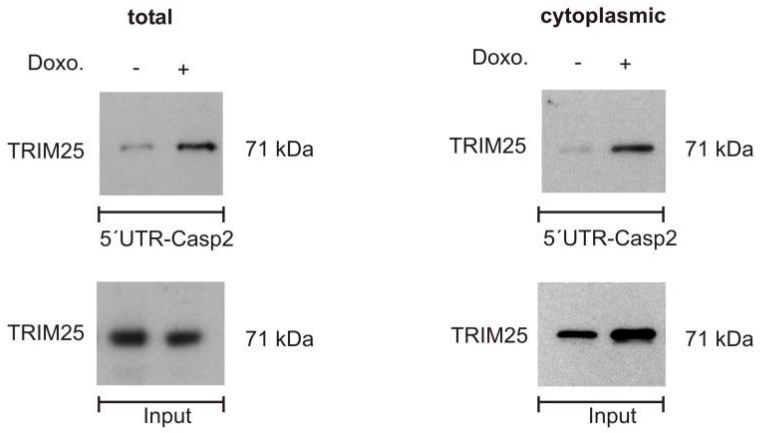

Figure 18. Doxorubicin-enhances TRIM25 affinity to the 5´-UTR of caspase-2. The biotinylated transcript encompassing the full-length 5´-UTR-caspase-2 was incubated with either total cell lysate (left panel) or with cytoplasmic cell lysates (right panel) from vehicle-treated DLD-1 cells (−) or from cells stimulated with the indicated dose of doxorubicin (+) for 6 h. RNA binding of TRIM25 to the pull-down material was evaluated by Western blot analysis, and equal input TRIM25 levels were determined by Western blot analysis (input). Data represent two independent experiments with similar results**.**

6.11. Determination of TRIM25 localization by using confocal-microscopy

Since TRIM25 is reported to be mainly localized in the cytoplasm and nucleoplasm (ATLAS 2020. March 16), I conducted fluorescent microscopy to confirm a similar intracellular localization in colon carcinoma cells. Confocal-microscopy revealed the predominant cytoplasmic localization of TRIM25 in DLD-1 cells **(Fig. 19)** (Nasrullah *et al.* 2019). Importantly, this localization was not affected after stimulation of cells with doxorubicin, indicating that the drug-induced increase in caspase-2 mRNA binding is not due to intracellular relocalization of TRIM25 protein as we have previously reported for the caspase-2-binding protein HuR (Badawi *et al.* 2018).

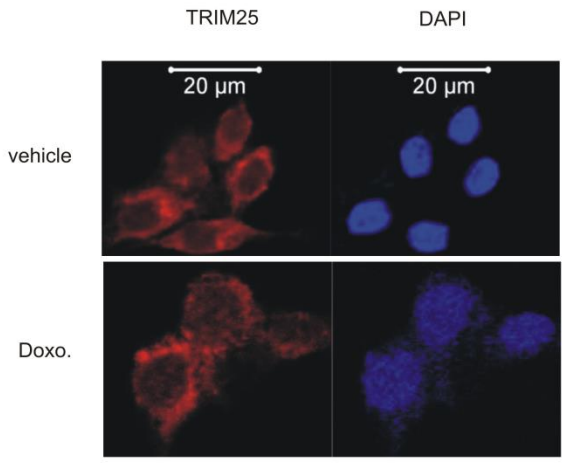

Figure 19. Intracellular localization of TRIM25. DLD-1 cells were treated for 6 h with either vehicle or with 10 µg/ml doxorubicin (Doxo.) before cells were fixed and successively stained with anti-TRIM25 and anti-mouse Alexa-488 antibodies. Thereafter, cell nuclei were visualized by DAPI staining (blue panel) Bar: 20 µm**.**

6.12. Binding of TRIM25 to the 5'UTR-caspase-2 impairs translation of caspase-2

In the next set of experiments, I tested whether the doxorubicin-induced increase in TRIM25 binding to the 5'UTR-caspase-2 could modulate the translation of caspase-2. Since doxorubicin-induced a cleavage of caspase-2, changes in the level of mature pro-caspase-2 protein could not reliably be monitored by Western blot analysis. As a more useful technique to monitor changes in caspase-2 translation, I analyzed for possible drug-induced changes in ribosome occupancy of caspase-2 mRNA by polysome/RNP fractionation by using sucrose density gradient ultracentrifugation. As we have previously demonstrated, long-term treatment of DLD-1 cells with doxorubicin induces global inhibition in protein translation (Badawi *et al.* 2018). For this reason, I chose only a short incubation period of 6 h, which did additionally fit with the time point I used for the analysis of caspase-2 mRNA binding and intracellular localization of TRIM25. As shown in **(Fig. 20)** (Nasrullah *et al.* 2019), doxorubicin significantly reduced the basal content

of caspase-2 mRNA in polysomes when compared with GAPDH mRNA levels. Notably, doxorubicin did not change the contents of corresponding mRNAs associating with RNPs **(Fig. 20)**. These data indicate that the increase in TRIM25 binding to the 5'UTR of caspase-2 upon doxorubicin is accompanied by a reduction in caspase-2 translation.

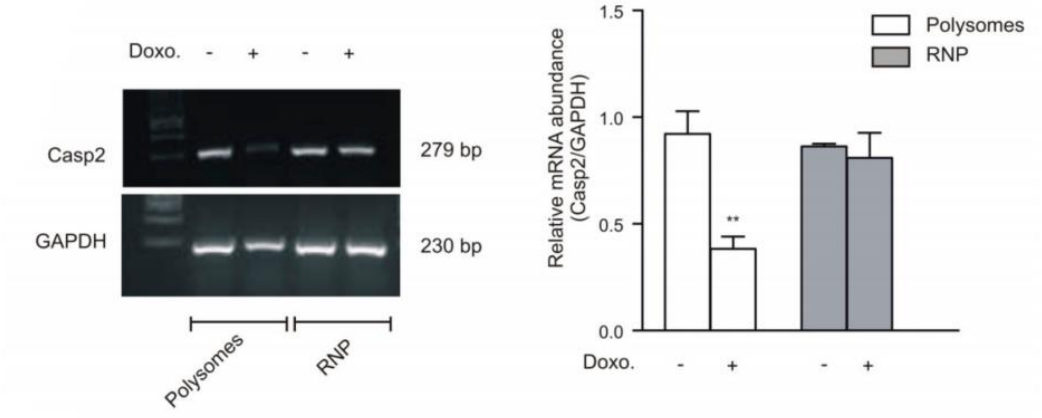

Figure 20. Doxorubicin-induced binding of TRIM25 to the 5'UTR-caspase-2 is accompanied by a reduction of caspase-2 translation. DLD-1 cells were treated for 6 h either with vehicle (−) or doxorubicin (+) before fractions of translational inactive RNPs were segregated from translationally active polysomes by ultracentrifugation. The amount of caspase-2 and GAPDH mRNA levels were determined by semiquantitative RT-PCR using primer pairs that were complementary and specific to the coding region of both genes. The graph on the right panel shows means ± SD (n = 3) and depicts the amount of caspase-2 mRNA levels normalized to GAPDH mRNA in polysomes (open bars) relative to those in RNP (grey bars) fractions. ** $p \leq 0.01$, doxorubicin vs. vehicle-treated cells.

6.13. Effects of transient TRIM25 knockdown on cell cycle

The cell cycle describes a sequence of different events characteristically relevant to the growth and division of a cell and is based on changes in the DNA content. In eukaryotic cells, the cell cycle is divided into G_1, S, G_2, and M phases, which the latter one is critical for DNA duplication and segregation of chromosomes to two daughter cells. Besides, the G_0 phase refers to the resting phase of the cell and, in most cases, is a characteristic feature of differentiated cells. Importantly, under DNA damaging conditions, e.g., exposure to genotoxic agents, cell cycle

progression is blocked due to cell cycle checkpoints mainly during G_1, S, or G_2 phases (Lippincott-Schwartz 2007, April 18). In order to investigate the possible impact of time-dependent transient knockdown of TRIM25 on the cell cycle of DLD-1 cells, flow cytometry was utilized for cell cycle analysis. DLD-1 cells were transiently transfected with either siRNA duplexes targeting human TRIM25 or with a non-gene-related scrambled siRNA for 24 h or 48 h before the addition of **P**ropidium **i**odide (PI). As shown in **Fig. 21**, there were no significant changes in cell cycle distribution upon TRIM25 silencing. Instead, there was a clear increase in the number of cells residing within the G_1 phase after 48 h of TRIM25 knockdown concomitant with a reduced cell number in the S phase **(Fig. 21)**. The reduction in cells residing in the S phase is presumably a direct consequence of serum deprivation for longer periods of cell cultivation. The results from these experiments, therefore, implicate that siRNA-mediated TRIM25 silencing has only weak effects on the cell cycle phases of DLD-1 cells.

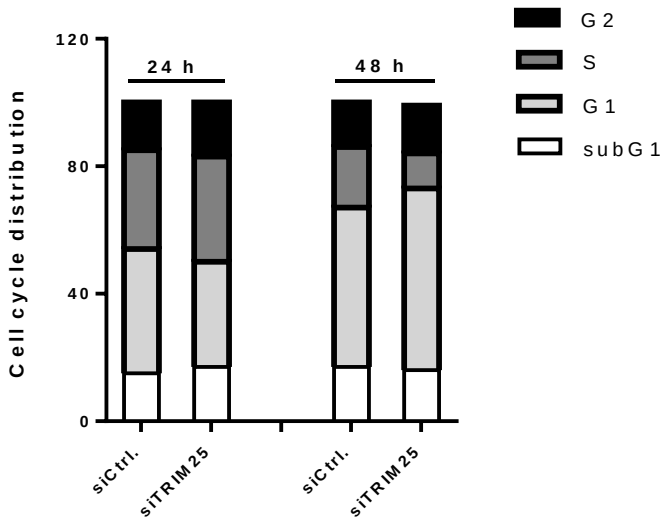

Figure 21. TRIM25 has only weak effects on the cell cycle distribution of DLD-1 cells. Subconfluent DLD-1 cells were either transfected with control siRNA duplexes (siCtrl.) or with siRNA duplexes targeting TRIM25 (siTRIM25) for 24 h or 48 h. The cells were harvested with trypsin/EDTA before the cell cycle was determined by using PI staining. Subsequently, cells were subjected to FACS analysis for the determination of different cell cycle phases indicated by different colored bars. Data represent the means of two independent experiments.

6.14. Effects of CRISPR-Cas9-mediated caspase-2 knockout on apoptotic sensitivity of DLD-1 cells

As mentioned before, I could demonstrate that transient silencing of caspase-2 can increase the sensitivity of colon carcinoma cells to drug-induced intrinsic apoptosis (see section 3.8). To confirm the hypothesis that caspase-2 is critical for TRIM25 silencing-dependent sensitivity of carcinoma cells towards drug-induced apoptosis, I made use of a CRISPR-Cas9-caspase-2 DLD-1 knockout cell line, which was kindly provided by Dr. G. Imre (Institute of Pharmacology and Toxicology, Goethe University Frankfurt). "CRISPR" is the abbreviation for "clusters of regularly interspaced short palindromic repeats." It is a specific area of DNA containing nucleotide repeats and spacers. Repeated sequences of nucleotides are distributed extensively throughout a CRISPR region, while spacers are tiny bits that are scattered among recurring nucleotide repeats. In the CRISPR/Cas system, intruding DNA is processed into small fragments of DNA by the Cas 9 nuclease, which then specifically integrated into CRISPR locus flanked by the spacers (Zhang *et al.* 2014). The stable caspase-2 knockout cells were generated by using a single lentiviral CRISPR/Cas9 system (GeCKO vector) from Addgene using the popular lentiviral envelope (pMD2.G) as well as the lentiviral packaging plasmids (psPAX2) under constant puromycin selection. Puromycin-resistant cells were seeded on a 96 well plate in a dilution of 0.4 cells/well to exclude the growth of cells that originated from mixed clones. Subsequently, to confirm the knockout of caspase-2 in the CRISPR-Cas9-caspase-2 deficient DLD-1 cells “DLD-1 Casp.2 -/-” in comparison to DLD-1 cells which had been transduced with non-targeting sgRNAs “DLD-1 wt”. Western blot analysis revealed an almost complete knockdown of caspase-2 protein in DLD-1 Casp.2 -/- cells when compared to the DLD-1 wt cells **(Fig. 22A)**. Also, a strong

knockdown of TRIM25 was evident upon the transient transfection of both cell clones with siRNA duplexes for TRIM25 **(Fig. 22A).** Intriguingly, the exposure of both cell clones with doxorubicin-induced a similar robust induction of caspase-3 cleavage independent of which cell clone was analyzed, indicating that the constant knockout of caspase-2 has no limiting effects on drug-induced intrinsic apoptosis of colon carcinoma cells. In accordance, stimulation of untransfected cell clones with doxorubicin **(Fig. 22B)**, or with etoposide **(Fig. 22C)** revealed a robust and dose-dependent induction of caspase-3 processing in both cell clones independent of which chemotherapeutic drug was employed. These results are in clear contrast to the data observed with a transient knockdown approach **(Fig. 16)**. The identical sensitivity of both cell clones towards TRIM25 transient knockdown may implicate that under permanent depletion of caspase-2, some unknown compensatory mechanism could rescue the lack of caspase-2 and caspase-2 dependent effects on caspase-3 cleavage.

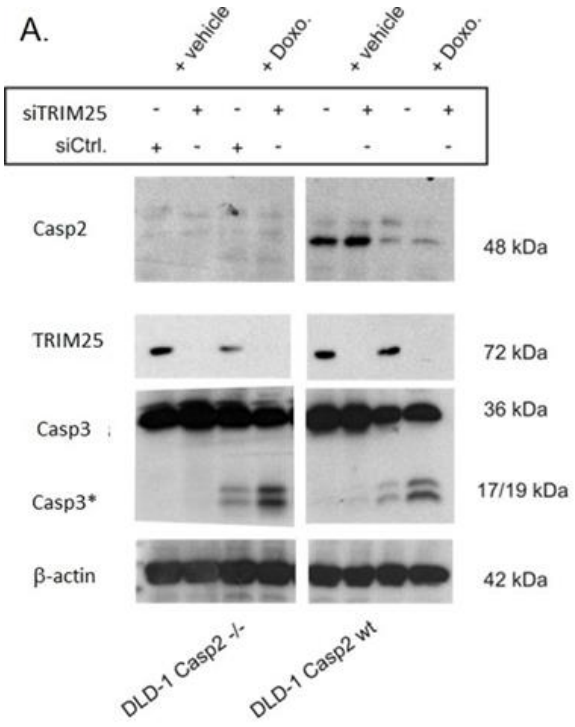

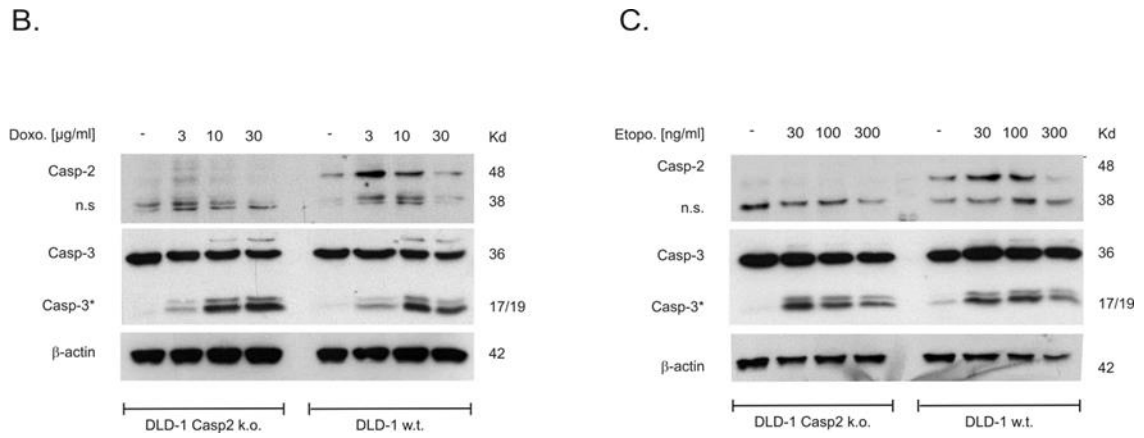

Figure 22. Doxorubicin-induced a robust induction of caspase-3 cleavage in both DLD-1 Casp.2 -/- and wild type cells. (A) Subconfluent DLD-1 Casp.2 -/- and wild type cells were transfected with control siRNA duplexes (siCtrl.) or with siRNA of Trim25 (siTrim25) or both in combination for 24 h before stimulation with 10 µg/ml doxorubicin (Doxo.). After a further 24 h, cells were harvested for total protein extraction, and the cleavage of caspase-2, caspase-3 as well as the knockdown efficiency of Trim25 was determined by Western blot using β-actin as a loading control. Data shown are representative of two independent experiments giving similar results. Concentration-dependent activation of cleaved caspase-3 by chemotherapeutics in DLD-1 Casp.2 -/- and wild type cells. Subconfluent DLD-1 Casp.2 -/- and wild-type cells were stimulated with indicated doses of **(B)** doxorubicin or **(C)** etoposide for 24 h. Subsequently, the cells were harvested, and equal amounts of protein (20 µg) from total cell lysates were subjected to SDS-PAGE and successively immunoblotted with anti-caspase-2, anti-caspase-3, and anti-β-actin antibodies, respectively. Data shown are representative of two independent experiments giving similar results (n.s: nonspecific).

7. DISCUSSION

7.1. TRIM25: A novel RNA binding protein with a direct impact on protein translation

In this study, the ubiquitin E3 ligase TRIM25 was identified as a so far undescribed potential regulator of caspase-2 translation in human colon carcinoma cells. By using RNA-affinity chromatography with the 5´-UTR served as bait, TRIM25 associated with 5´UTR of caspase-2, and this finding was confirmed by different approaches, including TRIM25 antibody-based immunoprecipitation approaches (RNP-IP) and RNA pull-down assay with a biotinylated RNA encompassing the 5´UTR of caspase-2, respectively. Importantly, besides TRIM25, we identified a large number of functionally different candidate 5´-UTR caspase-2 binding proteins including designated ribosomal proteins (e.g., several proteins of 40S and 60S ribosomes) and various eukaryotic translation initiation factors including the eukaryotic translation initiation factors 2A and 5B as well as various established RNA-binding proteins including the hnRNP H, the cold-inducible RNA binding protein and the ubiquitous ELAV-1 like protein HuR. Importantly, the latter one was previously identified as a 5´UTR-caspase-2 binding protein by our group, and therefore, this finding underlines the validity of the experimental approach used for the identification of novel caspase-2 mRNA binding proteins. Another functional class of 5´UTR - caspase-2 associated proteins included ubiquitination-regulatory proteins, e.g., the ubiquitin 40S ribosomal protein S27A and the E3 ligase TRIM25 (Nasrullah *et al.* 2019). For deeper analysis, we chose TRIM25 because several previous publications have validated TRIM25 as an RNA binding protein that is crucial for stem-cell physiology (Kwon *et al.* 2013) and which additionally plays a key role in the post-transcriptional regulation of breast cancer metastasis

(Walsh *et al.* 2017). The finding that several members of E3 ligases have meanwhile been identified as RNA-binding proteins implicates a dual role of E3 ligases in RNA regulation and ubiquitination pathways. This hypothesis is furthermore underscored by the fact that currently, more than 15 members of E3 ligases were found to contain predicted RNA binding domains (Cano *et al.* 2010). In clear contrast to the observations of those publications which demonstrated a critical role of E3 ligases (Cano *et al.* 2010) and particularly of TRIM25 in the regulation of RNA stability (Cano *et al.* 2012; Kwon *et al.* 2013; Choudhury *et al.* 2014; Walsh *et al.* 2017) and the activity of miRNAs (Choudhury *et al.* 2017) the herein presented data from TRIM25 silencing experiments implicate that TRIM25 does mainly interfere with the translation of caspase-2 without affecting the stability of caspase-2 transcripts **(see Fig. 11).** Questioning whether TRIM25 may recognize a specific *cis*-regulatory element, it needs to be mentioned that so far no distinct consensus motif for RNA-binding could be identified neither in the 3´UTR nor in exons of known mRNA targets although a certain tendency of TRIM25 to preferentially bind to G-and C-rich sequences is implicated from photoactivatable-ribonucleoside-enhanced crosslinking and immunoprecipitation (PAR-CLIP) experiments (Choudhury *et al.* 2017). Notably, in this study, TRIM25 was identified to bind mainly to the 5´UTR of caspase-2, which our group previously found as a target of IRES-triggered translation (Badawi *et al.* 2018). Since I did not further investigate whether TRIM25 is additionally able to bind to other mRNA regions of the caspase-2 message (coding region and/or 3´UTR), it can only be speculated that the herein described affinity is unique for the 5´UTR. Further experiments are definitely needed to decipher whether other caspase-2 mRNA regions are additional targets of TRIM25. Another critical issue that needs to be addressed is the determination of TRIM25 domain that is critical

for caspase-2 binding. Up to now, only a few publications reported on the mapping of TRIM25 domains critical for RNA recognition, although with some contradictory results. Truncations with deleted N-terminal RING domain and B-boxes or the C-terminal PRY/SPRY domain were found to still be capable of binding RNA, while mutants with deleted CC domain were shown to be unable to associate with RNA, thus indicating that the CC domain plays a vital role in TRIM25 RNA binding activity (Kwon *et al.* 2013). Contrary to these results, a more recent study identified a putative RBD within the C-terminal PRY/SPRY being critical for RNA binding (Choudhury *et al.* 2017). Importantly, the study by Kwon and colleagues was performed in embryonic stem cells from wild-type mice, which still express high levels of endogenous TRIM25. Based on the knowledge that the CC domain is critical for dimerization which itself is an important prerequisite for RNA binding (Lunde *et al.* 2007; Feracci *et al.* 2016), overexpression of any mutant construct including those which lacking a PRY/SPRY domain would still exert RNA binding capacity due to the formation of hetero-dimeric complexes with wild type TRIM25. Indeed this tendency may pretend that PRY/SPRY is dispensable for RNA binding. For this reason, the data from Choudhury's group, which were derived from TRIM25 knockout cells, are presumably more reliable. Another possible explanation for both discrepant findings is the fact that both studies evaluated structural requirements for binding to different RNAs. It is additionally tempting to speculate that binding to different RNA species may structurally depend on different TRIM25 domains. Conclusively, a mapping of TRIM25 domains, which are specifically relevant for caspase-2 mRNA binding, is an indispensable requirement for more conclusive predictions.

7.2. Potential mechanisms underlying caspase-2 suppression by TRIM25

To the best of my knowledge, this is the first report demonstrating that TRIM25 is able to interfere with the translation of mRNAs. This suggestion is substantiated by the following findings. Firstly, results from loss of function experiments clearly demonstrate that the increase in caspase-2 upon TRIM25 silencing is exclusively on the protein level without affecting the corresponding mRNA levels (see **Fig. 9**). In addition, the TRIM25 silencing-induced increase in caspase-2 protein is fully impaired in the presence of cycloheximide and, accompanied by a significant redistribution of caspase-2 mRNA from translationally inactive RNP to polysomes **(Fig. 10),** demonstrating that TRIM25 constitutively interferes with the *de novo* synthesis of caspase-2. However, further experiments are needed to unveil the underlying mechanisms. Previously, we could show that the ubiquitous RNA-binding protein HuR via binding to the 5´UTR of caspase-2 inhibits the IRES-mediated translation of caspase-2 (Eberhardt *et al.* 2019). However, preliminary experiments with the mTOR kinase inhibitor rapamycin, which negatively interferes with cap-dependent translation, indicate that TRIM25, in contrast to HuR, does not interfere with IRES-dependent translation, but instead mainly affects cap-dependent translation of TRIM25 (K. Häussler, personal communication). Together these data implicate that in colon carcinoma cells, the constitutive translation of caspase-2 is controlled by IRES-dependent but in addition through cap-dependent mechanisms. Hereby, TRIM25 and HuR can specifically interfere with only one alternative translation regulatory principles. Further experiments are needed to investigate which specific stimuli could induce a switch between both translation mechanisms. In that case, the therapeutic benefit of inhibiting strategies of either TRIM25 or HuR may critically rely on whether IRES-or cap-dependent translation of caspase-2 dominates in

a given tumor. Another critical question that needs to be answered is whether modulation of caspase-2 translation by TRIM25 requires E3 ligase activity of TRIM25 or is instead mediated independently of ubiquitination. Importantly, so far, an RNA dependence of TRIM25's catalytic activity has been described by several studies (Choudhury *et al.* 2017; Koliopoulos *et al.* 2018; Sanchez *et al.* 2018). In contrast, the requirement of prior ubiquitination for the RNA-binding capacity of TRIM25 has not been addressed so far. It is speculated that the RNA binding of TRIM25 may increase the ubiquitination activity either by facilitating the recruitment of a substrate, which is simultaneously binding the same RNA or, alternatively, may induce some allosteric changes in the TRIM25 protein which may finally increase its catalytic activity (Choudhury *et al.* 2017).

Potentially, one scenario to speculate is that binding of TRIM25 to caspase-2 mRNA may lead to ubiquitination and subsequent degradation of translation regulatory proteins, which are highly relevant for the synthesis of caspase-2. In accordance with this assumption, data from several laboratories have highlighted the critical involvement of the ubiquitin-proteasome system in the control of mRNA translation. Prominent examples include the proteasome-mediated degradation of the **e**ukaryotic **i**nitiation **f**actors (eIFs) eIF3a, eIF4G, and eIF4E, which are principally involved in the regulation of cap-dependent translation (Brooks 2010). Alternatively, it cannot be excluded that the binding of TRIM25 to caspase-2 RNA may initiate ubiquitination of some eIFs or adjacent RNA-binding proteins relevant for the control of caspase-2 translation in colon carcinoma cells. Hereby, TRIM25 may utilize the bound caspase-2 mRNA as a scaffold, which enhances the ubiquitination activity of TRIM25 or through allosteric changes (Choudhury *et al.* 2017). Another mechanism of how TRIM25 could presumably repress

caspase-2 translation is the increased recruitment of caspase-2 inhibiting miRNAs. So far, several caspase-2 suppressing miRs have been identified, including miR-708 (Brown *et al.* 2011), miR-494 (Zhang *et al.* 2019), miR-34a, miR-1247-3p, and others (Li *et al.* 2019; Zhang *et al.* 2019; Yang *et al.* 2020). The cooperative activation of a miR leading to a facilitated suppression has been previously demonstrated for the RNA-binding HuR. Hereby, HuR inhibits the expression of the tumor protein c-Myc by increasing the recruitment of let-7 miRNA in close proximity to the let-7 binding site (Kim *et al.* 2009). Since HuR and TRIM25 are both negative regulators of caspase-2, it would be interesting to check whether HuR or TRIM25 could additionally accelerate the recruitment of caspase-2 suppressive miRs in colon carcinoma cells. Notably, in this context, a previous study has identified that TRIM25 is an RNA-specific cofactor of the Lin28a protein, an RNA-binding protein that triggers the **t**erminal **u**ridylyl**t**ransferase 4 (TuT4)-mediated uridylation of the miRNA let-7. Functionally, the increased uridylation of pre-let 7 leads to enhanced degradation of let-7 and, consequently, to the increased stability of let-7 target mRNAs (Choudhury *et al.* 2014). However, herein I demonstrate that TRIM25 has a clear negative effect on caspase-2 translation. Therefore, it is tempting to suggest that TRIM25, in addition to exert a degradative activity on let-7, may additionally convey some stabilizing effects on particular miRNAs. Further studies are needed to evaluate this interesting aspect.

7.3. TRIM25: tumorigenic versus tumor-suppressing features

A considerable number of TRIM family members have been described to either positively or negatively modulate oncogenic pathways (Hatakeyama 2011; Hatakeyama 2017). The current

thesis presents TRIM25 as a negative regulator of caspase-2 translation, which may constitute a novel cell survival factor that prevents chemotherapeutic drug-induced apoptosis in colon carcinoma cells. In accordance with this proposed novel tumorigenic function, TRIM25 has been found to increase proliferation and invasion of colorectal cancer cells via activation of the TGF-β triggered signaling pathway, which underlines the oncogenic potential of TRIM25 in the gut (Sun *et al.* 2017). In a further agreement to data presented in this thesis, TRIM25 was previously identified as a critical regulator of the p53/Mdm2 circuit in the colon carcinoma cells line with a knockdown of TRIM25 caused an increase in p53-dependent apoptosis (Zhang *et al.* 2015). Another example further example where TRIM25 exerts a clear tumorigenic role via modulation of p53 is a previous publication from lung cancer cells. The authors of the study demonstrated that the depletion of TRIM25 markedly reduced proliferation and migration of tumor cells and increased the sensitivity to doxorubicin-induced apoptosis via increasing the expression of the p53 inhibiting E3 ligase Mdm2 (Qin *et al.* 2016). In addition to TRIM25, several other members of the TRIM protein family, including TRIM24, TRIM28, TRIM29, and TRIM32, were found to inhibit p53 levels via increasing proteasome-dependent degradation. In contrast, some other TRIM proteins, including TRIM2, TRIM8, TRIM13, and TRIM19, can positively regulate the level and/or activity of p53. These data indicate the diverse interrelationships of the tumor suppressor p53 with particular TRIM proteins (Lee *et al.* 2014). Importantly at the same time, p53 can modulate the transcription of some TRIM members either positively or negatively, which again underscores the complex interrelationship between both regulatory proteins. Since the herein described caspase-2 modulation by TRIM25 was observed in both p53 wild type

(RKO) as well as in p53 mutated (DLD-1) colon carcinoma cell lines, it is most likely that the TRIM25-caspase-2 axis acts independently of p53.

Despite the studies which commonly demonstrated a tumorigenic role of TRIM25, other reports have confirmed a clear tumor-suppressive function of TRIM25. E.g., TRIM25 inhibits the migration and invasion of HCC cells by targeting the **m**e**t**astasis-**a**ssociated 1 protein (MTA1) to proteasomal degradation (Zang *et al.* 2017). Another described TRIM25 target, which conveys a tumor-suppressive activity of TRIM25, is the ETS related gene (ERG), a transcription factor that can induce the expression of various carcinogenic genes. Upon binding to ERG, TRIM25 facilitates the degradation of ERG and thereby inhibits the progression of prostate cancer cells (Wang *et al.* 2016). It is worth mentioning that in contrast to the effects relying on the direct interaction of TRIM25 with a protein target, the herein described study points to a tumor modulatory role of TRIM25, which is mainly achieved through the interaction with the mRNA of the corresponding target.

7.4. Potential role TRIM25 silencing for sensitizing cancer cells to drug-induced apoptosis

In this study, I demonstrate a novel principle that could be applied for the sensitization of human colon carcinoma cells towards chemotherapeutic drug-induced apoptosis. The cell lines which were used in this study included human colon carcinoma cell lines expressing either mutated (DLD-1), or wild type p53 (RKO), respectively. Importantly, under diverse stress conditions, p53, in many cases, induces the initiation of apoptosis through upregulating prominent pro-apoptotic factors, including PUMA, BAX, and BAK (Kumar 2009). The finding that

TRIM25 depletion-mediated sensitization of cells to drug-induced apoptosis by topoisomerase inhibitors such as doxorubicin and etoposide was fully impaired after the additional knockdown of caspase-2 underlines the crucial role of caspase-2 for cell death sensitizing effects by TRIM25 knockdown. Interestingly, when monitoring for a possible impact on another effector caspase (caspase-7), I observed that rescuing effects on drug-induced caspase-7 induction after additional caspase-2 silencing was only observed in the p53 mutated DLD-1 cells, which suggests a differential role of p53 in the regulation of both effector caspases.

In full accordance with the results presented in my thesis, the previous study from my research group demonstrated a critical impact of caspase-2 in HuR depletion-dependent apoptosis sensitization (Badawi *et al.* 2018). It demonstrates that a forced increase in caspase-2 levels can be achieved by different (independent) approaches. However, when testing for possible potentiating effects by employing a double knockdown of HuR plus TRIM25, I found no significant increase in apoptosis when compared to the effects of single knockdown (data not shown). These results strengthen the hypothesis mentioned in section 7.2 that HuR and TRIM25 may interfere with different modes of constitutive caspase-2 translation, namely with either IRES triggered translation which is affected by HuR (Badawi *et al.* 2018) or, alternatively with the cap-dependent translation which is possibly impaired by TRIM25 (Nasrullah *et al.* 2019).

Considering the fact that caspase-2, in addition, to regulate DNA-damaged induced apoptosis, is furthermore implied in various non-apoptotic functions, it is most likely that the decreased translation of caspase-2 by TRIM25 affects nonapoptotic functions by caspase-2 including regulation of autophagy or the DNA damage response.

7.5. Future perspectives

A major challenge in the effective treatment of colon cancer is the lack of eradication of the whole cancer cell population and the subsequent development of chemotherapy resistance (Bostan *et al.* 2016). Currently, there are three major anticancer therapy approaches used in colon cancer, namely chemotherapy, radiation, and targeted therapies (Zhang and Yu 2013). Among these different cancer treatments, chemotherapy constitutes the most effective one to combat cancer. Accordingly, first-line anticancer drugs are aimed to kill specifically cancer cells without affecting healthy cells, thereby improving the survival rate of cancer patients (Yu and Zhang 2004; Adams and Cory 2007; Ashkenazi 2008; McCubrey *et al.* 2011).

The E3 ubiquitin ligase TRIM25 has been associated with many different types of human cancers. Representatively, overexpression of TRIM25 has been demonstrated in breast cancer, gastric cancer, lung cancer, and ovarian cancer (Hatakeyama 2011). Furthermore, various *in vitro* experiments revealed that the knockdown of TRIM25 resulted in suppression of cancer cell proliferation within lung and breast cancer cells (Horie *et al.* 2003; Qin *et al.* 2016), supporting a tumorigenic role of TRIM25 in all these cancers.

Currently, there are only a few studies which did investigate the expression and possible function of TRIM25 in the pathogenesis of colorectal cancer (Sun *et al.* 2017). The present study identified TRIM25 as a so far unrecognized RNA-binding protein of caspase-2 mRNA that negatively interferes with the translation of caspase-2, thereby contributing to chemotherapeutic drug resistance of colon carcinoma cells. For this reason, a specific interference with the negative TRIM25-caspase-2 axis may offer an attractive avenue for novel

target-specific anti-tumor therapies. In this context, different strategies could be principally used for targeting TRIM25.

One of the strategies is the implementation of transient TRIM25 knockdown approaches as adjuvant therapy of established anticancer therapies. This requires the successful application of siRNAs to inhibit the expression of TRIM25, specifically within the colon carcinoma cells. Importantly, several siRNAs approaches have already reached clinical trials for cancer therapy (Mahmoodi Chalbatani *et al.* 2019). One of the first RNAi-based drugs, which is currently in the clinical use is Patisiran, which targets the RNA coding for transthyretin and which is designed for the treatment of familial amyloid polyneuropathy (Hoy 2018). The successful use of siRNA mediated depletion of TRIM25 may, therefore, interfere with its different tumorigenic activities described before. Mechanistically, the delivery of siRNA within the cell will reduce the expression of TRIM25, mainly at the RNA level, without affecting the TRIM25 gene. Thus the transient silencing by the siRNA can be applied at any stage of disease as a kind of adjuvant therapy, especially before the administration of chemotherapeutic drugs. Technically, the effective delivery of unstable siRNA to the target tumor sites could be facilitated by the use of nanoparticles that protect the siRNAs from rapid plasmatic degradation or any undesirable immune responses (Tatiparti *et al.* 2017). A major problem that remains is the specific targeting of the siRNAs to only the tumor cells. Another attractive strategy to interfere efficiently with dysregulated TRIM25 activities in colorectal cancer includes the manipulation of gene expression of TRIM25 on the genome level by using CRISPR/Cas9-mediated gene editing. Currently, CRISPR/Cas9 gene-mediated editing of several oncogenes are tested in clinical trials for different human cancers, e.g., the **p**rogrammed **d**eath protein PD-1, which puts the brakes

on a cell's immune response and which is critical for the increased proliferation of B-lymphoma cells (Cyranoski 2016). In contrast to the effects which may occur upon transient TRIM25 silencing approaches, the depletion of TRIM25 by CRISPR/Cas9 may disrupt the constitutive interaction between TRIM25 and caspase-2 and thereby inducing long term inhibition of tumor cell survival. Concerning the fact that TRIM25 is also critically involved in a variety of diverse physiological functions (described in section 3.5), the potential benefits and side effects of targeting TRIM25 should be thoroughly balanced before implementing this approach in any human studies. Finally, an approach which specifically targets the ligase activity of TRIM25 is the use of pharmacological E3 ligase inhibitors. Meanwhile, there are several E3 inhibitors which are tested in clinical trials e.g. those targeting the E3 ligase MDM2 or inhibitors of apoptosis proteins (IAPs) (Landre *et al.* 2014). Consequently, if the E3 ligase activity of TRIM25 is crucial for its tumorigenic effects, these inhibitors may be additionally be used for blocking the caspase-2 inhibitory effects by TRIM25. However, to best of my knowledge, curretnly there is no specific inhibitor available for TRIM25. Here, I could demonstrate that TRIM25 may constitute a putative target of auto-ubiquitination that needs to be determined by further experiments. Hence, the use of E3 ligase inhibitors for inhibition of TRIM25 seems only reasonable if the auto-ubiquitination of TRIM25 would impair rather than promote its degradation. Therefore, the understanding of the E3 ligase function in the control of the negative TRIM25-caspase-2 axis is an essential requirement for evaluating the potential benefits of using pharmacological E3 ligase inhibitors in colon carcinoma.

Graphical summary

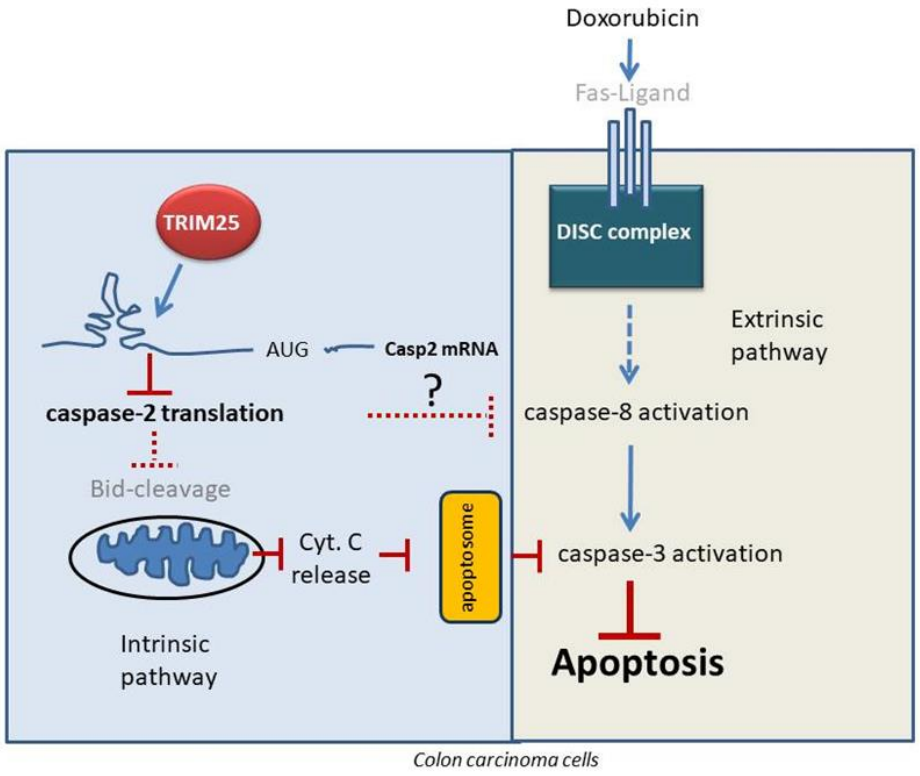

Figure 23. The postulated consequences of constitutive caspase-2 inhibition by TRIM25: An inhibition of caspase-2 synthesis as a result of constitutive TRIM25 binding to the 5´UTR of caspase-2-5´UTR leads to impaired intrinsic apoptosis (blue box) mainly via reducing BID cleavage and subsequently cytochrome c release from mitochondria. This will result in the impaired apoptosome complex formation. As a further consequence, the activation of executioner caspases induced, e.g., via the extrinsic and Fas ligand-mediated apoptosis pathway (green box) by chemotherapeutic agents, e.g., doxorubicin, will be blunted. The activation of executioner caspases induced parallelly by extrinsic Fas ligand-mediated chemotherapeutic agents, e.g., doxorubicin will be blunted. Thus the decrease of the thresholds which activate both cell death pathways (intrinsic and extrinsic) via lowering caspase-2 protein contents may essentially contribute to the increased resistance of cancer cells towards drug-induced apoptosis and represent a so far unrecognized cell survival mechanism in tumor cells.

8. References

1) Adams, J. M. and S. Cory (**2007**). The Bcl-2 apoptotic switch in cancer development and therapy. **Oncogene** 26(9):1324-1337.

2) Aghabozorgi, A. S., A. Bahreyni, A. Soleimani, A. Bahrami, M. Khazaei, G. A. Ferns, A. Avan and S. M. Hassanian (**2019**). Role of adenomatous polyposis coli (APC) gene mutations in the pathogenesis of colorectal cancer; current status and perspectives. **Biochimie** 157:64-71.

3) Ashkenazi, A. (**2008**). Directing cancer cells to self-destruct with pro-apoptotic receptor agonists. **Nat Rev Drug Discov** 7(12):1001-1012.

4) ATLAS, T. H. P. (2020, March 6). "CASP2." from https://www.proteinatlas.org/ENSG00000106144-CASP2/pathology.

5) ATLAS, T. H. P. (2020. March 16). "TRIM25." from https://www.proteinatlas.org/ENSG00000121060-TRIM25/cell.

6) Audic, Y. and R. S. Hartley (**2004**). Post-transcriptional regulation in cancer. **Biol Cell** 96(7):479-498.

7) Badawi, A., A. Biyanee, U. Nasrullah, S. Winslow, T. Schmid, J. Pfeilschifter and W. Eberhardt (**2018**). Inhibition of IRES-dependent translation of caspase-2 by HuR confers chemotherapeutic drug resistance in colon carcinoma cells. **Oncotarget** 9(26):18367-18385.

8) Badawi, A., S. Hehlgans, J. Pfeilschifter, F. Rodel and W. Eberhardt (**2017**). Silencing of the mRNA-binding protein HuR increases the sensitivity of colorectal cancer cells to ionizing radiation through upregulation of caspase-2. **Cancer Lett** 393:103-112.

9) Baliga, B. C., S. H. Read and S. Kumar (**2004**). The biochemical mechanism of caspase-2 activation. **Cell Death Differ** 11(11):1234-1241.

10) Bao, Q. and Y. Shi (**2007**). Apoptosome: a platform for the activation of initiator caspases. **Cell Death Differ** 14(1):56-65.

11) Benke, S., B. Agerer, L. Haas, M. Stoger, A. Lercher, L. Gabler, I. Kiss, S. Scinicariello, W. Berger, A. Bergthaler, A. C. Obenauf and G. A. Versteeg (**2018**). Human tripartite motif protein 52 is required for cell context-dependent proliferation. **Oncotarget** 9(17):13565-13581.

12) Bergeron, L., G. I. Perez, G. Macdonald, L. Shi, Y. Sun, A. Jurisicova, S. Varmuza, K. E. Latham, J. A. Flaws, J. C. Salter, H. Hara, M. A. Moskowitz, E. Li, A. Greenberg, J. L. Tilly and J. Yuan (**1998**). Defects in regulation of apoptosis in caspase-2-deficient mice. **Genes Dev** 12(9):1304-1314.

13) Boatright, K. M. and G. S. Salvesen (**2003**). Mechanisms of caspase activation. **Curr Opin Cell Biol** 15(6):725-731.

14) Bostan, M., M. Mihaila, C. Hotnog, C. Bleotu, G. Anton, V. Roman and L. I. Brasoveanu (**2016**). Modulation of Apoptosis in Colon Cancer Cells by Bioactive Compounds. **Colorectal Cancer - from Pathogenesis to Treatment**:51-87.

15) Bouchier-Hayes, L. (**2010**). The role of caspase-2 in stress-induced apoptosis. **J Cell Mol Med** 14(6A):1212-1224.

16) Bouchier-Hayes, L. and D. R. Green (**2012**). Caspase-2: the orphan caspase. **Cell Death Differ** 19(1):51-57.

17) Brooks, S. A. (**2010**). Functional interactions between mRNA turnover and surveillance and the ubiquitin proteasome system. **Wiley Interdiscip Rev RNA** 1(2):240-252.

18) Brown, C. J., C. F. Cheok, C. S. Verma and D. P. Lane (**2011**). Reactivation of p53: from peptides to small molecules. **Trends Pharmacol Sci** 32(1):53-62.

19) Butt, A. J., N. L. Harvey, G. Parasivam and S. Kumar (**1998**). Dimerization and autoprocessing of the Nedd2 (caspase-2) precursor requires both the prodomain and the carboxyl-terminal regions. **J Biol Chem** 273(12):6763-6768.

20) Callis, J. (**2014**). The ubiquitination machinery of the ubiquitin system. **Arabidopsis Book** 12:e0174.

21) Cano, F., H. Bye, L. M. Duncan, K. Buchet-Poyau, M. Billaud, M. R. Wills and P. J. Lehner (**2012**). The RNA-binding E3 ubiquitin ligase MEX-3C links ubiquitination with MHC-I mRNA degradation. **EMBO J** 31(17):3596-3606.

22) Cano, F., D. Miranda-Saavedra and P. J. Lehner (**2010**). RNA-binding E3 ubiquitin ligases: novel players in nucleic acid regulation. **Biochem Soc Trans** 38(6):1621-1626.

23) Cano, F., D. M. Saavedra and P. J. Lehner (**2010**). RNA-binding E3 ubiquitin ligases: novel nucleic acid regulation. **Biochem Soc Trans** 38:1621-1626.

24) Casiano, C. A., R. L. Ochs and E. M. Tan (**1998**). Distinct cleavage products of nuclear proteins in apoptosis and necrosis revealed by autoantibody probes. **Cell Death Differ** 5(2):183-190.

25) Castanier, C., N. Zemirli, A. Portier, D. Garcin, N. Bidere, A. Vazquez and D. Arnoult (**2012**). MAVS ubiquitination by the E3 ligase TRIM25 and degradation by the proteasome is involved in type I interferon production after activation of the antiviral RIG-I-like receptors. **BMC Biol** 10:44.

26) Choudhury, N. R., G. Heikel, M. Trubitsyna, P. Kubik, J. S. Nowak, S. Webb, S. Granneman, C. Spanos, J. Rappsilber, A. Castello and G. Michlewski (**2017**). RNA-binding activity of TRIM25 is mediated by its PRY/SPRY domain and is required for ubiquitination. **BMC Biol** 15.

27) Choudhury, N. R., J. S. Nowak, J. Zuo, J. Rappsilber, S. H. Spoel and G. Michlewski (**2014**). Trim25 Is an RNA-Specific Activator of Lin28a/TuT4-Mediated Uridylation. **Cell Rep** 9(4):1265-1272.

28) Conaway, R. C., C. S. Brower and J. W. Conaway (**2002**). Emerging roles of ubiquitin in transcription regulation. **Science** 296(5571):1254-1258.

29) Crawford, L. J., C. K. Johnston and A. E. Irvine (**2018**). TRIM proteins in blood cancers. **J Cell Commun Signal** 12(1):21-29.

30) Cyranoski, D. (**2016**). CRISPR gene-editing tested in a person for the first time. **Nature** 539(7630):479.

31) Dai, H., P. Zhang, S. Zhao, J. Zhang and B. Wang (**2009**). Regulation of the vascular endothelial growth factor and growth by estrogen and antiestrogens through Efp in Ishikawa endometrial carcinoma cells. **Oncol Rep** 21(2):395-401.

32) Danial, N. N. and S. J. Korsmeyer (**2004**). Cell death: critical control points. **Cell** 116(2):205-219.

33) Dawar, S., Y. Lim, J. Puccini, M. White, P. Thomas, L. Bouchier-Hayes, D. R. Green, L. Dorstyn and S. Kumar (**2017**). Caspase-2-mediated cell death is required for deleting aneuploid cells. **Oncogene** 36(19):2704-2714.

34) De Rosa, M., U. Pace, D. Rega, V. Costabile, F. Duraturo, P. Izzo and P. Delrio (**2015**). Genetics, diagnosis and management of colorectal cancer (Review). **Oncol Rep** 34(3):1087-1096.

35) Degterev, A., M. Boyce and J. Yuan (**2003**). A decade of caspases. **Oncogene** 22(53):8543-8567.

36) Deol, K. K., S. Lorenz and E. R. Strieter (**2019**). Enzymatic Logic of Ubiquitin Chain Assembly. **Frontiers in Physiology** 10.

37) Di, K., M. E. Linskey and D. A. Bota (**2013**). TRIM11 is overexpressed in high-grade gliomas and promotes proliferation, invasion, migration and glial tumor growth. **Oncogene** 32(42):5038-5047.

38) Dorstyn, L. and S. Kumar (**2009**). Putative functions of caspase-2. **F1000 Biol Rep** 1:96.

39) Droin, N., M. Beauchemin, E. Solary and R. Bertrand (**2000**). Identification of a caspase-2 isoform that behaves as an endogenous inhibitor of the caspase cascade. **Cancer Res** 60(24):7039-7047.

40) Droin, N., M. Beauchemin, E. Solary and R. Bertrand (**2000**). Identification of a caspase-2 isoform that behaves as an endogenous inhibitor of the caspase cascade. **Cancer Res** 60(24):7039-7047.

41) Eberhardt, W., U. Nasrullah and K. Haeussler (**2019**). Inhibition of Caspase-2 Translation by the mRNA Binding Protein HuR: A Novel Path of Therapy Resistance in Colon Carcinoma Cells? **Cells** 8(8).

42) Eckhart, L., C. Ballaun, M. Hermann, J. L. VandeBerg, W. Sipos, A. Uthman, H. Fischer and E. Tschachler (**2008**). Identification of novel mammalian caspases reveals an important role of gene loss in shaping the human caspase repertoire. **Mol Biol Evol** 25(5):831-841.

43) Elmore, S. (**2007**). Apoptosis: a review of programmed cell death. **Toxicol Pathol** 35(4):495-516.

44) Feracci, M., J. N. Foot, S. N. Grellscheid, M. Danilenko, R. Stehle, O. Gonchar, H. S. Kang, C. Dalgliesh, N. H. Meyer, Y. Liu, A. Lahat, M. Sattler, I. C. Eperon, D. J. Elliott and C. Dominguez (**2016**). Structural basis of RNA recognition and dimerization by the STAR proteins T-STAR and Sam68. **Nat Commun** 7:10355.

45) Ferlay, J., M. Colombet, I. Soerjomataram, T. Dyba, G. Randi, M. Bettio, A. Gavin, O. Visser and F. Bray (**2018**). Cancer incidence and mortality patterns in Europe: Estimates for 40 countries and 25 major cancers in 2018. **Eur J Cancer** 103:356-387.

46) Fu, J. J., X. Y. Lv, H. Y. Lin, L. Wu, R. Wang, Z. Zhou, B. H. Zhang, Y. L. Wang, B. K. Tsang, C. Zhu and H. M. Wang (**2010**). Ubiquitin Ligase Cullin 7 Induces Epithelial-Mesenchymal Transition in Human Choriocarcinoma Cells. **Journal of Biological Chemistry** 285(14):10870-10879.

47) Fuentes-Prior, P. and G. S. Salvesen (**2004**). The protein structures that shape caspase activity, specificity, activation and inhibition. **Biochem J** 384(Pt 2):201-232.

48) Fulda, S. and K. M. Debatin (**2003**). Death receptor signaling in cancer therapy. **Curr Med Chem Anticancer Agents** 3(4):253-262.

49) Gack, M. U., A. Kirchhofer, Y. C. Shin, K. S. Inn, C. Liang, S. Cui, S. Myong, T. Ha, K. P. Hopfner and J. U. Jung (**2008**). Roles of RIG-I N-terminal tandem CARD and splice variant in TRIM25-mediated antiviral signal transduction. **Proc Natl Acad Sci U S A** 105(43):16743-16748.

50) Gack, M. U., Y. C. Shin, C. H. Joo, T. Urano, C. Liang, L. Sun, O. Takeuchi, S. Akira, Z. Chen, S. Inoue and J. U. Jung (**2007**). TRIM25 RING-finger E3 ubiquitin ligase is essential for RIG-I-mediated antiviral activity. **Nature** 446(7138):916-920.

51) Gillen, C. D., H. A. Andrews, P. Prior and R. N. Allan (**1994**). Crohn's disease and colorectal cancer. **Gut** 35(5):651-655.

52) Goldar, S., M. S. Khaniani, S. M. Derakhshan and B. Baradaran (**2015**). Molecular mechanisms of apoptosis and roles in cancer development and treatment. **Asian Pac J Cancer Prev** 16(6):2129-2144.

53) Gong, J., J. Cao, G. Liu and J. R. Huo (**2015**). Function and mechanism of F-box proteins in gastric cancer (Review). **Int J Oncol** 47(1):43-50.

54) Green, D. R. and G. Kroemer (**2004**). The pathophysiology of mitochondrial cell death. **Science** 305(5684):626-629.

55) Green, D. R. and F. Llambi (**2015**). Cell Death Signaling. **Cold Spring Harb Perspect Biol** 7(12).

56) Guicciardi, M. E. and G. J. Gores (**2009**). Life and death by death receptors. **FASEB J** 23(6):1625-1637.

57) Guo, Y., S. M. Srinivasula, A. Druilhe, T. Fernandes-Alnemri and E. S. Alnemri (**2002**). Caspase-2 induces apoptosis by releasing proapoptotic proteins from mitochondria. **J Biol Chem** 277(16):13430-13437.

58) Gushchina, L. V., T. A. Kwiatkowski, S. Bhattacharya and N. L. Weisleder (**2018**). Conserved structural and functional aspects of the tripartite motif gene family point towards therapeutic applications in multiple diseases. **Pharmacol Ther** 185:12-25.

59) Han, C. H., R. Zhao, J. Kroger, M. H. Qu, A. A. Wani and Q. E. Wang (**2013**). Caspase-2 Short Isoform Interacts with Membrane-Associated Cytoskeleton Proteins to Inhibit Apoptosis. **PLoS One** 8(7).

60) Harrigan, J. A., X. Jacq, N. M. Martin and S. P. Jackson (**2018**). Deubiquitylating enzymes and drug discovery: emerging opportunities. **Nat Rev Drug Discov** 17(1):57-78.

61) Hassan, M., H. Watari, A. AbuAlmaaty, Y. Ohba and N. Sakuragi (**2014**). Apoptosis and molecular targeting therapy in cancer. **Biomed Res Int** 2014:150845.

62) Hatakeyama, S. (**2011**). TRIM proteins and cancer. **Nat Rev Cancer** 11(11):792-804.

63) Hatakeyama, S. (**2017**). TRIM Family Proteins: Roles in Autophagy, Immunity, and Carcinogenesis. **Trends Biochem Sci** 42(4):297-311.

64) Heikel, G., N. R. Choudhury and G. Michlewski (**2016**). The role of Trim25 in development, disease and RNA metabolism. **Biochem Soc Trans** 44(4):1045-1050.

65) Ho, L. H., R. Taylor, L. Dorstyn, D. Cakouros, P. Bouillet and S. Kumar (**2009**). A tumor suppressor function for caspase-2. **Proc Natl Acad Sci U S A** 106(13):5336-5341.

66) Horie, K., T. Urano, K. Ikeda and S. Inoue (**2003**). Estrogen-responsive RING finger protein controls breast cancer growth. **J Steroid Biochem Mol Biol** 85(2-5):101-104.

67) Hoy, S. M. (**2018**). Patisiran: First Global Approval. **Drugs** 78(15):1625-1631.

68) Imre, G., J. Heering, A. N. Takeda, M. Husmann, B. Thiede, D. M. zu Heringdorf, D. R. Green, F. G. van der Goot, B. Sinha, V. Dotsch and K. Rajalingam (**2012**). Caspase-2 is an initiator caspase responsible for pore-forming toxin-mediated apoptosis. **EMBO J** 31(11):2615-2628.

69) Inoue, S., A. Orimo, T. Hosoi, S. Kondo, H. Toyoshima, T. Kondo, A. Ikegami, Y. Ouchi, H. Orimo and M. Muramatsu (**1993**). Genomic binding-site cloning reveals an estrogen-responsive gene that encodes a RING finger protein. **Proc Natl Acad Sci U S A** 90(23):11117-11121.

70) Jin, Z. and W. S. El-Deiry (**2005**). Overview of cell death signaling pathways. **Cancer Biol Ther** 4(2):139-163.

71) Joazeiro, C. A., S. S. Wing, H. Huang, J. D. Leverson, T. Hunter and Y. C. Liu (**1999**). The tyrosine kinase negative regulator c-Cbl as a RING-type, E2-dependent ubiquitin-protein ligase. **Science** 286(5438):309-312.

72) Kano, S., N. Miyajima, S. Fukuda and S. Hatakeyama (**2008**). Tripartite motif protein 32 facilitates cell growth and migration via degradation of Abl-interactor 2. **Cancer Res** 68(14):5572-5580.

73) Kerr, J. F., A. H. Wyllie and A. R. Currie (**1972**). Apoptosis: a basic biological phenomenon with wide-ranging implications in tissue kinetics. **Br J Cancer** 26(4):239-257.

74) Keum, N. and E. Giovannucci (**2019**). Global burden of colorectal cancer: emerging trends, risk factors and prevention strategies. **Nat Rev Gastroenterol Hepatol** 16(12):713-732.

75) Kim, I. R., K. Murakami, N. J. Chen, S. D. Saibil, E. Matysiak-Zablocki, A. R. Elford, M. Bonnard, S. Benchimol, A. Jurisicova, W. C. Yeh and P. S. Ohashi (**2009**). DNA damage- and stress-induced apoptosis occurs independently of PIDD. **Apoptosis** 14(9):1039-1049.

76) Kiraz, Y., A. Adan, M. Kartal Yandim and Y. Baran (**2016**). Major apoptotic mechanisms and genes involved in apoptosis. **Tumour Biol** 37(7):8471-8486.

77) Kitevska, T., S. J. Roberts, D. Pantaki-Eimany, S. E. Boyd, F. L. Scott and C. J. Hawkins (**2014**). Analysis of the minimal specificity of caspase-2 and identification of Ac-VDTTD-AFC as a caspase-2-selective peptide substrate. **Biosci Rep** 34(2).

78) Koliopoulos, M. G., M. Lethier, A. G. van der Veen, K. Haubrich, J. Hennig, E. Kowalinski, R. V. Stevens, S. R. Martin, E. S. C. Reis, S. Cusack and K. Rittinger (**2018**). Molecular mechanism of influenza A NS1-mediated TRIM25 recognition and inhibition. **Nat Commun** 9(1):1820.

79) Kroemer, G., L. Galluzzi and C. Brenner (**2007**). Mitochondrial membrane permeabilization in cell death. **Physiol Rev** 87(1):99-163.

80) Krumschnabel, G., B. Sohm, F. Bock, C. Manzl and A. Villunger (**2009**). The enigma of caspase-2: the laymen's view. **Cell Death Differ** 16(2):195-207.

81) Kumar, S. (**2007**). Caspase function in programmed cell death. **Cell Death Differ** 14(1):32-43.

82) Kumar, S. (**2009**). Caspase 2 in apoptosis, the DNA damage response and tumour suppression: enigma no more? **Nature Reviews Cancer** 9(12):897-903.

83) Kumar, S., M. Kinoshita, M. Noda, N. G. Copeland and N. A. Jenkins (**1994**). Induction of apoptosis by the mouse Nedd2 gene, which encodes a protein similar to the product of the Caenorhabditis elegans cell death gene ced-3 and the mammalian IL-1 beta-converting enzyme. **Genes Dev** 8(14):1613-1626.

84) Kuribayashi, K., P. A. Mayes and W. S. El-Deiry (**2006**). What are caspases 3 and 7 doing upstream of the mitochondria? **Cancer Biol Ther** 5(7):763-765.

85) Kwon, S. C., H. Yi, K. Eichelbaum, S. Fohr, B. Fischer, K. T. You, A. Castello, J. Krijgsveld, M. W. Hentze and V. N. Kim (**2013**). The RNA-binding protein repertoire of embryonic stem cells. **Nat Struct Mol Biol** 20(9):1122-+.

86) Laemmli, U. K. (**1970**). Cleavage of structural proteins during the assembly of the head of bacteriophage T4. **Nature** 227(5259):680-685.

87) Landre, V., B. Rotblat, S. Melino, F. Bernassola and G. Melino (**2014**). Screening for E3-Ubiquitin ligase inhibitors: challenges and opportunities. **Oncotarget** 5(18):7988-8013.

88) Lavrik, I. N., A. Golks, S. Baumann and P. H. Krammer (**2006**). Caspase-2 is activated at the CD95 death-inducing signaling complex in the course of CD95-induced apoptosis. **Blood** 108(2):559-565.

89) Lavrik, I. N., A. Golks and P. H. Krammer (**2005**). Caspases: pharmacological manipulation of cell death. **J Clin Invest** 115(10):2665-2672.

90) Lee, J. Y., S. B. Jee, W. Y. Park, Y. J. Choi, B. Kim, Y. H. Kim and Y. Jun do (**2014**). Tumor suppressor protein p53 promotes 2-methoxyestradiol-induced activation of Bak and Bax, leading to mitochondria-dependent apoptosis in human colon cancer HCT116 cells. **J Microbiol Biotechnol** 24(12):1654-1663.

91) Legrand, N., D. A. Dixon and C. Sobolewski (**2019**). AU-rich element-binding proteins in colorectal cancer. **World J Gastrointest Oncol** 11(2):71-90.

92) Li, H., L. Bergeron, V. Cryns, M. S. Pasternack, H. Zhu, L. Shi, A. Greenberg and J. Yuan (**1997**). Activation of caspase-2 in apoptosis. **J Biol Chem** 272(34):21010-21017.

93) Li, J. and J. Yuan (**2008**). Caspases in apoptosis and beyond. **Oncogene** 27(48):6194-6206.

94) Li, M. M., Z. Lau, P. Cheung, E. G. Aguilar, W. M. Schneider, L. Bozzacco, H. Molina, E. Buehler, A. Takaoka, C. M. Rice, D. P. Felsenfeld and M. R. MacDonald (**2017**). TRIM25 Enhances the Antiviral Action of Zinc-Finger Antiviral Protein (ZAP). **PLoS Pathog** 13(1):e1006145.

95) Li, Q. Q., T. J. Liu, S. S. Yang and Z. L. Zhang (**2019**). Upregulation of miR-34a by Inhibition of IRE1 alpha Has Protective Effect against A beta-Induced Injury in SH-SY5Y Cells by Targeting Caspase-2. **Oxid Med Cell Longev**.

96) Lippincott-Schwartz, T. P. W. E. J. L.-S. T. P. W. E. J. (2007, April 18). Introduction to the Cell Cycle, Elsevier.

97) Liu, H., D. Su, J. Zhang, S. Ge, Y. Li, F. Wang, M. Gravel, A. Roulston, Q. Song, W. Xu, J. G. Liang, G. Shore, X. Wang and P. Liang (**2017**). Improvement of Pharmacokinetic Profile of TRAIL via Trimer-Tag Enhances its Antitumor Activity in vivo. **Sci Rep** 7(1):8953.

98) Liu, X., Q. Ji, Z. Fan and Q. Li (**2015**). Cellular signaling pathways implicated in metastasis of colorectal cancer and the associated targeted agents. **Future Oncol** 11(21):2911-2922.

99) Locksley, R. M., N. Killeen and M. J. Lenardo (**2001**). The TNF and TNF receptor superfamilies: integrating mammalian biology. **Cell** 104(4):487-501.

100) Lomonosova, E. and G. Chinnadurai (**2008**). BH3-only proteins in apoptosis and beyond: an overview. **Oncogene** 27 Suppl 1:S2-19.

101) Lopez-Garcia, C., L. Sansregret, E. Domingo, N. McGranahan, S. Hobor, N. J. Birkbak, S. Horswell, E. Gronroos, F. Favero, A. J. Rowan, N. Matthews, S. Begum, B. Phillimore, R. Burrell, D. Oukrif, B. Spencer-Dene, M. Kovac, G. Stamp, A. Stewart, H. Danielsen, M. Novelli, I. Tomlinson and C. Swanton (**2017**). BCL9L Dysfunction Impairs Caspase-2 Expression Permitting Aneuploidy Tolerance in Colorectal Cancer. **Cancer Cell** 31(1):79-93.

102) Lorick, K. L., J. P. Jensen, S. Fang, A. M. Ong, S. Hatakeyama and A. M. Weissman (**1999**). RING fingers mediate ubiquitin-conjugating enzyme (E2)-dependent ubiquitination. **Proc Natl Acad Sci U S A** 96(20):11364-11369.

103) Lunde, B. M., C. Moore and G. Varani (**2007**). RNA-binding proteins: modular design for efficient function. **Nat Rev Mol Cell Biol** 8(6):479-490.

104) Mahmoodi Chalbatani, G., H. Dana, E. Gharagouzloo, S. Grijalvo, R. Eritja, C. D. Logsdon, F. Memari, S. R. Miri, M. R. Rad and V. Marmari (**2019**). Small interfering RNAs (siRNAs) in cancer therapy: a nano-based approach. **Int J Nanomedicine** 14:3111-3128.

105) Mandell, M. A., A. Jain, J. Arko-Mensah, S. Chauhan, T. Kimura, C. Dinkins, G. Silvestri, J. Munch, F. Kirchhoff, A. Simonsen, Y. Wei, B. Levine, T. Johansen and V. Deretic (**2014**). TRIM proteins regulate autophagy and can target autophagic substrates by direct recognition. **Dev Cell** 30(4):394-409.

106) Manzl, C., G. Krumschnabel, F. Bock, B. Sohm, V. Labi, F. Baumgartner, E. Logette, J. Tschopp and A. Villunger (**2009**). Caspase-2 activation in the absence of PIDDosome formation. **J Cell Biol** 185(2):291-303.

107) Marley, A. R. and H. Nan (**2016**). Epidemiology of colorectal cancer. **Int J Mol Epidemiol Genet** 7(3):105-114.

108) Martinon, F. and J. Tschopp (**2007**). Inflammatory caspases and inflammasomes: master switches of inflammation. **Cell Death Differ** 14(1):10-22.

109) McCubrey, J. A., L. S. Steelman, C. R. Kempf, W. H. Chappell, S. L. Abrams, F. Stivala, G. Malaponte, F. Nicoletti, M. Libra, J. Basecke, D. Maksimovic-Ivanic, S. Mijatovic, G. Montalto, M. Cervello, L. Cocco and A. M. Martelli (**2011**). Therapeutic resistance resulting from mutations in Raf/MEK/ERK and PI3K/PTEN/Akt/mTOR signaling pathways. **J Cell Physiol** 226(11):2762-2781.

110) McNab, F. W., R. Rajsbaum, J. P. Stoye and A. O'Garra (**2011**). Tripartite-motif proteins and innate immune regulation. **Curr Opin Immunol** 23(1):46-56.

111) Meroni, G. and G. Diez-Roux (**2005**). TRIM/RBCC, a novel class of 'single protein RING finger' E3 ubiquitin ligases. **Bioessays** 27(11):1147-1157.

112) Morreale, F. E. and H. Walden (**2016**). Types of Ubiquitin Ligases. **Cell** 165(1):248-248 e241.

113) Nasrullah, U., K. Haeussler, A. Biyanee, I. Wittig, J. Pfeilschifter and W. Eberhardt (**2019**). Identification of TRIM25 as a Negative Regulator of Caspase-2 Expression Reveals a Novel Target for Sensitizing Colon Carcinoma Cells to Intrinsic Apoptosis. **Cells** 8(12).

114) Neochoritis, C. G., K. Wang, N. Estrada-Ortiz, E. Herdtweck, K. Kubica, A. Twarda, K. M. Zak, T. A. Holak and A. Domling (**2015**). 2,30-Bis(10H-indole) heterocycles: New p53/MDM2/MDMX antagonists. **Bioorg Med Chem Lett** 25(24):5661-5666.

115) Norbury, C. J. and I. D. Hickson (**2001**). Cellular responses to DNA damage. **Annu Rev Pharmacol Toxicol** 41:367-401.

116) Oines, M., L. M. Helsingen, M. Bretthauer and L. Emilsson (**2017**). Epidemiology and risk factors of colorectal polyps. **Best Pract Res Clin Gastroenterol** 31(4):419-424.

117) Olsson, M., J. Forsberg and B. Zhivotovsky (**2015**). Caspase-2: the reinvented enzyme. **Oncogene** 34(15):1877-1882.

118) Olsson, M., H. Vakifahmetoglu, P. M. Abruzzo, K. Hogstrand, A. Grandien and B. Zhivotovsky (**2009**). DISC-mediated activation of caspase-2 in DNA damage-induced apoptosis. **Oncogene** 28(18):1949-1959.

119) Ozato, K., D. M. Shin, T. H. Chang and H. C. Morse, 3rd (**2008**). TRIM family proteins and their emerging roles in innate immunity. **Nat Rev Immunol** 8(11):849-860.

120) Parrish, A. B., C. D. Freel and S. Kornbluth (**2013**). Cellular mechanisms controlling caspase activation and function. **Cold Spring Harb Perspect Biol** 5(6).

121) Petroski, M. D. and R. J. Deshaies (**2003**). Context of multiubiquitin chain attachment influences the rate of Sic1 degradation. **Mol Cell** 11(6):1435-1444.

122) Petroski, M. D. and R. J. Deshaies (**2005**). Function and regulation of cullin-RING ubiquitin ligases. **Nat Rev Mol Cell Biol** 6(1):9-20.

123) Pfeffer, C. M. and A. T. K. Singh (**2018**). Apoptosis: A Target for Anticancer Therapy. **Int J Mol Sci** 19(2).

124) Pfoh, R., I. K. Lacdao and V. Saridakis (**2015**). Deubiquitinases and the new therapeutic opportunities offered to cancer. **Endocr Relat Cancer** 22(1):T35-54.

125) Pistritto, G., D. Trisciuoglio, C. Ceci, A. Garufi and G. D'Orazi (**2016**). Apoptosis as anticancer mechanism: function and dysfunction of its modulators and targeted therapeutic strategies. **Aging (Albany NY)** 8(4):603-619.

126) Plati, J., O. Bucur and R. Khosravi-Far (**2008**). Dysregulation of apoptotic signaling in cancer: molecular mechanisms and therapeutic opportunities. **J Cell Biochem** 104(4):1124-1149.

127) Pop, C. and G. S. Salvesen (**2009**). Human caspases: activation, specificity, and regulation. **J Biol Chem** 284(33):21777-21781.

128) Puccini, J., L. Dorstyn and S. Kumar (**2013**). Caspase-2 as a tumour suppressor. **Cell Death Differ** 20(9):1133-1139.

129) Qin, Y., H. Cui and H. Zhang (**2016**). Overexpression of TRIM25 in Lung Cancer Regulates Tumor Cell Progression. **Technol Cancer Res Treat** 15(5):707-715.

130) Rajsbaum, R., R. A. Albrecht, M. K. Wang, N. P. Maharaj, G. A. Versteeg, E. Nistal-Villan, A. Garcia-Sastre and M. U. Gack (**2012**). Species-specific inhibition of RIG-I ubiquitination and IFN induction by the influenza A virus NS1 protein. **PLoS Pathog** 8(11):e1003059.

131) Read, S. H., B. C. Baliga, P. G. Ekert, D. L. Vaux and S. Kumar (**2002**). A novel Apaf-1-independent putative caspase-2 activation complex. **J Cell Biol** 159(5):739-745.

132) Reymond, A., G. Meroni, A. Fantozzi, G. Merla, S. Cairo, L. Luzi, D. Riganelli, E. Zanaria, S. Messali, S. Cainarca, A. Guffanti, S. Minucci, P. G. Pelicci and A. Ballabio (**2001**). The tripartite motif family identifies cell compartments. **EMBO J** 20(9):2140-2151.

133) Sadowski, M., R. Suryadinata, A. R. Tan, S. N. Roesley and B. Sarcevic (**2012**). Protein monoubiquitination and polyubiquitination generate structural diversity to control distinct biological processes. **IUBMB Life** 64(2):136-142.

134) Sakamaki, K. and Y. Satou (**2009**). Caspases: evolutionary aspects of their functions in vertebrates. **J Fish Biol** 74(4):727-753.

135) Sakuma, M., J. Akahira, T. Suzuki, S. Inoue, K. Ito, T. Moriya, H. Sasano, K. Okamura and N. Yaegashi (**2005**). Expression of estrogen-responsive finger protein (Efp) is associated with advanced disease in human epithelial ovarian cancer. **Gynecol Oncol** 99(3):664-670.

136) Sanchez, J. G., K. M. J. Sparrer, C. Chiang, R. A. Reis, J. J. Chiang, M. A. Zurenski, Y. Wan, M. U. Gack and O. Pornillos (**2018**). TRIM25 Binds RNA to Modulate Cellular Anti-viral Defense. **J Mol Biol** 430(24):5280-5293.

137) Schweizer, A., C. Briand and M. G. Grutter (**2003**). Crystal structure of caspase-2, apical initiator of the intrinsic apoptotic pathway. **J Biol Chem** 278(43):42441-42447.

138) Senda, T., A. Shimomura and A. Iizuka-Kogo (**2005**). Adenomatous polyposis coli (Apc) tumor suppressor gene as a multifunctional gene. **Anat Sci Int** 80(3):121-131.

139) Shalini, S., L. Dorstyn, S. Dawar and S. Kumar (**2015**). Old, new and emerging functions of caspases. **Cell Death Differ** 22(4):526-539.

140) Shen, X., J. Li, W. Liao, J. Wang, H. Chen, Y. Yao, H. Liu and K. Ding (**2016**). microRNA-149 targets caspase-2 in glioma progression. **Oncotarget** 7(18):26388-26399.

141) Siegel, R., C. Desantis and A. Jemal (**2014**). Colorectal cancer statistics, 2014. **CA Cancer J Clin** 64(2):104-117.

142) Singh, N. and A. B. Singh (**2016**). Deubiquitinases and cancer: A snapshot. **Crit Rev Oncol Hematol** 103:22-26.

143) Slee, E. A., C. Adrain and S. J. Martin (**1999**). Serial killers: ordering caspase activation events in apoptosis. **Cell Death Differ** 6(11):1067-1074.

144) Smith, P. K., R. I. Krohn, G. T. Hermanson, A. K. Mallia, F. H. Gartner, M. D. Provenzano, E. K. Fujimoto, N. M. Goeke, B. J. Olson and D. C. Klenk (**1985**). Measurement of protein using bicinchoninic acid. **Anal Biochem** 150(1):76-85.

145) Sohn, D., W. Budach and R. U. Janicke (**2011**). Caspase-2 is required for DNA damage-induced expression of the CDK inhibitor p21(WAF1/CIP1). **Cell Death Differ** 18(10):1664-1674.

146) Song, T., X. Zhang, L. Zhang, J. Dong, W. Cai, J. Gao and B. Hong (**2013**). miR-708 promotes the development of bladder carcinoma via direct repression of Caspase-2. **J Cancer Res Clin Oncol** 139(7):1189-1198.

147) Stringer, D. K. and R. C. Piper (**2011**). Terminating protein ubiquitination: Hasta la vista, ubiquitin. **Cell Cycle** 10(18):3067-3071.

148) Sun, N., Y. Xue, T. Dai, X. Li and N. Zheng (**2017**). Tripartite motif containing 25 promotes proliferation and invasion of colorectal cancer cells through TGF-beta signaling. **Biosci Rep** 37(4).

149) Sun, N. F., Y. Xue, T. Dai, X. D. Li and N. X. Zheng (**2017**). Tripartite motif containing 25 promotes proliferation and invasion of colorectal cancer cells through TGF-beta signaling. **Biosci Rep** 37.

150) Suzuki, T., T. Urano, T. Tsukui, K. Horie-Inoue, T. Moriya, T. Ishida, M. Muramatsu, Y. Ouchi, H. Sasano and S. Inoue (**2005**). Estrogen-responsive finger protein as a new potential biomarker for breast cancer. **Clin Cancer Res** 11(17):6148-6154.

151) Swatek, K. N. and D. Komander (**2016**). Ubiquitin modifications. **Cell Res** 26(4):399-422.

152) Tatiparti, K., S. Sau, S. K. Kashaw and A. K. Iyer (**2017**). siRNA Delivery Strategies: A Comprehensive Review of Recent Developments. **Nanomaterials (Basel)** 7(4).

153) Tinel, A. and J. Tschopp (**2004**). The PIDDosome, a protein complex implicated in activation of caspase-2 in response to genotoxic stress. **Science** 304(5672):843-846.

154) Tiwari, M., L. K. Sharma, D. Vanegas, D. A. Callaway, Y. Bai, J. D. Lechleiter and B. Herman (**2014**). A nonapoptotic role for CASP2/caspase 2: modulation of autophagy. **Autophagy** 10(6):1054-1070.

155) Torok, M. and L. D. Etkin (**2001**). Two B or not two B? Overview of the rapidly expanding B-box family of proteins. **Differentiation** 67(3):63-71.

156) Ueyama, K., K. Ikeda, W. Sato, N. Nakasato, K. Horie-Inoue, S. Takeda and S. Inoue (**2010**). Knockdown of Efp by DNA-modified small interfering RNA inhibits breast cancer cell proliferation and in vivo tumor growth. **Cancer Gene Ther** 17(9):624-632.

157) Upton, J. P., K. Austgen, M. Nishino, K. M. Coakley, A. Hagen, D. Han, F. R. Papa and S. A. Oakes (**2008**). Caspase-2 cleavage of BID is a critical apoptotic signal downstream of endoplasmic reticulum stress. **Mol Cell Biol** 28(12):3943-3951.

158) Upton, J. P., K. Austgen, M. Nishino, K. M. Coakley, A. Hagen, D. Han, F. R. Papa and S. A. Oakes (**2008**). Caspase-2 cleavage of BID is a critical apoptotic signal downstream of endoplasmic reticulum stress. **Mol Cell Biol** 28(12):3943-3951.

159) Versteeg, G. A., S. Benke, A. Garcia-Sastre and R. Rajsbaum (**2014**). InTRIMsic immunity: Positive and negative regulation of immune signaling by tripartite motif proteins. **Cytokine Growth Factor Rev** 25(5):563-576.

160) Walsh, L. A., M. J. Alvarez, E. Y. Sabio, M. Reyngold, V. Makarov, S. Mukherjee, K. W. Lee, A. Desrichard, S. Turcan, M. G. Dalin, V. K. Rajasekhar, S. B. Chen, L. T. Vahdat, A. Califano and T. A. Chan (**2017**). An Integrated Systems Biology Approach Identifies TRIM25 as a Key Determinant of Breast Cancer Metastasis. **Cell Rep** 20(7):1623-1640.

161) Wang, L., M. Miura, L. Bergeron, H. Zhu and J. Yuan (**1994**). Ich-1, an Ice/ced-3-related gene, encodes both positive and negative regulators of programmed cell death. **Cell** 78(5):739-750.

162) Wang, S., R. K. Kollipara, C. G. Humphries, S. H. Ma, R. Hutchinson, R. Li, J. Siddiqui, S. A. Tomlins, G. V. Raj and R. Kittler (**2016**). The ubiquitin ligase TRIM25 targets ERG for degradation in prostate cancer. **Oncotarget** 7(40):64921-64931.

163) Watanabe, M. and S. Hatakeyama (**2017**). TRIM proteins and diseases. **J Biochem** 161(2):135-144.

164) Waterman, H., G. Levkowitz, I. Alroy and Y. Yarden (**1999**). The RING finger of c-Cbl mediates desensitization of the epidermal growth factor receptor. **J Biol Chem** 274(32):22151-22154.

165) Winkler, C., A. Doller, G. Imre, A. Badawi, T. Schmid, S. Schulz, N. Steinmeyer, J. Pfeilschifter, K. Rajalingam and W. Eberhardt (**2014**). Attenuation of the ELAV1-like protein HuR sensitizes adenocarcinoma cells to the intrinsic apoptotic pathway by increasing the translation of caspase-2L. **Cell Death & Disease** 5.

166) Xu, G. X., Y. F. Guo, D. B. Xu, Y. Wang, Y. F. Shen, F. F. Wang, Y. Y. Lv, F. L. Song, D. W. Jiang, Y. Q. Zhang, Y. Lou, Y. K. Meng, Y. J. Yang and Y. F. Kang (**2017**). TRIM14 regulates cell proliferation and invasion in osteosarcoma via promotion of the AKT signaling pathway. **Sci Rep** 7.

167) Xue, D., S. Shaham and H. R. Horvitz (**1996**). The Caenorhabditis elegans cell-death protein CED-3 is a cysteine protease with substrate specificities similar to those of the human CPP32 protease. **Genes Dev** 10(9):1073-1083.

168) Yang, L., Y. Dou, Z. Sui, H. Cheng, X. Liu, Q. Wang, P. Gao, Y. Qu and M. Xu (**2020**). Upregulated miRNA-182-5p expression in tumor tissue and peripheral blood samples from patients with non-small cell lung cancer is associated with downregulated Caspase 2 expression. **Exp Ther Med** 19(1):603-610.

169) Yoo, N. J., J. W. Lee, Y. J. Kim, Y. H. Soung, S. Y. Kim, S. W. Nam, W. S. Park, J. Y. Lee and S. H. Lee (**2004**). Loss of caspase-2, -6 and -7 expression in gastric cancers. **APMIS** 112(6):330-335.

170) Yu, J. and L. Zhang (**2004**). Apoptosis in human cancer cells. **Curr Opin Oncol** 16(1):19-24.

171) Zaman, S., R. Wang and V. Gandhi (**2014**). Targeting the apoptosis pathway in hematologic malignancies. **Leuk Lymphoma** 55(9):1980-1992.

172) Zang, H. L., S. N. Ren, H. Cao and X. F. Tian (**2017**). The ubiquitin ligase TRIM25 inhibits hepatocellular carcinoma progression by targeting metastasis associated 1 protein. **IUBMB Life** 69(10):795-801.

173) Zhang, F., Y. Wen and X. Guo (**2014**). CRISPR/Cas9 for genome editing: progress, implications and challenges. **Human Molecular Genetics** 23(R1):R40-46.

174) Zhang, L. and J. Yu (**2013**). Role of apoptosis in colon cancer biology, therapy, and prevention. **Curr Colorectal Cancer Rep** 9(4).

175) Zhang, P., S. Elabd, S. Hammer, V. Solozobova, H. Yan, F. Bartel, S. Inoue, T. Henrich, J. Wittbrodt, F. Loosli, G. Davidson and C. Blattner (**2015**). TRIM25 has a dual function in the p53/Mdm2 circuit. **Oncogene** 34(46):5729-5738.

176) Zhang, Q., Y. Li, M. Zhao, H. Lin, W. J. Wang, D. D. Li, W. Cui, C. H. Zhou, J. L. Zhong and C. Z. Huang (**2019**). MiR-494 acts as a tumor promoter by targeting CASP2 in non-small cell lung cancer. **Sci Rep** 9.

177) Zhang, R., W. P. Zhou, Z. J. Yu, L. Yang, G. Q. Liu, H. T. Yu, Q. Y. Zhou, Z. L. Min, C. X. Zhang, Q. M. Wu, X. M. Hu and Q. Yuan (**2019**). miR-1247-3p mediates apoptosis of cerebral neurons by targeting caspase-2 in stroke. **Brain Research** 1714:18-26.

178) Zhao, K. W., D. Sikriwal, X. Dong, P. Guo, X. Sun and J. T. Dong (**2011**). Oestrogen causes degradation of KLF5 by inducing the E3 ubiquitin ligase EFP in ER-positive breast cancer cells. **Biochem J** 437(2):323-333.

179) Zheng, X., X. Wang, F. Tu, Q. Wang, Z. Fan and G. Gao (**2017**). TRIM25 Is Required for the Antiviral Activity of Zinc Finger Antiviral Protein. **J Virol** 91(9).

180) Zou, W., J. Wang and D. E. Zhang (**2007**). Negative regulation of ISG15 E3 ligase EFP through its autoISGylation. **Biochem Biophys Res Commun** 354(1):321-327.

181) Zou, W. and D. E. Zhang (**2006**). The interferon-inducible ubiquitin-protein isopeptide ligase (E3) EFP also functions as an ISG15 E3 ligase. **J Biol Chem** 281(7):3989-3994.

9. Appendix

9.1. Publications

Usman Nasrullah, Kristina Haeussler, Abhiruchi Biyanee, Ilka Wittig, Josef Pfeilschifter, Wolfgang Eberhardt. Identification of TRIM25 as a Negative Regulator of Caspase-2 Expression Reveals a Novel Target for Sensitizing Colon Carcinoma Cells to Intrinsic Apoptosis. Cells 2019 Dec 12;8(12):1622

Amel Badawi, Abhiruchi Biyanee, **Usman Nasrullah**, Sofia Winslow, Tobias Schmid, Josef Pfeilschifter, Wolfgang Eberhardt. Inhibition of IRES-dependent Translation of caspase-2 by HuR Confers Chemotherapeutic Drug Resistance in Colon Carcinoma Cells. Oncotarget. 2018 Apr 6;9(26):18367-18385

Wolfgang Eberhardt, **Usman Nasrullah**, Josef Pfeilschifter. Activation of Renal Profibrotic TGFβ Controlled Signaling Cascades by Calcineurin and mTOR Inhibitors. Review Cell Signal. 2018 Dec;52:1-11

Wolfgang Eberhardt, **Usman Nasrullah**, Kristina Haeussler. Inhibition of Caspase-2 Translation by the mRNA Binding Protein HuR: A Novel Path of Therapy Resistance in Colon Carcinoma Cells? Review Cells. 2019 Jul 30;8(8):797

9.2. Presentations

2017, 2018, 2019	Project presentations, Pharmazentrum Seminar meeting, Frankfurt am Main
2017, 2018	Project presentations, Pharmazentrum Annual meeting, Rauischholzhausen
2-5 March 2020	Annual Meeting of the 5th German Pharm-Tox Summit German Society for Experimental and Clinical Pharmacology and Toxicology (DGPT), Leipzig 2020.

9.3. D E C L A R A T I O N

I herewith declare that I have not previously participated in any doctoral examination procedure in a mathematics or natural science discipline.

Frankfurt am Main, 19-05-2020

(Signature)

Author's Declaration I herewith declare that I have produced my doctoral dissertation on the topic of "**The E3 ligase TRIM25 negatively interferes with the translation of caspase-2 – therapeutic implications for sensitizing colon carcinoma cells to intrinsic apoptosis**" independently and using only the tools indicated therein. In particular, all references borrowed from external sources are clearly acknowledged and identified. I confirm that I have respected the principles of good scientific practice and have not made use of the services of any commercial agency in respect of my doctorate.

Frankfurt am Main, 19-05-2020

(Signature)